THE ASTROPHYSICAL JOURNAL

AN INTERNATIONAL REVIEW OF SPECTROSCOPY AND ASTRONOMICAL PHYSICS

VOLUME 86 NOVEMBER 1937 NUMBER 4

THE SODIUM CONTENT OF THE HEAD OF THE GREAT DAYLIGHT COMET SKJELLERUP 1927 K

ARTHUR ADEL, V. M. SLIPHER

AND R. LADENBURG

ABSTRACT

Spectrograms of the great daylight comet, Skjellerup, December, 1927, taken near perihelion passage, reveal the D-lines of sodium in emission with very nearly equal intensity. On the assumption that the D-lines are due to the absorption and re-emission of resonance radiation and that the absorption of this radiation in the interior of the comet is governed by the combined action of the Doppler and radiation damping agencies, the observed intensity ratio $0.9 \leqslant (D_2/D_1) \leqslant 1.1$ yields, for the concentration of normal sodium atoms in the comet's temporary atmosphere, $50 \leqslant N \leqslant 2500/\text{cm}^3$. The concentration of normal sodium atoms is subsequently confined to the region of the lower limit by an analysis of the monochromatic magnitude of the comet.

I. INTRODUCTION

Visual, photographic, spectrographic, and radiometric observations of Skjellerup's brilliant comet (1927 k) were secured on December 16–19 under good conditions of transparency.[1]

On the evening of December 15 an object was reported closely following the sun as it set. The next morning the comet was found to be an easy naked-eye object. The experienced observer saw it readily during that day by extending the hand to shade the eyes from the sun, which was only about 5° southwest of the comet.

[1] V. M. Slipher and E. C. Slipher, *Pop. Ast.*, **36**, 300, 1928; C. O. Lampland, *ibid.*, **36**, 240, 1928.

Venus, to the west of the comet, was available for comparison. Early in the day of December 16, the comet was many times brighter than Venus and was a relatively conspicuous object by reason of its brightness and tail.

The nucleus was of an orange-yellow color and was small but not quite stellar in form or sharpness. At times it appeared distinctly elongated. The nucleus was enveloped by the arching hoods commonly seen in bright comets. The tail was broad and was about 45′ long. By early afternoon (December 16) the comet had faded, and the tail had also changed in appearance.

After Saturday, December 17, the comet was seen, during the day, only with the aid of the telescope. It was last observed late in the afternoon of December 19. Attempts to direct the telescope on it the next day in full daylight were unsuccessful.

The comet's spectrum was first examined visually on the morning of December 16. However, it showed—on the sky-spectrum background—only a strong continuous spectrum of the nucleus, of the solar type. Examination with both low and high dispersion then showed the same result, disclosing none of the usual cometary bright bands. The next day, it was seen that the dark D-lines of sodium of the sky spectrum were bordered with faint bright D-lines of the comet. On December 18 these had strengthened until they were a very conspicuous pair of bright lines of equal intensity superposed upon the sky spectrum. The following day they were still brighter. They were long and very considerably displaced to the red side of their normal position, proving that the comet was receding from the earth at the rate of about 90 km/sec. The emitting sodium spread to a considerable distance from the nucleus and was most intense on December 19, the last day of observation. The two lines were very sharp and were conspicuous because they were so nearly of equal strength.

Although sought, no trace was found, visually or photographically, of the usual cometary bright bands. The long series of spectrograms included the spectrum region of two of these bands, 5165 A and 5635 A, the former being perhaps the most capable of the series of revealing itself under the conditions. It should be borne in mind, however, that the sky spectrum might have been effective in masking

PLATE VIII

a *b*

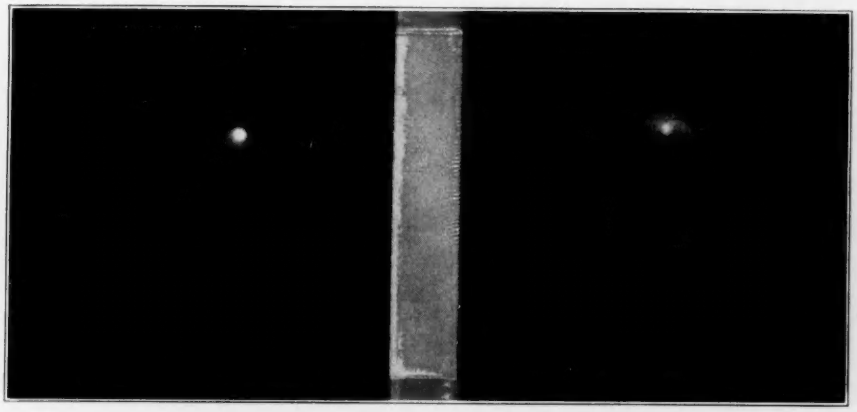

a) Comet (1927 k) Skjellerup

Photographed by E. C. Slipher at midafternoon, December 16, 1927, when the comet was only 5° from the sun.

b) Drawing of Comet Skjellerup

Made by E. C. Slipher on December 17, 1927

UNIV. OF MICH.

PLATE IX

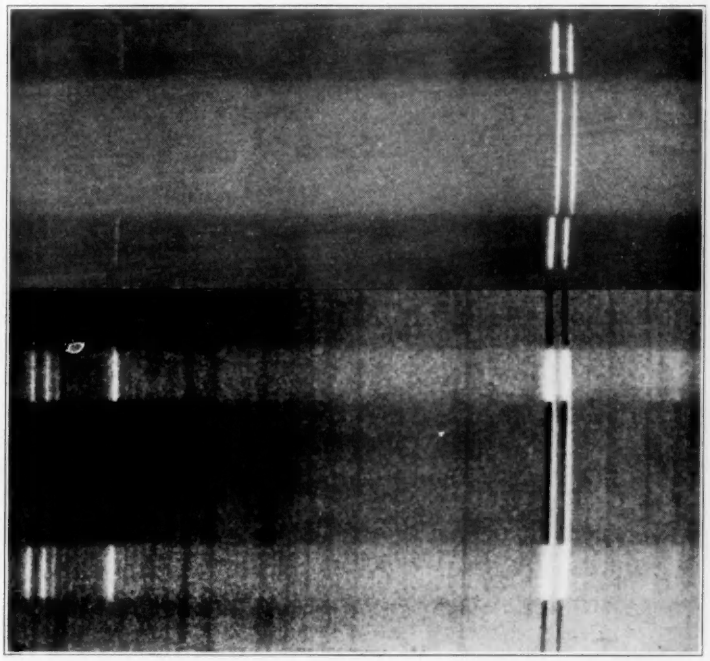

THE SPECTRUM OF COMET SKJELLERUP (1927 K)

The upper spectrum (*a*) with short exposure to record the comet's bright sodium D-lines with the least intensity of sky (solar) spectrum. This displays the strange equally intense D_1 and D_2 in the comet as compared with the usual unequal strength given by the D-lines in the comparison above and below those of the comet.

The lower spectrogram (*b*) with long exposure to record the comet's bright D-lines over the dark lined solar (sky) spectrum background. Superposed are to be seen short bright lines of the comparison spectrum. This spectrogram was made with a long slit for comet (and sky) to allow the bright comet lines to show their extension from the comet's nucleus (which occupied the middle of the slit). Both spectrograms reveal the marked displacement of the comet's lines in accord with its rapid recession from the earth at the time. The comparison spectrum is an iron-vanadium spark into which was dropped a pinch of salt.

weak emissions, inasmuch as all observations were made against a daylight sky, very close to the sun.

II. THE D-LINES IN EMISSION

The amount of vaporized material per unit volume of a comet's atmosphere may be considered to be minute. Accordingly, in discussing the processes governing the distribution of energy in spectral lines emitted, it is safe to assert that collision damping, pressure effects, and Stark effect may be neglected. The breadth of the D-lines, or the width at half-intensity, is therefore controlled by the combined action of radiation damping and the Doppler effect due to random motions. It is of interest to determine which of these mechanisms is dominant.

The Doppler half-intensity breadth is given by the familiar expression[2]

$$\omega_d = \frac{2\nu}{c}\left\{\frac{2RTln2}{M}\right\}^{\frac{1}{2}},$$

from which it follows that

$$\omega_d = 2.08 \times 10^9 \text{ sec}^{-1}.$$

The radiation damping half-intensity breadth is the sum of the half-intensity breadths of the resonance and ground levels. The half-intensity breadth of the ground level is substantially zero, apropos of the long mean life of the atom in this state. The upper-level half-intensity breadth is given by

$$\omega_r = \sum_m C_n 4\pi e^2 (\nu_n - \nu_m)^2 \frac{1}{3\mu c^3},$$

where

$$C_n = 3 \sum_m f_{nm} \frac{g_m}{g_n}.$$

[2] The value of T will be taken equal to $(277^\circ + 329^\circ)/2\sqrt{r}$, where $277^\circ/\sqrt{r}$ is the temperature obtained when the nuclear masses are assumed to be approximately spherical black bodies absorbing solar radiation in an amount corresponding to their cross-sections, and reradiating this energy in an amount corresponding to their entire surfaces; and where $329^\circ/\sqrt{r}$ is the value obtained when reradiation occurs only from the hemisphere exposed to the sun. r (taken ≈ 0.17) is the heliocentric distance in astronomical units. The meteoric masses are assumed to be in near equilibrium with the solar radiation, and the gas, having been effused by these masses, is assumed to have partaken of their temperatures. $T = 750^\circ$ K.

The sums are extended over all levels for which $E_n > E_m$, E being the energy. For a resonance level this becomes

$$\omega_r = \frac{3 f_{no} g_o}{g_n} \times \frac{4\pi e^2 \nu_n^2}{3\mu c^3},$$

where f_{no} is the oscillator strength of the transition, and g_o and g_n are the weights of the normal and resonance states, respectively. The transitions in question are

$$D_1, \quad {}^2P_{1/2} \rightarrow {}^2S_{1/2}$$
$$D_2, \quad {}^2P_{3/2} \rightarrow {}^2S_{1/2},$$

for which we have

$$g_{S_{1/2}} = 2, \quad g_{P_{1/2}} = 2, \quad g_{P_{3/2}} = 4;$$

and[3]

$$f_{P_{3/2}} = 2 f_{P_{1/2}} = 0.71.$$

It follows that ${}_{D_1}\omega_r = {}_{D_2}\omega_r = 10^7 \text{ sec}^{-1}$. (The value of ω_r has actually been observed for the D-lines by R. Minkowski.[4] He has found $2\pi\omega_r = 0.63 \times 10^8$, from which it follows that $\omega_r = 10^7$.)

The large ratio $\omega_d/\omega_r = 208$ indicates that the distribution of energy in the cometary D-lines is predominantly of Doppler origin.

III. THE COMETARY D-LINES

We seek an explanation for the observed equality of intensity of the D-lines emitted by the sodium in the temporary atmosphere of Comet Skjellerup. The intensity in question is clearly the total or integrated emission, since it is manifest from Section II and from the fact that the slit width was 0.78 A that the spectrograph was incapable of resolving the true contours of the emissions.

Schwarzschild and Kron[5] have satisfactorily accounted for the luminosity of comet tails by the mechanism of absorption and re-emission of sunlight. Zanstra[6] has been similarly successful in the

[3] R. Ladenburg and E. Thiele, *Zs. f. Phys.*, **72**, 697, 1931.

[4] *Ibid.*, **86**, 839, 1926.

[5] *Ap. J.*, **34**, 342, 1911.

[6] *M.N.*, **89**, 178, 1928.

case of the comet heads. It seems appropriate, therefore, to assume that the sodium atoms in the atmosphere of Comet Skjellerup were excited by solar radiation. The problem then resolves itself into determining the set of conditions which prevailed in the cloud to make it possible for the gas of sodium atoms to absorb in such manner as to emit equally in the regions D_1 and D_2. It is sufficient, as in Section II, to consider radiation damping and the Doppler effect as the agencies governing the absorption of sunlight. It has been assumed, of course, that in so rare a medium the resonance absorption and emission are equal for each volume element.

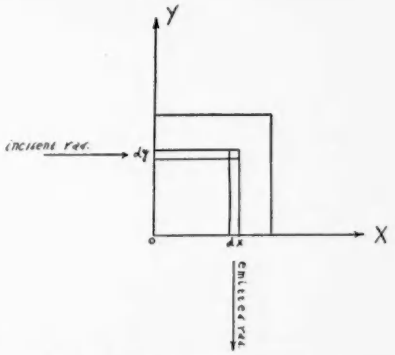

FIG. 1.—Model of comet's head

To take into account the differential absorption suffered by the re-emitted resonance radiations as they pass through the body of the cloud to the boundary, it suffices to represent the atmosphere of the comet as a two-dimensional rectangular layer illuminated in the X-direction by the D-region of the solar spectrum. We shall determine the intensity of the resonance radiation emitted by the sodium vapor in the comet in the Y-direction. The absorption coefficient of the sodium vapor is a function of the frequency ν and will be designated by $\alpha(\nu)$. With negligible error, we assume that the intensity of the sunlight incident upon the vapor is constant over the small spectral region D_1 and over the small spectral region D_2 of the vapor. Denote this by ${}_{D_1}I_0$ and by ${}_{D_2}I_0$. Neglecting the effect of scattering from surrounding space elements, the amount of radiation absorbed by the element $dxdy$ is proportional to

$$I_0 e^{-\alpha(\nu)z}\alpha(\nu)dxdy\,.$$

A quantity proportional to $e^{-\alpha(\nu)y}$ of this amount will escape through the boundary $y = 0$ and will proceed, let us say, toward the earth. In consequence, the total radiation of frequency ν emitted in the direction of the negative y-axis is proportional to the integral of the

product of these factors taken over the area occupied by the sodium cloud. That is to say,

$$I(\nu) = I_0 \iint \alpha(\nu) e^{-\alpha(\nu)(x+y)} dx dy .$$

If l is taken to be the length of the layer in both the X- and Y-directions, it follows that

$$I(\nu) = \frac{I_0 \{1 - e^{-\alpha(\nu) l}\}^2}{\alpha(\nu)} .$$

The total energy radiated as a D-line is consequently represented by

$$P = \int_0^\infty I(\nu) d\nu = I_0 \int_0^\infty \frac{\{1 - e^{-\alpha(\nu) l}\}^2}{\alpha(\nu)} d\nu .$$

The absorption coefficient determined by the combined action of radiation damping and the Doppler effect may be stated explicitly[7]:

$$\alpha(\nu) = \frac{NK\delta Mc^2}{2RT\nu_0^2 \pi^{1/2}} \int_{-\infty}^{+\infty} \frac{e^{-y^2}}{(\omega - y)^2 + D^2} dy ,$$

where

N = the number of normal atoms per cm^3,

$K = \dfrac{f_{n0} e^2}{\mu c}$,

$\delta = \dfrac{f_{n0}}{4\pi\tau} = \frac{1}{2}\omega_r$, τ = mean life,

$\omega = (\nu_0 - \nu) \dfrac{c}{\nu_0} \left(\dfrac{M}{2RT}\right)^{1/2} = \dfrac{(\nu_0 - \nu)}{\omega_d} 2 (ln\ 2)^{1/2}$,

$y = u \left(\dfrac{M}{2RT}\right)^{1/2}$, u = the velocity of an atom in the line of sight,

$D = \dfrac{\delta c}{\nu_0} \left(\dfrac{M}{2RT}\right)^{1/2} = \dfrac{\omega_r}{\omega_d} (ln\ 2)^{1/2}$.

[7] Cf. S. Rosseland, *Theoretical Astrophysics*, p. 100, 1936.

F. Reiche[8] has shown that, when $D \leqslant 0.01$, the absorption coefficient may be expressed in the form

$$a(\nu) = k_0 \left\{ e^{-\omega^2} - \frac{a}{\pi^{1/2}} (1 - 2\omega F(\omega)) \right\},$$

where

$$k_0 = \frac{2\pi e^2}{\mu c} N \cdot f \left(\frac{ln\ 2}{\pi} \right)^{1/2} \frac{1}{\omega_d}$$

$$F(\omega) = e^{-\omega^2} \int_0^{\omega} e^{y^2} dy$$

$$a = 2D = \frac{2\omega_r}{\omega_d} (ln\ 2)^{1/2}.$$

The factor preceding the integral in Rosseland's expression for $a(\nu)$ is identical with the product

$$\frac{k_0 a}{2\pi}.$$

The simplification presented above is applicable to the present problem in virtue of the fact that $D = 0.004$ for Comet Skjellerup.

Before proceeding with the evaluation of the integral P, it will be instructive to find the solution in the first approximation by neglecting the effect of the differential absorption exercised by the sodium cloud upon the escaping radiations. In this approximation, the integral P becomes l times the integral Q:

$$Q = I_0 \int_0^{\infty} \{1 - e^{-a(\nu) l}\}\, d\nu.$$

This integral has been evaluated not only for the limiting cases of the Doppler effect and radiation damping[9] but also for the general

[8] Cf. A. C. G. Mitchell and M. W. Zemansky, *Resonance Radiation and Excited Atoms* (New York: Macmillan Co., 1934), pp. 101 and 321.

[9] R. Ladenburg and S. Levy, *Zs. f. Phys.*, **65**, 189, 1930. R. Ladenburg and F. Reiche, *Ann. d. Phys.*, **42**, 181, 1913; *C.R.*, **158**, 1788, 1914.

case of the combined effects.[10] In the general case of the combined effects, the manner in which Q depends upon the optical density of the gas, that is, upon the product Nfl, is depicted by the curves of growth (Fig. 2) taken from the paper by E. F. M. van der Held. The

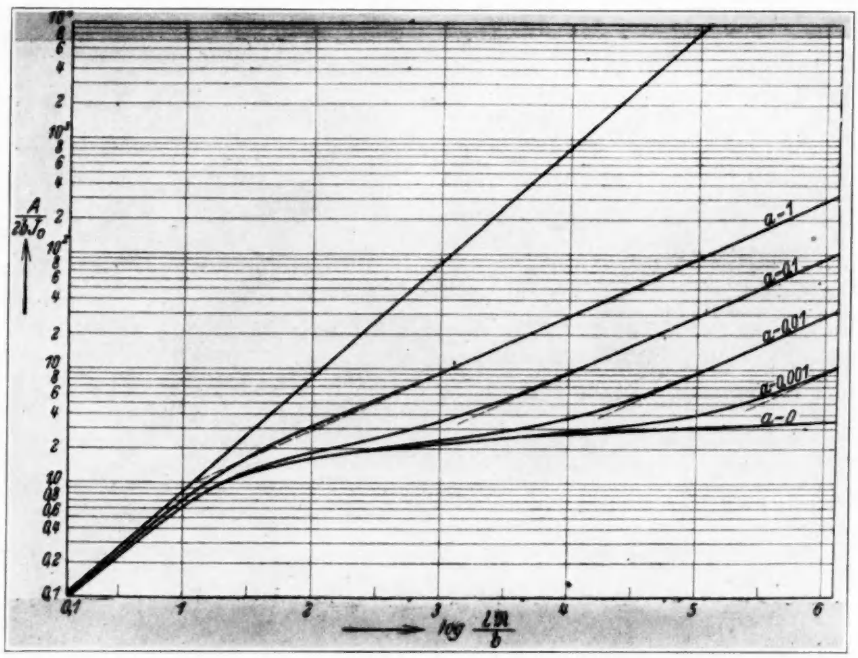

FIG. 2.—Curve of growth in the first approximation

arabic $\mathfrak{N}$ is equal to the product $N \cdot f$. The curve is a plot of $\pi Q/b I_0$ against log Nfl/b, where

$$b = \frac{2\pi\nu_0}{c}\left(\frac{2RT}{M}\right)^{1/2} = \frac{\pi}{(ln\ 2)^{1/2}}\,\omega_d = 3.77\omega_d .$$

The parameter of the family of curves is

$$a = 2\,\frac{\omega_r}{\omega_d}\,(ln\ 2)^{1/2} \equiv \tfrac{1}{2}\,D\ ;$$

[10] W. Schütz, *Zs. f. Phys.*, **64**, 682, 1930; *Zs. f. Ap.*, **1**, 300, 1932. E. F. M. van der Held, *Zs. f. Phys.*, **70**, 514, 1931; see also Rosseland, *op. cit.*, p. 166.

that is, the ratio of radiation damping and Doppler half-intensity breadths multiplied by 1.66. In the case of Comet Skjellerup,[11]

$$\omega_d = 2.08 \times 10^9,\ b = 7.85 \times 10^9,\ l = 5 \times 10^9 \text{ cm},\ f_{D_2} = 2f_{D_1} = 0.71 .$$

Consequently, for D_2,

$$\frac{Nf_2 l}{b} = N \times 0.454 = \frac{N}{2.2},$$

and for D_1,

$$\frac{Nf_1 l}{b} = \frac{N}{4.4}.$$

The curves of growth express the fact, which was first pointed out by Ladenburg and Reiche, that the total absorption is proportional to the optical density for small values of the latter regardless of whether the absorption coefficient is determined by radiation damping, Doppler effect, or both; whereas, in the event that radiation damping is an appreciable agent for the absorption ($a > 0.01$), the total absorption is proportional to the square root of the optical density for large values of the latter.

In the case of Comet Skjellerup

$$a = \frac{2 \times 10^7 \, (ln\ 2)^{1/2}}{2.08 \times 10^9} = 0.008 ,$$

and we are therefore concerned with the intermediate portion of the curves of growth. This section, in which Nfl/b ranges between 10^2 and 2×10^4, supplies the clue for the approximately equal total emission of D_2 and D_1. It is evident that in this region the emission increases very slowly with increasing optical density. Specifically, the ratio of the total emission of the two lines, for which the ratio of the optical density is 2:1, differs from unity by only 10–15 per cent.

A more exact determination of the optical density demands recognition of the fact that the intensity of sunlight $I_{0,2}$ in the cometary spectral region of D_2 will, in general, differ from $I_{0,1}$ in the region D_1. This is due to the different contours of the D-lines in the solar

[11] In this calculation the comet's atmosphere has been assumed to be spherical and its diameter has been taken to be l, as determined from the length of the D-lines.

TABLE 1

log Nlf/b	Nlf/b	$A/2bI_0 = Q\pi/bI_0$		
		$a=0$	$a=0.001$	$a=0.01$
0.2	1.585	0.155	.....	.....
0.3	2.0	.177	.....	.....
0.4	2.51	.218	.....	.....
0.5	3.17	.267	.....	.....
0.6	3.98	.320	.....	.....
0.7	5.01	.388	.....	.....
0.8	6.30	.460	.....	.....
0.9	7.94	.545	.....	.....
1.0	10.0	.652	.....	.....
1.1	12.6	.762	.....	.....
1.2	16	.875	.....	.....
1.3	20	1.00	.....	.....
1.4	25	1.12	.....	.....
1.5	32	1.23	.....	.....
1.6	40	1.32	.....	.....
1.7	50	1.40	.....	.....
1.8	63	1.48	.....	.....
1.9	80	1.57	.....	.....
2.0	100	1.65	.....	.....
2.1	126	1.71	.....	.....
2.2	160	1.77	.....	.....
2.3	200	1.83	.....	.....
2.4	250	1.89	.....	1.90
2.5	320	1.95	.....	1.98
2.6	400	2.01	.....	2.05
2.7	500	2.07	.....	2.12
2.8	630	2.12	.....	2.20
2.9	800	2.18	.....	2.29
3.0	1000	2.23	.....	2.38
3.1	1260	2.29	.....	2.48
3.2	1600	2.34	.....	2.58
3.3	2000	2.40	.....	2.68
3.4	2500	2.44	.....	2.79
3.5	3200	2.49	.....	2.90
3.6	4000	2.54	.....	3.02
3.7	5000	2.59	2.61	3.17
3.8	6300	2.64	2.67	3.32
3.9	8000	2.68	2.73	3.49
4.0	10000	2.72	2.80	3.67
4.1	12600	2.78	2.89	3.90
4.2	16000	2.82	2.98	4.20
4.3	20000	2.86	3.07	4.56
4.4	25000	2.90	3.16	5.00
4.5	32000	2.94	3.27	5.47
4.6	40000	2.98	3.38	6.0
4.7	50000	3.02	3.56	6.6
4.8	63000	3.06	3.63	7.4
4.9	80000	3.10	3.80	8.25
5.0	100000	3.14	4.00	9.2
5.1	126000	3.18	4.22	.....
5.2	160000	3.22	4.50	.....
5.3	200000	3.25	4.81	.....

spectrum and to the fact that the comet possessed an appreciable radial velocity relative to the sun, the latter resulting in a Doppler displacement of the D-lines. Unsöld[12] and Korff[13] have mapped the experimental contours of the solar D-lines. From the known heliocentric radial velocity of the comet[14] and the work of Korff and Unsöld, it appears that

$$\frac{I_{0,2}}{I_{0,1}} \cong 0.96 .$$

The ratio Q_2/Q_1 of the observed total emission of the D-lines in the comet appears to be $0.9 \leqslant Q_2/Q_1 \leqslant 1.1$. The corresponding ratio of the quotient Q/I_0 for the lines D_2 and D_1 is

$$0.86 \leqslant \frac{\dfrac{Q_2}{I_{0,2}}}{\dfrac{Q_1}{I_{0,1}}} \leqslant 1.14 .$$

The corresponding possible limits of the density N of normal

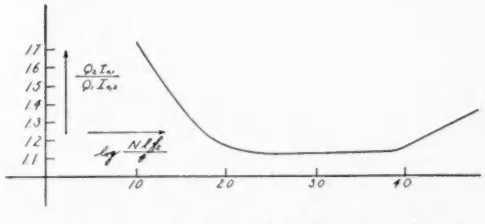

FIG. 3.—Relative intensity as function of optical density

sodium atoms are easily obtained from Table 1. They may also be obtained from Figure 3, which exhibits the dependence of

$$\frac{\dfrac{Q_2}{I_{0,2}}}{\dfrac{Q_1}{I_{0,1}}}$$

[12] *Zs. f. Phys.*, **46**, 772, 1928.

[13] *Ap. J.*, **76**, 291, 1932.

[14] The orbital elements for Comet Skjellerup (1927 k) have been given by A. C. D. Crommelin in the *M.N.R.A.S.*, **88**, 597, 1928, as

T = 1927 Dec. 18.18340 U.T. $\quad i = 85°6'22''.01$
$\omega = 47°11'\ 13''.24 \quad \log q = 9.2462789$
$\Omega = 77°13'\ 29''.62$

upon the optical density Nf_2l/b. The lower limit of the density is rather sharply defined, yielding $N > 170$ atoms/cm^3; the upper limit is not quite so sharply defined, yielding $N < 22{,}000$ atoms/cm^3. Consequently we may conclude, in the first approximation, that the density of normal sodium vapor lies between 10^2 and 2.5×10^4 atoms/cm^3.

The second approximation to the solution of the problem is achieved by evaluating the integral P (see Appen.). The results of

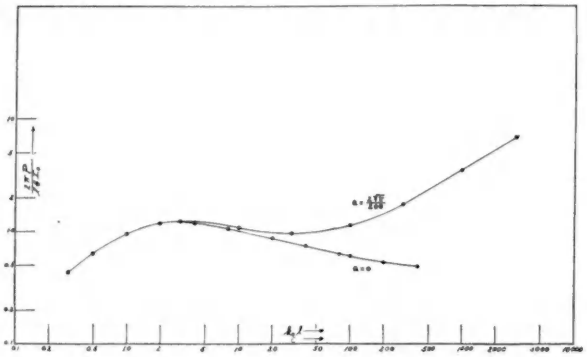

FIG. 4.—Curves of growth in the second approximation

these approximate calculations are collected in Figure 4. The quantity

$$k_0 l = C = Nfl \frac{2e^2}{\mu c} \frac{\pi^{3/2}}{b} = 2Nf \times 0.03 ,$$

which is plotted as abscissa, is found by introducing the values $e^2/\mu c = 8.45 \times 10^{-3}$, $b = 7.85 \times 10^9$, and $l = 5 \times 10^9$; it follows that $N = C_{D_2} \times 25 = C_{D_1} \times 50$; the ordinates are the values of $2\pi\ P/b\, I_0\, l$. The lower curve is drawn for $a = 0$, and the upper one for $a/2 = \sqrt{\pi}/200 = 0.00887$, where, as before, $a = 2\omega_r/\omega_d$ $(ln2)^{1/2} = 1.66\ \omega_r/\omega_d$.

In the same manner in which Figure 3 was interpreted, we now consider the dependency of the ratio

$$\frac{\dfrac{P_2}{I_{0,2}}}{\dfrac{P_1}{I_{0,1}}}$$

upon C_{D_2}. For the temporary atmosphere of Comet Skjellerup, this ratio lies between 0.86 and 1.14, and we conclude from Figure 4 that the upper limit of the density of the normal sodium atoms lies in the neighborhood of 2500 atoms/cm^3 (instead of 22,000 as was determined in the first approximation) and that the lower limit may be as low as 50 atoms/cm^3 (instead of 170).

It must be borne in mind that the inequalities involving N should, strictly speaking, be expressed in the form of limits. Thus, the first approximation yields either $N = 170$ or $N = 22{,}000$, and the second approximation yields either $N = 50$ or $N = 2{,}500$. We must, therefore, find an independent method of approach which will indicate which limit is to be considered the solution to the problem. It is clear that if the lower limit is the appropriate one, then the effect of the cometary sodium upon the escaping radiation is negligible, and the second approximation adds little to the first.

IV. THE CALCULATED MONOCHROMATIC MAGNITUDE OF COMET SKJELLERUP

A knowledge of the approximate dimensions of the comet's atmosphere combined with the density of the normal sodium as determined in Section III, makes it possible to form an estimate of the magnitude of the cometary head in the light of the D-lines.

The energy of a single D-emission is $1/3 \times 10^{-11}$ ergs. The number of transitions in the entire cloud per second is equal to the volume of the cloud multiplied by the mean density, multiplied by the number of transitions per atom per second, or

$$\frac{\pi D^3 N}{6t},$$

where t is the time required by a sodium atom to execute an absorption and emission of a D-quantum. The total energy emitted per second by the cloud is $1/3 \times 10^{-11} \times \pi D^3 N/6t$ ergs. The luminous power output of the sun is 5×10^{32} ergs/sec. and its apparent magnitude is -26.7. The sun's apparent brightness, therefore, exceeded that of Comet Skjellerup's head by a factor

$$F = \frac{5 \times 10^{32}}{\frac{1}{3} \times 10^{-11} \times \frac{\pi D^3 N}{6t}}.$$

Since $50 \leqslant N \leqslant 2500$, the limits of this factor are

$$10^{12}t \leqslant F \leqslant 5 \times 10^{13}t ,$$

and the monochromatic brightness of the cloud is $-26.7 + x$, where $2.5^x = F$. We must now determine t. This may be done by the application of Milne's method of finding the resultant momentum acquired by a sodium atom during the time t. The momentum acquired in falling toward the sun is mgt. The mean momentum acquired away from the sun in virtue of absorption (radiation pressure) is $h\nu/c$. The momenta toward and away from the sun are in the same ratio as the forces of gravitation and repulsion due to radiation pressure. Baade and Pauli[15] have determined this ratio and have shown it to be

$$Z = \frac{8\pi^2 e^2 h e^{-\frac{h\nu}{kT}}}{\mu m c G \lambda^3} = \frac{\text{radiation}}{\text{gravitation}} ,$$

where e is the electronic charge, μ is the electronic mass, m is the mass of the sodium atom, and T is the sun's temperature. Wurm[16] has shown that better agreement is secured when it is assumed that the ratio as determined by Baade and Pauli is too great by a factor of 2. We arrive, therefore, at the relationship

$$\frac{h\nu}{c} = \frac{Z}{2} mgt ,$$

from which it follows that $t = 0.5 \times 10^{-3}$ seconds. Consequently,

$$5 \times 10^8 \leqslant F \leqslant 2.5 \times 10^{10} ,$$

and therefore $22 \lessapprox \times \lessapprox 26$. It would appear that the monochromatic magnitude of the comet's head was $-4.7 \lessapprox M \lessapprox -0.7$. (The comet was very nearly one astronomical unit distant from the earth at the time of observation.)

Reference to the description of the comet given in Section I indi-

[15] W. Baade and W. Pauli, *Naturwissenschaften*, **15**, 50, 1927.

[16] K. Wurm, *Zs. f. Ap.*, **10**, 287, 1935.

cates that the sodium magnitude of the comet was much nearer -0.7 than -4.7 and was probably in the neighborhood of magnitude -1. This would seem to indicate that the density of normal sodium atoms in the cloud was in the immediate neighborhood of the lower limit given in Section III, that is, in the immediate neighborhood of 50 or 100 atoms/cm^3.

V. THE PROPORTION OF NORMAL TO IONIZED SODIUM ATOMS IN THE TEMPORARY ATMOSPHERE OF COMET SKJELLERUP

Owing to the high degree of ionization, the total number of sodium atoms per cm^3 must have exceeded by far the density of normal sodium. An approximation to the degree of ionization prevalent in the comet's atmosphere can be ascertained from Saha's relation. The expression

$$\log \frac{x^2 p}{1 - x^2} = -5048 \frac{I}{T} + \tfrac{5}{2} \log T - 6.5 + \log \frac{R^2}{4r^2},$$

where

x = the fraction of atoms ionized
p = the gas pressure
I = the ionization potential of sodium = 5.1 electron volts
T = the sun's temperature = 6000°
$(R^2/4r^2)$ = the factor of dilution of the sun's black-body radiation at the distance r of the comet from the sun,

leads to the value $Ni^2/N = 10^{15}$, where N_i = the number of ionized atoms per cm^3, and N = the number of normal atoms per cm^3. Since N appears to be in the neighborhood of 100 atoms per cm^3, we have N_i approximately equal to 3×10^8. It follows that for every normal sodium atom present in the head of Comet Skjellerup there were approximately 3,000,000 ionized ones.

APPENDIX

The evaluation of the integral P given below is due to Mr. John Sweer, of Princeton University.

Evaluation of the integral

$$I = \int_0^\infty \frac{\{1 - e^{-a(\nu)l}\}^2}{a(\nu)} d\nu ,$$

which is identical with P when $I_0 = 1$.

$$a(\nu) = k_0 \left\{ e^{-\omega^2} - \frac{a}{\sqrt{\pi}} (1 - 2\omega F(\omega)) \right\}$$

$$F(\omega) = e^{-\omega^2} \int_0^\omega e^{y^2} dy$$

$a = 2\,\omega_r/\omega_d\,(ln\ 2)^{1/2}$ is taken to be $\leqq 0.02$.

Case I

Taking $a = 0$ and writing $k_2 = C \times l$, we find

$$I = \frac{l}{C} \int_0^\infty \frac{\{1 - e^{Ce^{-\omega^2}}\}^2}{e^{-\omega^2}} d\nu = \frac{lb}{2\pi C} \int_{-\infty}^{+\infty} \frac{\{1 - e^{-Ce^{\omega^2}}\}^2}{e^{-\omega^2}} d\omega ,$$

where $b = \pi\omega_d/(ln\ 2)^{1/2}$, and where the lower limit is set at $-\infty$ because the integrand approaches zero very rapidly for values of $-\omega$ greater than approximately $100 \times \omega_d$. In order to carry out the above integration, let us first consider the function

$$T(C) = \int_{-\infty}^{+\infty} \{1 - e^{-Ce^{-\omega^2}}\}\, d\omega .$$

We may now write

$$\int_0^C T(C)dC = \int_{-\infty}^{+\infty} \left\{ C + \frac{e^{-Ce^{-\omega^2}} - 1}{e^{-\omega^2}} \right\} d\omega ,$$

from which it follows that

$$\int_0^{2C} TdC - 2\int_0^C TdC = \int_{-\infty}^{+\infty} \left\{ 2C + \frac{e^{-2Ce^{-\omega^2}} - 1}{e^{-\omega^2}} - 2C - 2\,\frac{e^{-Ce^{-\omega^2}} - 1}{e^{-\omega^2}} \right\} d\omega$$

$$= \int_{-\infty}^{+\infty} \frac{\{1 - e^{-Ce^{-\omega^2}}\}^2}{e^{-\omega^2}} d\omega .$$

The function $T(C)$ has been tabulated.[9] It is equal to $\sqrt{\pi}$ times the product $C \cdot S(C)$, which is given on page 204 of the first reference in note 9 above. We may now put the integral in the form

$$I = \frac{l}{C}\frac{b}{2\pi}\left\{\int_0^{2C} TdC - 2\int_0^{C} TdC\right\}$$

$$= \frac{l}{C}\frac{b}{2\sqrt{\pi}}\left\{\int_0^{2C} C \cdot S(C)dC - 2\int_0^{C} C \cdot S(C)dC\right\}.$$

The values of the intensity function for $a = 0$ have been calculated from this formula by means of numerical integration of the tabulated function given in the first reference under note 9 above.

CASE II

For $a \neq 0$ the integral becomes

$$I = \frac{lb}{2\pi}\int_{-\infty}^{+\infty} \frac{\left\{1 - e^{-C\left(e^{-\omega^2} - \frac{a}{\sqrt{\pi}}\{1-2\omega F(\omega)\}\right)}\right\}^2}{C\left\{e^{-\omega^2} - \frac{a}{\sqrt{\pi}}(1 - 2\omega F(\omega))\right\}} d\omega .$$

Numerical integration is again employed in this case, from $\omega = 0$ to that value $\underline{\omega}$ of ω for which $e^{-\omega^2}$ may be neglected, and for which a power series expansion of

$$e^{-C\left(e^{-\omega^2} - \frac{a}{\sqrt{\pi}}\{1-2\omega F(\omega)\}\right)}$$

may be assumed to be valid when fourth-degree terms of the argument are dropped. For these greater values of ω, we may write (putting $aC/\sqrt{\pi} = A$):

$$\frac{\pi I'}{bl} = \int_{\underline{\omega}}^{\infty} \frac{1 - 2e^{A(1-2\omega F)} + e^{2A(1-2\omega F)}}{-A(1-2\omega F)} d\omega$$

$$= \int_{\underline{\omega}}^{\infty} \{-A(1-2\omega F) - A^2(1-2\omega F)^2 - \tfrac{7}{12}A^3(1-2\omega F)^3 - \ldots .\} d\omega$$

$$= \left| -AF - A^2F - A^2\left\{\int F^2 d\omega - \omega F^2\right\}\right.$$

$$\left. - \tfrac{7}{12}A^3\left\{F - 2\omega F^2 + \tfrac{4}{3}\left(\omega^2 F + \frac{F^3}{3}\right) + \tfrac{2}{3}\right\}\int F^2 d\omega \right|_{\underline{\omega}}^{\infty} .$$

The foregoing follows readily from the relation

$$1 - 2\omega F = \frac{dF}{d\omega} .$$

Upon the introduction of the semi-convergent series

$$F(\omega) = \frac{1}{2\omega}\left\{1 + \frac{1}{2\omega^2} + \frac{1\cdot 3}{(2\omega^2)^2} + \frac{1\cdot 3\cdot 5}{(2\omega^2)^3} + \frac{1\cdot 3\cdot 5\cdot 7}{(2\omega^2)^4} + \ldots\right\},$$

we find

$$\frac{\pi I'}{bl} = \frac{1}{2\omega}A + \frac{1}{4\omega^3}(A - \tfrac{1}{3}A^2) + \frac{1}{8\omega^5}(3A - \tfrac{6}{5}A^2 + \tfrac{7}{10}A^3) + \frac{1}{16\omega^7}(15A - \tfrac{39}{7}A^2 + \tfrac{3}{4}A^3).$$

This formula was employed to evaluate the integrals over the edges of the line.

LOWELL OBSERVATORY
FLAGSTAFF, ARIZONA
AND
PRINCETON UNIVERSITY
PRINCETON, NEW JERSEY
July 1937

RADIAL VELOCITIES OF CEPHEID VARIABLE STARS*

ALFRED H. JOY

ABSTRACT

Uniform radial-velocity determinations have been made for 128 variable stars of the δ Cephei type with periods from 1.5 to 45 days. With low-dispersion spectrographs the observations have been extended to the fourteenth photographic magnitude. Tests for systematic errors were made by comparing results for stars having similar spectra with Lick determinations.

Velocity-curves were drawn for 106 stars. From these curves the normal velocity, range, and certain characteristic features were deduced. Incomplete data were also obtained for 22 additional stars. Diagrams were plotted showing the relationship between period and certain properties of the stars such as light- and velocity-range, shape of the curves, and lag of the velocity-curve at maximum and minimum of light.

Radial-velocity determinations for variable stars of the δ Cephei type are of especial value for extending our knowledge of the activities taking place in the atmospheres of unstable stars as well as for obtaining data concerning the motions of distant stars and the movement of the galaxy as a whole. In general, Cepheids are situated close to the galactic plane and are well distributed in longitude.

The characteristics of individual velocity-curves of several of the brighter Cepheid variables have been known for a number of years through the results obtained, mostly at the Lick Observatory, from three-prism spectrograms. Previous to 1920 about a dozen stars had been observed in detail and the relationship of the light- and velocity-changes carefully studied.

In planning a comprehensive program of spectroscopic observation of stars of this type, it seemed advisable to survey the whole group down to the faintest limit of magnitude possible with the instruments available rather than to continue the practice of intensive observation of certain selected stars. It was hoped that ten, or even fewer, spectrograms of each star, if properly distributed in phase, would be sufficient to determine a reliable normal velocity for the star and give a first approximation to the form of its velocity-curve.

* *Contributions from the Mount Wilson Observatory, Carnegie Institution of Washington*, No. 578.

Up to the present time spectrographic velocity-observations for 29 variable stars of the δ Cephei type have been published, exclusive of Polaris, which is peculiar in its behavior. They are as follows:

η Aql	DT Cyg	W Sgr
U Aql	β Dor	X Sgr
FF Aql	ζ Gem	Y Sgr
RT Aur	W Gem	RV Sco
l Car	T Mon	SZ Tau
SU Cas	S Mus	R TrA
TU Cas	S Nor	S TrA
δ Cep	Y Oph	T Vul
X Cyg	κ Pav	U Vul
SU Cyg	S Sge	

Twenty stars were observed at the Lick Observatory by 14 different observers, 12 at Mount Wilson, mostly by Sanford, 2 at Michigan, and 1 each at the Pulkowa and the Cape observatories. In a few cases observations were made at more than one observatory. The present investigation adds to this number 126 stars and leaves only 35 stars, mostly fainter than fourteenth magnitude, north of declination $-40°$ for which no observations are now available.

The observations and reductions have been kept as uniform as possible during the period of time involved. One-prism spectrographs were used, and the camera employed depended on the brightness of the star so that the exposure-times could be limited to three hours or less.

The spectra of Cepheids are known for their wide deep lines and for the presence of numerous strong lines of ionized atoms. These characteristics are especially favorable to the use of low dispersion. It was found that most of the lines used could be seen and readily measured on small-scale spectrograms, if attention was given to the proper exposure of the photographic plate. Although the observations of each star usually extended over several years, the resulting velocities, when sufficient in number, may be used to plot a mean velocity-curve, if the period is reasonably constant. It is necessary to depend upon the period of variation given by photometric observers. The photographic results, especially those of Robinson of the Harvard Observatory, have been used if available. In most cases preference has been given to elements based on data covering as long a

period of time as possible. A number of the elements are apparently in need of further observations for confirmation or revision.

In Table 1, data are listed concerning 106 stars for which the observations indicate the course of the velocity-curve. Table 2 contains similar data for 22 stars for which curves could not be drawn, either because of insufficient observations or because the agreement among the velocities was too poor to determine the curve. The phases are expressed as fractions of the period. The symbols "a," "b," and "c" in the sixth column indicate dispersions of approximately 35, 75, and 120 A per millimeter, respectively, at $H\gamma$. The estimated weight, given in the last column, is based on the dispersion and the quality of the plate. The radial velocities for each of the 106 stars are plotted against phase in Figures 1–18, and rough velocity-curves are drawn through the points with due consideration of the weight of the observations as given in the table.

The normal velocity for each curve was determined to the nearest half-kilometer per second by the method of equal areas and is indicated on the diagram by a dashed line. Light-curves from various sources, to which reference is made in Table 1, have been placed alongside for convenience in comparing certain features of the light- and velocity-variations.

On the assumption that the curves, as drawn, represent the true course of the velocity variations, the average unweighted residual is about 3 km/sec, and the probable error of the normal velocity for a star is of the order of 1.0 km/sec. Tests for systematic error were made by comparing with Lick Observatory results the velocities of 8 stars having constant velocity and Cepheid-like spectra. Fifty-five spectrograms were obtained with the shorter cameras at both the 60- and 100-inch telescopes and measured in the customary way. The results are shown in Table 3. The mean of the differences is ± 2.4 km/sec, and the systematic deviation -0.14 km/sec. Thirteen plates of δ Cephei may also be used for comparison with Jacobsen's curve, which is shown in Figure 6. The mean of the residuals is ± 3.4 km/sec, and the systematic difference (Mt. Wilson *minus* Lick) -0.3 km/sec. Similarly, 11 plates of T Vulpeculae give a mean residual of ± 3.3 km/sec and a systematic difference of -0.1 km/sec relative to Albrecht's curve.[1]

[1] *Lick Obs. Bull.*, **4**, 137, 1907.

TABLE 1

OBSERVATIONS OF CEPHEID VARIABLES FOR WHICH VELOCITY-CURVES ARE ILLUSTRATED

Plate	Date	JD*	Phase	Vel. Km/Sec	Disp.	Wt.
SZ Aquilae $18^h59^m35^s$, $+1°9'$†; 9.4–11.4 pg.						
Max. = JD 2420258.765 + $17^d.137939E$						
Elements and photographic light-curve by Robinson, *Harvard Bull.*, No. 872, 16, 1930.						
C 1241	1921 Aug. 20	2422922.701	0.441	+ 4.3	b	1.0
1361	Oct. 6	2969.641	.180	−20.8	a	1.5
3764	1926 Apr. 24	4630.993	.120	−22.7	b	1.0
4979	1928 Sept. 24	5514.706	.684	+34.7	b	0.3
γ 16703	1929 July 14	5807.844	.789	+36.8	b	0.7
C 5274	Aug. 18	5842.765	.827	+45.4	b	0.7
5284	Aug. 21	5845.802	.004	+ 9.4	b	1.0
γ 17575	1930 July 11	6169.868	0.913	+17.8	b	0.7
TT Aquilae $19^h3^m9^s$, $+1°8'$; 7.4–9.1 pg.						
Max. = JD 2420097.705 + $13^d.754980E$						
Elements and photographic light-curve by Robinson, *Harvard Ann.*, **90**, 49, 58, 1933.						
γ 7221	1918 Aug. 19	2421825.795	0.634	+18.4	b	1.0
8131	1919 May 7	2086.948	.620	+13.3	b	0.7
8164	May 12	2091.908	.980	−12.4	b	1.0
16036	1928 July 31	5459.788	.828	+26.0	a	0.5
16255	Oct. 28	5548.639	.288	− 9.3	b	1.0
16589	1929 May 20	5752.977	.144	−26.5	a	0.5
16754	July 23	5816.790	.783	+27.4	a	1.0
16759	July 24	5817.831	.858	+ 4.5	a	0.5
17488	1930 June 4	6132.985	.770	+26.1	b	1.0
17511	June 8	6136.976	0.061	−20.5	a	1.5
FM Aquilae $19^h4^m32^s$, $+10°24'$; 8.3–8.9 vis.						
Max. = JD 2425882.80 + $6^d.107E$						
Elements and visual light-curve by Lause, *Acta Astronomica*, Ser. c, **1**, 145, 1930. The period is doubtful.						
γ 18900	1932 June 19	2426878.977	0.120	−19.1	b	1.0
19028	Aug. 20	6940.809	.245	−29.2	b	1.0
C 6148	Oct. 10	6991.735	0.584	−18.3	c	0.6

* All Julian days refer to G.M.T.

† The epoch is 1900 in all cases.

TABLE 1—*Continued*

Plate	Date	JD	Phase	Vel. Km/Sec	Disp.	Wt.
FM Aquilae—*Continued*						
γ 19564	1933 Apr. 2	2427165.004	0.956	+14.4	b	0.7
C 6275	July 14	7268.668	.931	− 1.9	b	0.7
6289	Aug. 29	7314.644	.459	−17.7	b	1.0
γ 20398	1934 May 21	7579.891	.893	+ 5.9	b	1.0
C 6437	June 19	7608.983	0.656	− 2.5	b	1.0
FN Aquilae $19^h7^m48^s$, $+3°23'$; 9.9–10.9 pg.						
Max. = JD 2425853.36 + 9^d480E						
Elements and photographic light-curve by Prager, *A.N.*, **243**, 360, 1931.						
γ 18914	1932 June 23	2426882.882	0.599	+30.0	b	1.0
C 6109	Aug. 23	6943.634	.008	+ 0.2	b	1.0
6114	Aug. 24	6944.632	.113	−14.1	b	1.0
γ 19116	Sept. 13	6964.659	.226	+ 4.6	b	1.0
19563	1933 Apr. 1	7164.962	.356	− 3.3	c	0.6
C 6244	May 14	7207.981	.893	+ 1.8	b	1.0
γ 20015	Nov. 2	7379.649	.002	+ 7.2	b	1.0
20774	1935 June 13	7967.910	.055	− 1.0	b	1.0
20777	June 14	7968.969	.166	− 7.9	b	1.0
20796	July 12	7996.924	.115	−21.8	c	0.4
20841	Oct. 20	8096.678	0.638	+18.2	c	0.6
PZ Aquilae $18^h50^m42^s$, $-3°1'$; 12.4–13.5 pg.						
Max. = JD 2426174.853 + $8^d75546E$						
Elements by Harwood, *Harvard Bull.*, No. 893, 24, 1933. No light-curve available.						
C 6444	1934 June 22	2427611.858	0.127	−38.6	c	0.4
6513	Aug. 23	7673.719	.192	44.6	c	.4
6694	1935 June 10	7964.892	.448	21.3	c	.4
6750	July 8	7992.816	.638	17.0	c	.6
6754	July 9	7993.769	.746	26.0	c	.6
6943	1936 July 30	8380.726	0.942	−49.5	c	0.6
V 336 Aquilae $18^h56^m11^s$, $-0°1'$; 9.4–10.4 vis.						
Max. = JD 2427600.31 + $7^d30765E$						
Elements from *A.N.*, **258**, 199, 1936. Visual light-curve by Beyer, *ibid.*, **258**, 276, 1936.						
γ 21004	1936 May 1	2428290.943	0.508	+27.7	c	0.6
C 6913	May 2	8291.950	.646	+28.8	c	.6
6920	May 27	8316.970	0.070	− 8.5	c	0.6

TABLE 1—*Continued*

	Plate	Date	JD	Phase	Vel. Km/Sec	Disp.	Wt.
		V 336 Aquilae—*Continued*					
γ	21012.....	1936 May 31	248320.985	0.619	+45.8	c	0.4
	21031.....	July 1	8351.757	.830	+ 1.3	c	.6
	21034.....	July 7	8357.771	.653	+41.6	c	.6
C	6930.....	July 11	8361.691	.190	− 3.2	c	.6
	6945.....	July 30	8380.905	0.819	+16.2	c	0.6

Y Aurigae $5^h21^m32^s$, $+42°21'$; 9.2–10.2 pg.

Max. = JD 2419866.903 + $3^d.859435E$

Elements and photographic light-curve by Robinson, *Harvard Ann.*, **90**, 46, 56, 1933.

C	4131.....	1926 Dec. 14	2424864.929	0.013	− 6.5	b	1.0
	4135.....	Dec. 15	4865.882	.260	+ 6.8	b	1.0
	4554.....	1927 Nov. 30	5215.874	.944	−12.7	b	0.3
	4642.....	1928 Jan. 10	5256.829	.556	+14.2	b	1.0
	4977.....	Sept. 23	5513.997	.189	− 0.8	b	1.0
	5336.....	1929 Oct. 12	5897.000	.427	+22.4	b	1.0
	5697.....	1931 Mar. 29	6430.667	.702	+21.8	b	1.0
	6146.....	1932 Oct. 9	6990.006	0.629	+32.5	b	0.7

RX Aurigae $4^h54^m28^s$, $+39°49'$; 7.8–8.8 pg.

Max. = JD 2419698.357 + $11^d.623331E$

Elements and photographic light-curve by Robinson, *Harvard Ann.*, **90**, 46, 58, 1933.

γ	6451.....	1917 Dec. 5	2421568.795	0.921	−27.4	a	1.5
	6514.....	Dec. 30	1593.938	.084	29.5	a	1.0
	6689.....	1918 Feb. 1	1626.689	.902	28.0	a	1.5
	6752.....	Mar. 21	1674.691	.032	30.4	a	1.0
	7622.....	Dec. 12	1940.946	.939	25.6	a	1.5
	7675.....	Dec. 19	1947.863	.534	18.0	a	0.5
	7767.....	1919 Jan. 14	1973.736	.760	19.5	a	1.0
	7796.....	Jan. 18	1977.757	.106	27.4	a	1.5
	14790.....	1927 Jan. 18	4899.679	.490	19.1	b	1.0
C	4976.....	1928 Sept. 23	5513.940	.337	23.4	b	1.0
γ	16259.....	Oct. 28	5548.951	.349	24.9	b	1.0
	17135.....	1929 Dec. 14	5960.853	.787	15.1	b	1.0
C	5381.....	1930 Jan. 8	5985.816	.934	32.1	b	1.0
	5396.....	Feb. 11	6019.676	.847	18.7	b	1.0
γ	17369.....	Apr. 8	6075.642	.662	5.6	b	0.7
	17374.....	Apr. 9	6076.633	.748	9.7	b	1.0
C	5433.....	Apr. 11	6078.633	0.920	−27.6	b	1.0

TABLE 1—*Continued*

Plate	Date	JD	Phase	Vel. Km/Sec	Disp.	Wt.

SY Aurigae $5^h5^m31^s$, $+42°42'$; 9.0–10.1 pg.

Max. = JD 2419172.082 + 10^d.144890 E

Elements and photographic light-curve by Robinson, *Harvard Ann.*, **90**, 46, 58, 1933.

4130.....	1926 Dec. 14	2424864.859	0.147	− 3.5	b	1.0
4150.....	Dec. 19	4869.918	.646	+12.6	b	1.0
4184.....	1927 Feb. 8	4920.785	.660	+ 5.7	b	0.3
4443.....	Oct. 5	5159.938	.234	− 1.8	b	0.3
4641.....	1928 Jan. 10	5256.738	.775	− 9.1	b	1.0
4687.....	Feb. 27	5304.633	.496	+ 8.0	b	1.0
5071.....	Nov. 21	5572.847	.935	−13.6	b	1.0
5076.....	Nov. 22	5573.972	0.046	−10.4	b	1.0

YZ Aurigae $5^h8^m27^s$, $+39°58'$; 10.2–11.4 pg.

Max. = JD 2420420.436 + 18^d.193225 E

Elements and photographic light-curve by Robinson, *Harvard Ann.*, **90**, 46, 59, 1933.

C 5081.....	1928 Nov. 25	2425576.979	0.432	−14.6	b	0.3
6136.....	1932 Sept. 13	6964.035	.672	+ 4.2	c	0.6
γ 19270.....	Nov. 10	7022.901	.908	−13.1	b	1.0
C 6602.....	1934 Dec. 15	7787.715	.946	−12.9	c	0.6
6625.....	1935 Feb. 11	7845.644	.130	−49.1	c	0.2
γ 20823.....	Oct. 9	8085.031	.288	−43.1	c	0.6
20859.....	Nov. 6	8113.953	0.878	−18.0	c	0.6

AN Aurigae $4^h52^m43^s$, $+40°41'$; 11.3–12.3 pg.

Max. = JD 2421633.59 + 10^d.2908 E

Elements by Oosterhoff, *Harvard Bull.*, No. 900, 10, 1935. Photographic light-curve by Parenago, *N.N.V.S.*, **4**, 151, 1933.

C 6165.....	1932 Nov. 7	2427019.910	0.411	+19.9	c	0.6
6199.....	1933 Jan. 5	7078.667	.121	− 8.7	c	.6
6326.....	Oct. 27	7373.962	.816	−34.4	c	.6
6562.....	1934 Oct. 19	7730.894	.500	+ 0.1	c	.6
6591.....	Dec. 14	7786.796	.933	−24.1	c	.6
6969.....	1936 Sept. 25	8437.955	0.212	− 4.4	c	0.6

TABLE 1—*Continued*

	Plate	Date	JD	Phase	Vel. Km/Sec	Disp.	Wt.
	AO Aurigae $5^h41^m14^s$, $+31°59'$; 10.9–12.6 pg.						
	Max. = JD 2427193.08 + 6^d.76300 E						
	Elements and photographic light-curve by Parenago, *N.N.V.S.*, **4**, 351, 1934.						
C	6604	1934 Dec. 15	2427787.868	0.947	− 7.9	c	0.4
	6615	Dec. 17	7789.804	.234	−23.6	c	.4
	6635	1935 Mar. 17	7879.799	.540	−15.1	c	.2
γ	20847	Oct. 21	8097.035	.662	− 2.1	c	.4
C	6835	1936 Feb. 2	8201.754	.146	−34.4	c	.4
γ	20971	Mar. 28	8256.741	.276	−25.8	c	.2
	21078	Oct. 8	8450.007	.853	+ 9.4	c	.6
	21080	Oct. 9	8451.017	0.003	−35.0	c	0.6
	RW Camelopardalis $3^h46^m11^s$, $+58°21'$; 9.0–9.9 pg.						
	Max. = JD 2420876.579 + 16^d.411760 E						
	Elements and photographic light-curve by Robinson, *Harvard Ann.*, **90**, 46, 58, 1933.						
C	881	1921 Feb. 18	2422739.674	0.522	−19.5	b	0.7
	4037	1926 Sept. 21	4780.956	.901	−25.4	b	0.7
	4053	Oct. 19	4808.915	.605	+10.6	b	1.0
	4149	Dec. 19	4869.828	.316	−52.1	b	1.0
	4558	1927 Dec. 2	5217.759	.516	−20.2	b	1.0
	5067	1928 Nov. 20	5571.917	.096	−49.0	b	1.0
γ	17102	1929 Nov. 20	5936.878	.334	−42.5	b	1.0
	17730	1930 Sept. 3	6223.008	.768	− 5.6	b	0.7
C	5625	Dec. 1	6312.007	.191	−49.7	b	1.0
	5651	Dec. 27	6338.847	.826	− 4.2	b	1.0
	5905	1931 Nov. 2	6648.924	.720	+ 8.0	b	0.7
	5941	1932 Jan. 16	6723.698	0.276	−34.4	b	0.7
	RX Camelopardalis $3^h56^m42^s$, $+58°23'$; 8.2–9.3 pg.						
	Max. = JD 2420359.763 + 7^d.911978 E						
	Elements and photographic light-curve by Robinson, *Harvard Ann.*, **90**, 46, 58, 1933. Plate C4556, although of good quality, has not been used in drawing the velocity-curve.						
C	3963	1926 Aug. 19	2424747.994	0.631	−10.6	b	1.0
	3985	Aug. 23	4751.008	.012	44.2	b	1.0
	4048	Oct. 18	4807.992	.214	47.1	b	1.0
	4054	Oct. 19	4808.966	.336	49.5	b	1.0
	4556	1927 Dec. 1	5216.870	.893	57.5	b	1.0
	4627	1928 Jan. 8	5254.739	.679	22.1	b	0.7
	4972	Sept. 4	5494.016	.922	30.2	b	1.0
γ	16258	Oct. 28	5548.906	0.859	−20.3	b	1.0

TABLE 1—*Continued*

Plate	Date	JD	Phase	Vel. Km/Sec	Disp.	Wt.
RX Camelopardalis—*Continued*						
C 5068	1928 Nov. 20	2425571.979	0.775	− 9.0	b	1.0
5131	1929 Feb. 26	5669.663	.122	42.9	b	1.0
5360	Dec. 9	5955.858	.294	56.5	b	1.0
5363	Dec. 10	5956.854	.420	50.9	b	1.0
5365	Dec. 11	5957.908	0.553	−31.2	b	1.0

RW Canis Majoris $7^h8^m47^s$, $-18°34'$; 10.6–11.4 vis.

Max. = JD 2425234.31 + 5^d.7292 E

Elements by Oosterhoff, *Harvard Bull.*, No. 900, 10, 1935. Visual light-curve by Florja, *N.N.V.S.*, **4**, No. 2, Tafel I, 1932.

C 6221	1933 Mar. 3	2427135.706	0.878	+77.6	c	0.2
6345	Nov. 25	7402.978	.529	54.2	c	.4
6581	1934 Nov. 14	7756.941	.311	36.0	c	.2
6593	Dec. 14	7786.936	.547	57.5	c	.2
γ 20838	1935 Oct. 20	8096.026	.497	48.5	c	.2
C 6828	Dec. 7	8144.934	.033	37.9	b	.7
γ 20939	1936 Mar. 3	8231.705	0.179	+25.4	c	0.6

RY Canis Majoris $7^h11^m56^s$, $-11°18'$; 7.6–8.6 vis.

Max. = JD 2426718.86 + 4^d.659 E

Elements and visual light-curve by Lause, *A.N.*, **246**, 297, 1932. 1.4 days have been added to the epoch given to reduce it to maximum.

γ 19400	1933 Jan. 3	2427076.826	0.823	+67.4	b	1.0
19565	Apr. 2	7165.637	.895	47.2	b	1.0
19998	Oct. 29	7375.984	.044	48.5	b	1.0
C 6381	1934 Mar. 20	7517.774	.478	34.5	c	0.6
γ 20677	Dec. 18	7790.906	.102	12.9	c	0.6
20685	1935 Jan. 15	7818.786	.086	22.4	b	1.0
20890	Dec. 8	8145.951	0.308	+20.4	c	0.6

SS Canis Majoris $7^h21^m58^s$, $-25°4'$; 9.9–10.7 vis.

Max. = JD 2424916.21 + 12^d.3661 E

Elements by Oosterhoff, *Harvard Bull.*, No. 900, 10, 1935. Visual light-curve by Florja, *N.N.V.S.*, **4**, No. 2, Tafel I, 1932.

γ 19425	1933 Jan. 7	2427080.852	0.046	+57.4	c	0.6
19560	Apr. 1	7164.684	.826	68.1	c	.2
20269	1934 Mar. 22	7519.663	.531	60.6	c	.2
C 6592	Dec. 14	7786.858	.138	44.0	c	.6
γ 20946	1936 Mar. 4	8232.684	0.191	+53.2	c	0.4

TABLE 1—*Continued*

Plate	Date	JD	Phase	Vel. Km/Sec	Disp.	Wt.
TV Canis Majoris $7^h4^m40^s$, $-13°37'$; 10.8–11.3 vis.						
Max. = JD 2426974.51 + $4^d.6693E$						
Elements by Florja, *Tashkent Circ.*, No. 15, 1933. No light-curve available. The period is uncertain.						
C 6205	1933 Feb. 4	2427108.705	0.740	+47.6	c	0.2
γ 20106	Dec. 27	7434.833	.585	51.0	b	.3
C 6396	1934 Apr. 20	7548.642	.959	13.3	c	.6
6611	Dec. 17	7789.009	.437	50.4	c	.2
γ 20863	1935 Nov. 8	8115.021	.257	46.8	c	.6
20896	1936 Jan. 6	8174.837	.068	33.5	c	.4
20947	Mar. 4	8232.726	0.466	+37.7	c	0.4
TW Canis Majoris $7^h17^m27^s$, $-14°7'$; 9.4–9.9 vis.						
Max. = JD 2426985.08 + $6^d.994E$						
Elements by Florja, *Tashkent Circ.*, No. 15, 1933. No light-curve available.						
γ 19424	1933 Jan. 7	2427080.781	0.683	+83.7	b	0.7
C 6404	1934 Apr. 22	7550.654	.866	61.7	c	.6
γ 20678	Dec. 18	7790.955	.224	64.5	c	.6
20686	1935 Jan. 15	7818.882	.217	60.4	c	.6
20745	Apr. 21	7914.646	.909	53.5	c	.6
20864	Nov. 8	8115.052	.563	83.5	c	.6
20935	1936 Mar. 2	8230.717	0.101	+45.8	c	0.6
RS Cassiopeiae $23^h32^m36^s$, $+61°52'$; 11.0–12.2 pg.						
Max. = JD 2419617.580 + $6^d.2955890E$						
Elements and photographic light-curve by Robinson, *Harvard Ann.*, **90**, 50, 57, 1933.						
C 4446	1927 Oct. 7	2425161.818	0.654	−15.4	b	0.3
4640	1928 Jan. 10	5256.646	.717	18.9	b	0.3
4969	Sept. 3	5493.830	.392	13.9	b	0.3
5338	1929 Oct. 14	5899.802	.877	13.1	b	1.0
5842	1931 Sept. 21	6606.882	.190	32.4	b	1.0
5849	Sept. 23	6608.738	.485	22.8	b	0.7
6084	1932 July 24	6913.914	.960	42.1	c	0.4
6111	Aug. 23	6943.880	.720	9.4	b	1.0
γ 19118	Sept. 13	6964.788	0.040	−47.6	b	1.0

TABLE 1—*Continued*

Plate	Date	JD	Phase	Vel. Km/Sec	Disp.	Wt.
RW Cassiopeiae $1^h30^m43^s$, $+57°15'$; 9.5–10.7 pg.						
Max. = JD 2419651.941 + $14^d800676E$						
Elements and photographic light-curve by Robinson, *Harvard Ann.*, **90**, 46, 58, 1933.						
C 4166.....	1927 Jan. 13	2424894.752	0.228	−83.3	b	1.0
4392.....	Sept. 4	5128.001	.987	66.7	b	1.0
4993.....	1928 Sept. 27	5517.917	.332	59.7	b	1.0
5359.....	1929 Dec. 9	5955.712	.911	68.4	b	0.7
5923.....	1931 Dec. 17	6693.833	.782	42.6	c	0.3
γ 19121.....	1932 Sept. 14	6965.008	.104	97.1	b	1.0
C 6183.....	1933 Jan. 3	7076.684	0.649	−50.2	b	1.0
RY Cassiopeiae $23^h47^m10^s$, $+58°11'$; 9.3–10.5 vis.						
Max. = JD 2424502.724 + $12^d13819E$						
Elements and visual light-curve by Brun, *Bull. de l'association française d'obs. d'étoiles var.*, **1**, 121, 1932.						
C 4458.....	1927 Oct. 9	2425163.882	0.469	−56.4	b	0.3
4468.....	Oct. 11	5165.792	.627	49.8	b	1.0
4626.....	1928 Jan. 8	5254.659	.948	88.0	b	1.0
4998.....	Sept. 28	5518.869	.715	54.7	b	0.7
5529.....	1930 Sept. 3	6223.927	.801	73.3	b	0.7
5531.....	Sept. 5	6225.988	.970	82.2	b	0.3
5555.....	Sept. 19	6239.933	.119	90.5	b	0.7
5567.....	Oct. 6	6256.792	.508	47.3	c	0.6
5588.....	Oct. 30	6280.861	0.491	−62.2	b	0.3
SW Cassiopeiae $23^h2^m54^s$, $+58°1'$; 9.6–10.3 pg.						
Max. = JD 2419403.033 + $5^d441022E$						
Elements and photographic light-curve by Robinson, *Harvard Ann.*, **90**, 50, 57, 1933.						
C 4523.....	1927 Nov. 4	2425189.742	0.533	−33.7	b	1.0
4964.....	1928 Sept. 2	5492.928	.256	36.1	b	1.0
4975.....	Sept. 23	5513.861	.101	47.2	b	0.3
5599.....	1930 Nov. 2	6283.642	.580	24.9	b	1.0
5898.....	1931 Oct. 31	6646.767	.318	27.2	b	1.0
V 92.....	Nov. 1	6647.694	.489	36.5	a	0.5
γ 18916.....	1932 June 23	6882.990	.734	26.8	b	1.0
19030.....	Aug. 20	6940.942	.384	49.5	b	1.0
C 6108.....	Aug. 23	6943.000	.763	26.0	b	1.0
γ 19187.....	Oct. 11	6992.740	.904	48.6	b	1.0
C 6169.....	Nov. 8	7020.674	0.038	−54.0	b	1.0

TABLE 1—*Continued*

	Plate	Date	JD	Phase	Vel. Km/Sec	Disp.	Wt.
	SY Cassiopeiae $0^h9^m51^s$, $+57°52'$; 9.3–10.1 pg.						
	Max. = JD 2419336.475 + $4^d.070978E$						
	Elements and photographic light-curve by Robinson, *Harvard Ann.*, **90**, 46, 56, 1933.						
C	4447	1927 Oct. 7	2425161.947	0.976	−57.6	b	1.0
	4514	Nov. 2	5187.828	.333	47.6	b	1.0
	4633	1928 Jan. 9	5255.673	.999	60.0	b	1.0
	5282	1929 Aug. 20	5844.957	.751	27.0	b	0.3
	5821	1931 Aug. 26	6580.955	.543	11.2	c	0.6
	6091	1932 July 25	6914.983	.594	23.7	b	0.7
	6314	1933 Sept. 30	7346.706	.643	21.1	c	0.6
	6938	1936 July 28	8378.993	0.215	−59.8	c	0.4
	SZ Cassiopeiae $2^h19^m55^s$, $+59°1'$; 10.6–11.0 pg.						
	Max. = JD 2420718.724 + $13^d.601666E$						
	Elements and photographic light-curve by Robinson, *Harvard Ann.*, **90**, 46, 58, 1933.						
C	4134	1926 Dec. 15	2424865.785	0.894	−49.9	b	1.0
	4403	1927 Sept. 5	5129.999	.319	40.3	b	0.3
	4462	Oct. 10	5164.830	.880	49.6	b	0.7
	4971	1928 Sept. 3	5493.972	.078	41.7	b	1.0
	5080	Nov. 25	5576.833	.160	43.6	b	1.0
	5326	1929 Sept. 18	5873.992	.017	35.6	b	0.3
	5530	1930 Sept. 4	6224.010	.751	39.8	b	0.7
γ	17939	Dec. 4	6315.662	.489	37.8	b	0.3
V	132	1932 Jan. 17	6724.677	.550	24.3	c	0.2
C	6107	Aug. 22	6942.934	.606	32.8	b	1.0
	6304	1933 Sept. 1	7317.000	.108	46.0	c	0.6
	6312	Sept. 29	7345.915	.234	56.0	c	0.6
	6325	Oct. 27	7373.889	0.290	−59.3	b	1.0
	UZ Cassiopeiae $1^h6^m18^s$, $+60°41'$; 11.4–12.1 pg.						
	Max. = JD 2422687.42 + $4^d.25968E$						
	Elements by Oosterhoff, *Harvard Bull.*, No. 900, 10, 1935. Photographic light-curve by Lehmann-Balanowsky, *Pulkowa Obs. Circ.*, No. 2, 21, 1932.						
C	6149	1932 Oct. 10	2426991.795	0.495	−45.2	c	0.6
γ	19268	Nov. 10	7022.727	.754	35.3	b	.7
C	6296	1933 Aug. 31	7316.000	.603	20.1	c	.4
	6316	Sept. 30	7346.812	.836	44.3	c	.4
	6331	Oct. 28	7374.764	.398	46.2	c	.6
	6357	Dec. 26	7433.722	.239	61.6	c	.6
	6508	1934 Aug. 22	7672.000	.177	59.5	c	.6
γ	20858	1935 Nov. 6	8113.899	0.917	−72.9	c	0.6

TABLE 1—*Continued*

Plate	Date	JD	Phase	Vel. Km/Sec	Disp.	Wt.
VV Cassiopeiae $1^h44^m17^s$, $+59°23'$; 10.5–11.5 pg.						
Max. = JD 2422514.159+6^d.207747E						
Elements and photographic light-curve by Robinson, *Harvard Ann.*, **90**, 46, 57, 1933.						
C 5669	1930 Dec. 30	2426341.740	0.581	−51.0	c	0.4
5817	1931 Aug. 25	6579.929	.951	41.1	c	.6
5822	Aug. 27	6581.006	.124	62.3	c	.4
γ 19189	1932 Oct. 11	6992.859	.469	48.9	b	.7
19905	1933 Oct. 1	7347.941	.669	47.4	c	.6
20845	1935 Oct. 20	8096.894	.317	62.1	c	.6
20888	Dec. 8	8145.733	.185	61.3	c	.4
C 6831	1936 Jan. 3	8171.625	0.356	−64.1	c	0.6
VW Cassiopeiae $0^h59^m35^s$, $+61°14'$; 10.5–11.7 pg.						
Max. = JD 2420751.32+5^d.99386E						
Elements by Oosterhoff, *Harvard Bull.*, No. 900, 10, 1935. Photographic light-curve by Lehmann-Balanowsky, *Pulkowa Obs. Circ.*, No. 2, 20, 1932.						
C 6100	1932 Aug. 21	2426941.985	0.834	−42.0	b	1.0
6125	Sept. 9	6960.969	.002	60.6	c	0.6
γ 19119	Sept. 13	6964.889	.656	40.7	b	0.7
C 6317	1933 Sept. 30	7346.892	.388	62.5	c	0.6
6332	Oct. 28	7374.867	.055	70.9	b	0.6
6790	1935 Aug. 9	8024.002	.355	74.7	c	0.6
γ 20822	Oct. 8	8084.970	.527	41.3	c	0.4
20945	1936 Mar. 4	8232.642	0.164	−86.0	c	0.4
XY Cassiopeiae $0^h44^m7^s$, $+59°34'$; 10.2–10.8 pg.						
Max. = JD 2419403.784+4^d.501880E						
Elements and photographic light-curve by Robinson, *Harvard Ann.*, **90**, 46, 57, 1933.						
C 4938	1928 Aug. 23	2425482.868	0.343	−26.8	b	0.7
5812	1931 Aug. 24	6578.938	.813	42.3	c	0.6
6130	1932 Sept. 11	6962.963	.116	52.6	b	1.0
γ 19196	Oct. 12	6993.819	.970	55.6	b	1.0
C 6157	Nov. 6	7018.748	.508	32.9	c	0.6
6315	1933 Sept. 30	7346.743	.365	42.3	c	0.6
6832	1936 Jan. 3	8171.743	0.622	−31.9	c	0.4

TABLE 1—*Continued*

Plate	Date	JD	Phase	Vel. Km/Sec	Disp.	Wt.
AP Cassiopeiae $0^h27^m36^s$, $+62°21'$; 12.0–13.1 pg.						
Max. = JD 2426289.53 + $6^d.8465E$						
Elements by Oosterhoff, *Harvard Bull.*, No. 900, 10, 1935. No light-curve available.						
C 6079	1932 July 23	2426912.954	0.057	−51.1	c	0.6
6106	Aug. 22	6942.855	.425	42.4	c	.6
6133	Sept. 12	6963.875	.495	42.2	c	.6
6310	1933 Sept. 28	7344.834	.138	52.7	c	.6
6535	1934 Sept. 17	7698.965	.862	45.3	c	.6
6620	1935 Jan. 12	7815.663	.907	43.9	c	.6
6786	Aug. 7	8022.976	.187	51.0	c	.6
6965	1936 Sept. 10	8422.986	0.613	−36.7	c	0.6
BY Cassiopeiae $1^h40^m15^s$, $+60°55'$; 11.1–11.5 pg.						
Max. = JD 2426933.30 + $3^d.241E$						
Elements by Lange, *Leningrad Univ. Astr. Obs. Bull.*, No. 2, 10, 1933. Lange's visual curve seems uncertain and has been omitted.						
C 6507	1934 Aug. 21	2427671.943	0.906	−67.3	c	0.6
6534	Sept. 17	7698.861	.211	49.2	c	.4
6544	Sept. 20	7701.783	.113	53.4	c	.4
γ 20824	1935 Oct. 9	8085.910	.634	33.5	c	.6
20919	1936 Feb. 4	8203.615	.952	62.4	c	.4
C 6845	Feb. 28	8227.646	0.366	−30.0	c	0.2
CG Cassiopeiae $23^h55^m54^s$, $+60°25'$; 12.2–13.3 pg.						
Max. = JD 2426945.11 + $4^d.363E$						
Elements and visual light-curve by Lange, *Leningrad Univ. Astr. Obs. Bull.*, No. 2, 9, 1933.						
C 6503	1934 Aug. 20	2427670.979	0.369	−88.1	c	0.6
6510	Aug. 22	7672.892	.808	67.6	c	.4
6561	Oct. 19	7730.819	.084	105.7	c	.6
6789	1935 Aug. 8	8023.951	.270	96.6	c	.6
γ 20820	Oct. 8	8084.844	.227	111.2	c	.6
20857	Nov. 6	8113.826	0.870	−67.3	c	0.4
46.1932 Cassiopeiae $23^h52^m13^s$, $+62°9'$; 10.5–11.5 pg.						
Max. = JD 2427346.96 + $9^d.79E$						
Period by Stuker, *A.N.*, **246**, 407, 1932. The epoch is arbitrarily chosen so as to make the phase of plate C 6318 zero. No light-curve is available.						
C 6139	1932 Sept. 21	2426972.751	0.776	−64.1	c	0.4
γ 19194	Oct. 12	6993.707	.917	71.0	b	1.0
C 6318	1933 Sept. 30	7346.963	0.000	−91.1	b	1.0

TABLE 1—*Continued*

Plate	Date	JD	Phase	Vel. Km/Sec	Disp.	Wt.
46.1932 Cassiopeiae—*Continued*						
C 6343	1933 Nov. 25	2427402.757	0.700	−65.0	b	1.0
6471	1934 July 23	7642.989	.238	72.2	c	0.6
6541	Sept. 19	7700.933	.156	82.2	b	1.0
γ 20605	Oct. 20	7731.740	.303	69.2	c	0.6
20843	1935 Oct. 20	8096.783	0.590	−57.1	c	0.6

δ Cephei $22^h25^m27^s$, $+57°54'$; 3.9–4.6 pg.

Max. = JD $2393659.873+5^d366396E-0^d84\times10^{-8}E^2$

Elements by Prager, *Kleinere Veröff. Berlin-Babelsberg*, No. 15, 138, 1936. The velocity-curve is plotted according to Prager's elements from Jacobsen's observations made with the three-prism spectrograph of the Lick Observatory, *Lick Obs. Bull.*, No. 12, 145, 1926. Photographic light-curve by Robinson, *Harvard Ann.*, **90**, 57, 1933. Observations of this well-known star were carried out as a test of the usefulness of low dispersion in determining radial velocity-curves of Cepheid variables.

γ 17100	1929 Nov. 20	2425936.681	0.672	− 5.1	b	1.0
C 5558	1930 Sept. 22	6242.754	.708	− 2.5	b	1.0
γ 17790	Oct. 5	6255.799	.139	−37.5	b	1.0
C 5566	Oct. 6	6256.729	.312	−16.1	b	1.0
5571	Oct. 7	6257.808	.513	−14.5	b	1.0
5586	Oct. 30	6280.700	.779	+ 5.3	b	0.7
5593	Nov. 1	6282.621	.137	−28.6	b	1.0
5616	Nov. 29	6310.708	.371	−15.6	b	1.0
5622	Nov. 30	6311.740	.564	−13.8	b	1.0
5627	Dec. 1	6312.607	.725	+ 0.4	b	1.0
5655	Dec. 28	6339.614	.758	+ 7.9	b	1.0
5663	Dec. 29	6340.610	.943	−22.7	b	1.0
5667	Dec. 30	6341.607	0.129	−27.9	b	1.0

SZ Cygni $20^h29^m38^s$, $+46°16'$; 9.7–11.0 pg.

Max. = JD $2426399.219+15^d111056E$

Elements by Florja and Parenago, *N.N.V.S.*, **4**, 320, 1934. Photographic light-curve by Henroteau, *Dom. Obs. Pub.*, **9**, 69, 1925.

C 2797	1924 May 20	2423926.971	0.395	− 8.6	b	0.4
3863	1926 June 25	4692.981	.087	34.6	b	0.4
γ 16782	1929 Aug. 13	5837.910	.854	1.3	b	0.4
17573	1930 July 10	6168.915	.759	3.8	b	0.4
17631	Aug. 8	6197.887	.676	15.2	b	0.7
C 5815	1931 Aug. 25	6579.747	.947	3.9	b	1.0
5820	Aug. 26	6580.888	.022	33.8	b	1.0
5897	Oct. 31	6646.667	0.375	−21.4	b	1.0

TABLE 1—*Continued*

	Plate	Date	JD	Phase	Vel. Km/Sec	Disp.	Wt.

TX Cygni $20^h56^m26^s$, $+42°12'$; 10.5–12.4 pg.

Max. = JD 2422290.941 + $14^d.70791\,E + 0^d.000000138E^2$

Elements by Florja and Parenago, *N.N.V.S.*, **4**, 323, 1934. Photographic light-curve by Koolikovsky, *ibid.*, **4**, 86, 1932.

C	4396	1927 Sept. 4	2425128.882	0.950	−30.3	b	1.0
	4444	Oct. 7	5161.649	.178	35.2	b	0.7
	4517	Nov. 3	5188.647	.013	36.4	b	1.0
	5328	1929 Sept. 20	5875.833	.734	8.7	b	0.3
	5513	1930 Aug. 11	6200.844	.830	6.0	b	0.7
	6341	1933 Nov. 25	7402.646	.537	5.5	b	0.7
	6929	1936 July 10	8360.934	0.676	− 1.4	c	0.2

VX Cygni $20^h53^m34^s$, $+39°48'$; 10.1–10.8 pg.

Max. = JD 2420369.820 + $20^d.132467\,E$

Elements and photographic light-curve by Robinson, *Harvard Ann.*, **90**, 50, 59, 1933.

C	4368	1927 July 16	2425078.949	0.907	− 8.7	b	0.3
	4936	1928 Aug. 5	5464.935	.080	−45.1	b	1.0
	6160	1932 Nov. 7	7019.632	.303	−42.2	c	0.6
	6266	1933 July 1	7255.972	.042	−40.1	c	0.6
γ	19718	July 4	7258.977	.191	−50.9	c	0.6
	19913	Oct. 3	7349.635	.694	+14.0	c	0.4
	20604	1934 Oct. 20	7731.653	.670	+ 7.8	c	0.6
	20636	Nov. 14	7756.670	.912	−14.8	b	1.0
	20793	1935 July 11	7995.917	.796	+ 4.1	c	0.6
	21005	1936 May 1	8290.993	0.453	−10.6	c	0.4

VY Cygni $21^h0^m27^s$, $+39°34'$; 10.1–11.3 pg.

Max. = JD 2423497.144 + $7^d.856956E$

Elements and photographic light-curve by Parenago, *N.N.V.S.*, **4**, 407, 1935.

C	4445	1927 Oct. 7	2425161.721	0.860	+ 4.1	b	1.0
	4513	Nov. 2	5187.698	.166	−20.8	b	1.0
	4990	1928 Sept. 27	5517.723	.171	−18.9	b	1.0
γ	17570	1930 July 9	6167.978	.932	−15.4	b	0.7
	17637	Aug. 9	6198.922	.871	− 2.0	b	0.7
C	5511	Aug. 10	6199.922	.998	−26.2	b	1.0
	5816	1931 Aug. 25	6579.840	.352	−14.3	b	1.0
	6051	1932 June 21	6880.962	.678	− 5.5	b	1.0
	6957	1936 Sept. 8	8420.644	.613	+ 9.5	c	0.6
	6961	Sept. 9	8421.826	0.764	+ 3.3	c	0.6

TABLE 1—*Continued*

	Plate	Date	JD	Phase	Vel. Km/Sec	Disp.	Wt.
	VZ Cygni $21^h47^m41^s$, $+42°40'$; 9.0–9.9 pg.						
	Max. = JD 2420642.129 + 4^d.864691 E						
	Elements and photographic light-curve by Robinson, *Harvard Ann.*, **90**, 50, 57, 1933.						
C	1760	1922 July 2	2423238.890	0.798	− 6.1	a	0.5
	3372	1925 July 4	4336.934	.515	−10.9	b	1.0
	4388	1927 Sept. 3	5127.744	.076	−32.8	b	1.0
	5233	1929 June 24	5787.971	.794	+ 1.4	b	1.0
γ	16699	July 13	5806.938	.693	− 2.1	b	1.0
	16704	July 14	5807.946	.900	−23.8	b	1.0
C	5321	Sept. 16	5871.796	0.026	−26.5	b	1.0
	BZ Cygni $20^h42^m34^s$, $+44°56'$; 11.2–12.0 pg.						
	Max. = JD 2426674.10 + 10^d.1416 E						
	Elements by Beyer and photographic light-curve by Plaut, *A.N.*, **252**, 99, 1934.						
C	6506	1934 Aug. 21	2427671.821	0.379	−17.3	c	0.6
	6537	Sept. 18	7699.819	.140	−32.7	c	.6
	6601	Dec. 15	7787.663	.802	−10.9	c	.4
	6762	1935 July 10	7994.990	.245	−31.8	c	.4
	6785	Aug. 7	8022.899	.997	−48.1	c	.6
γ	21052	1936 Aug. 2	8383.875	.590	+ 3.6	c	.6
C	6968	Sept. 25	8437.833	0.911	−19.5	c	0.6
	CD Cygni $20^h0^m37^s$, $+33°50'$; 9.0–10.5 pg.						
	Max. = JD 2421501.035 + 17^d.071343 E						
	Elements and photographic light-curve by Robinson, *Harvard Ann.*, **90**, 49, 58, 1933.						
C	3951	1926 Aug. 16	2424744.874	0.017	−22.7	b	1.0
	4039	Sept. 25	4784.727	.351	−24.4	b	0.3
	4401	1927 Sept. 5	5129.844	.567	− 6.7	b	0.7
	4857	1928 June 25	5423.941	.795	+22.4	b	0.3
	4989	Sept. 27	5517.649	.284	−23.8	b	1.0
	5258	1929 July 24	5817.849	.869	+ 4.0	b	1.0
	5492	1930 July 7	6165.974	.261	−25.6	b	1.0
γ	17728	Sept. 2	6222.826	.592	+ 3.7	b	0.7
C	5528	Sept. 3	6223.819	.650	+ 8.1	b	0.7
	5590	Oct. 31	6281.651	.037	−31.6	b	1.0
	5790	1931 July 8	6531.969	.700	+24.2	b	1.0
V	67	Oct. 25	6640.700	0.070	−47.0	b	0.7

TABLE 1—*Continued*

Plate	Date	JD	Phase	Vel. Km/Sec	Disp.	Wt.
MW Cygni $20^h8^m27^s$, $+32°35'$; 10–11 pg.						
Max. = JD 2425173.40 + $5^d.9550E$						
Elements by Oosterhoff, *Harvard Bull.*, No. 900, 10, 1935. No light-curve in magnitudes available.						
C 6265	1933 July 1	2427255.903	0.707	− 5.1	c	0.4
γ 19713	July 3	7257.920	.045	−16.9	b	1.0
C 6282	July 31	7285.938	.750	− 0.4	b	0.3
6293	Aug. 30	7315.635	.737	+ 2.7	c	0.6
γ 19914	Oct. 3	7349.735	.463	− 6.1	b	0.7
C 6466	1934 July 21	7640.870	.353	−23.9	c	0.4
6475	July 24	7643.910	.863	−12.7	b	1.0
γ 20887	1935 Dec. 8	8145.630	0.115	−25.8	c	0.2
MZ Cygni $21^h17^m53^s$, $+37°2'$; 10.8–12.2 vis.						
Max. = JD 2427642.12 + $21^d.1655E$						
Elements and visual light-curve by Beyer, *A.N.*, **258**, 285, 1936.						
C 6252	1933 May 31	2427224.979	0.291	−70.1	c	0.4
6301	Aug. 31	7316.861	.632	43.4	c	.2
γ 19908	Oct. 2	7348.765	.140	66.5	c	.6
C 6323	Oct. 27	7373.754	.320	82.3	c	.6
γ 20834	1935 Oct. 19	8095.738	.432	64.0	c	.6
20856	Nov. 6	8113.739	.282	83.8	c	.4
C 6825	Dec. 7	8144.691	.745	24.3	c	.2
γ 21033	1936 July 1	8351.847	.532	47.8	c	.2
C 6937	July 28	8378.887	.810	24.3	c	.2
6978	Oct. 24	8466.772	0.962	−44.3	c	0.6
RZ Geminorum $5^h56^m35^s$, $+22°14'$; 10.0–11.1 pg.						
Max. = JD 2420409.203 + $5^d.530209E$						
Elements and photographic light-curve by Robinson, *Harvard Ann.*, **90**, 46, 57, 1933.						
C 4448	1927 Oct. 8	2425162.017	0.428	+13.3	b	0.7
4515	Nov. 2	5187.948	.116	−11.7	b	0.7
5620	1930 Nov. 30	6311.029	.198	+ 4.3	b	1.0
5942	1932 Jan. 16	6723.819	.840	+11.0	b	0.7
6621	1935 Feb. 10	7844.701	.524	+ 7.8	c	0.4
γ 20837	Oct. 19	8095.977	.961	− 6.4	c	0.6
20851	Nov. 5	8112.892	.020	+ 0.2	c	0.6
20905	1936 Jan. 9	8177.737	0.745	+ 9.8	c	0.4

TABLE 1—*Continued*

Plate	Date	JD	Phase	Vel. Km/Sec	Disp.	Wt.
AA Geminorum $6^h0^m21^s$, $+26°20'$; 10.2–11.0 pg.						
Max. = JD 2420726.34 + $11^d30111E$						
Elements and photographic light-curve by Kukarkin, *N.N.V.S.*, **3**, 29, 1930.						
C 6174.....	1932 Nov. 8	2427020.988	0.994	+ 8.4	c	0.6
γ 19276.....	Nov. 11	7023.860	.248	+ 6.5	b	1.0
C 6363.....	1934 Jan. 23	7461.632	.985	− 0.7	c	0.4
6628.....	1935 Mar. 16	7878.765	.896	− 1.7	c	0.6
γ 20852.....	Nov. 5	8112.934	.617	+20.2	c	0.6
20926.....	1936 Feb. 5	8204.752	.741	+22.0	c	0.6
20940.....	Mar. 3	8231.774	0.132	− 7.4	c	0.6
AD Geminorum $6^h37^m9^s$, $+21°3'$; 9.5–10.3 pg.						
Max. = JD 2420410.450 + $3^d787928E$						
Elements and photographic light-curve by Kukarkin, *N.N.V.S.*, **3**, 29, 1930.						
γ 19200.....	1932 Oct. 13	2426994.029	0.042	− 1.2	b	1.0
C 6200.....	1933 Jan. 5	7078.712	.398	+35.5	c	0.4
γ 19572.....	Apr. 3	7166.712	.630	+68.8	b	0.3
C 6361.....	1934 Jan. 22	7460.920	.300	+38.0	b	1.0
6364.....	Jan. 23	7461.674	.499	+46.2	c	0.6
γ 20607.....	Oct. 20	7731.913	.841	+50.8	c	0.6
C 6614.....	Dec. 17	7789.740	.107	+ 3.5	c	0.6
γ 20684.....	1935 Jan. 15	7818.688	0.749	+51.2	c	0.6
AP Herculis $18^h45^m57^s$, $+15°49'$; 10.5–11.2 vis.						
Max. = JD 2425394.94 + 10^d422E						
Elements and visual light-curve by Beyer, *A.N.*, **252**, 176, 1934; **226**, 324, 1926.						
C 5811.....	1931 Aug. 24	2426578.736	0.586	−29.8	c	0.4
6116.....	1932 Aug. 24	6944.792	.710	19.0	c	.4
6145.....	Oct. 8	6989.649	.014	19.1	c	.6
6239.....	1933 Apr. 5	7168.955	.218	41.7	c	.6
6246.....	May 15	7208.844	.046	24.8	c	.6
6383.....	1934 Mar. 21	7518.000	.709	32.9	c	.6
6440.....	June 21	7610.708	.605	24.9	c	.4
6952.....	1936 Aug. 28	8409.781	.277	54.5	c	.6
γ 21073.....	Oct. 7	8449.635	.101	22.9	c	.4
21082.....	Nov. 5	8478.642	0.884	−11.9	c	0.6

TABLE 1—*Continued*

	Plate	Date	JD	Phase	Vel. Km/Sec	Disp.	Wt.
	BB Herculis $18^h41^m16^s$, $+12°14'$; 9.6–10.6 pg.						
	Max. = JD 2426244.300 + $7^d.50712E$						
	Elements and photographic light-curve by Parenago, *N.N.V.S.*, **4**, 307, 1934.						
γ	19117	1932 Sept. 13	2426964.726	0.966	+ 82.4	b	1.0
	19186	Oct. 11	6992.684	.690	99.8	b	0.3
	19193	Oct. 12	6993.660	.820	99.2	b	0.3
C	6248	1933 May 15	7208.979	.502	92.5	b	1.0
	6263	July 1	7255.670	.721	104.7	c	0.6
γ	19716	July 4	7258.759	.133	83.8	b	1.0
	19838	Sept. 2	7318.781	.128	81.3	b	1.0
	19903	Oct. 1	7347.727	0.984	+81.9	b	1.0
	BL Herculis $17^h56^m38^s$, $+19°16'$; 10.1–11.1 pg.						
	Max. = JD 2426503.16 + $4^d.20345E$						
	Elements and photographic light-curve by Parenago, *N.N.V.S.*, **4**, 309, 1934. Both light- and velocity-curves are peculiar.						
C	6049	1932 June 21	2426880.830	0.848	+21.5	c	0.4
	6127	Sept. 11	6962.674	.318	5.6	b	1.0
γ	19185	Oct. 11	6992.627	.444	5.5	b	0.7
	19192	Oct. 12	6993.617	.680	25.5	b	1.0
	19526	1933 Mar. 6	7138.010	.031	14.3	b	1.0
	19570	Apr. 2	7165.993	.688	35.6	b	0.7
C	6260	June 30	7254.706	.793	16.9	b	1.0
	6267	July 2	7256.663	.258	11.5	c	0.2
	6433	1934 May 24	7582.812	.849	19.1	b	0.3
	6438	June 20	7609.694	.244	8.7	b	0.7
	6463	July 21	7640.684	.617	26.6	c	0.4
γ	20744	1935 Apr. 21	7914.001	.639	28.5	c	0.4
C	6697	June 11	7965.708	.964	14.3	b	1.0
	6844	1936 Feb. 28	8227.031	.109	8.6	b	1.0
γ	20951	Mar. 4	8232.972	.522	19.1	c	0.4
C	6914	May 2	8291.994	0.563	+14.6	b	0.7
	V Lacertae $22^h44^m33^s$, $+55°48'$; 8.7–9.9 pg.						
	Max. = JD 2418031.919 + $4^d.983443E$						
	Elements and photographic light-curve by Robinson, *Harvard Ann.*, **90**, 50, 57, 1933.						
C	4128	1926 Dec. 14	2424864.672	0.091	−22.7	b	1.0
	4499	1927 Oct. 28	5182.722	.912	+ 1.3	b	1.0
	4980	1928 Sept. 24	5514.778	0.544	−22.8	b	1.0

TABLE 1—*Continued*

Plate	Date	JD	Phase	Vel. Km/Sec	Disp.	Wt.
V Lacertae—*Continued*						
C 4997	1928 Sept. 28	2425518.798	0.351	−24.0	b	1.0
γ 16257	Oct. 28	5548.799	.371	−31.9	b	1.0
C 5255	1929 July 23	5816.931	.175	−45.6	b	1.0
5287	Aug. 21	5845.997	.008	−17.1	b	1.0
γ 17636	1930 Aug. 9	6198.817	.806	− 5.2	b	1.0
C 5514	Aug. 11	6200.972	0.240	−36.4	b	1.0

X Lacertae $22^h44^m58^s$, $+55°54'$; 8.8–9.4 pg.

Max. = JD 2418890.652 + 5^d.443996E

Elements and photographic light-curve by Robinson, *Harvard Ann.*, **90**, 50, 57, 1933.

C 3946	1926 Aug. 15	2424743.954	0.185	−37.5	b	1.0
4036	Sept. 21	4780.872	.966	30.7	b	1.0
4040	Sept. 25	4784.813	.690	16.8	b	1.0
4051	Oct. 19	4808.767	.090	42.6	b	1.0
4133	Dec. 15	4865.699	.548	17.6	b	1.0
4147	Dec. 19	4869.660	.276	30.6	b	1.0
4372	1927 July 17	5079.977	.908	30.2	b	1.0
4553	Nov. 30	5215.778	.853	16.2	b	0.3
4555	Dec. 1	5216.750	.032	32.5	b	1.0
4562	Dec. 5	5220.654	0.749	−16.7	b	1.0

Y Lacertae $22^h5^m13^s$, $+50°33'$; 8.3–8.8 pg.

Max. = JD 2418424.295 + 4^d.323844E

Elements and photographic light-curve by Robinson, *Harvard Ann.*, **90**, 50, 56, 1933.

C 4390	1927 Sept. 3	2425127.876	0.375	−22.3	b	1.0
4397	Sept. 4	5128.978	.630	−10.1	b	1.0
4925	1928 July 29	5457.882	.698	+ 5.3	b	1.0
5278	1929 Aug. 19	5843.840	.960	−20.8	b	1.0
5361	Dec. 10	5956.660	.053	−37.4	b	1.0
γ 17638	1930 Aug. 9	6198.994	.099	−29.1	b	1.0
C 5559	Sept. 22	6242.788	.227	−30.0	c	0.6
5587	Oct. 30	6280.750	.007	−50.0	b	1.0
γ 17935	Dec. 3	6314.690	.856	−11.8	b	1.0
C 6050	1932 June 21	6880.885	0.804	− 4.6	b	1.0

TABLE 1—*Continued*

Plate	Date	JD	Phase	Vel. Km/Sec	Disp.	Wt.
Z Lacertae $22^h36^m55^s$, $+56°18'$; 8.4–9.8 pg.						
Max. = JD 2418475.781 + $10^d.8855569E$						
Elements and photographic light-curve by Robinson, *Harvard Ann.*, **90**, 50, 58, 1933.						
C 1220	1921 Aug. 16	2422918.874	0.163	−38.7	a	1.5
1274	Sept. 8	2941.762	.266	−40.0	b	1.0
1297	Sept. 12	2945.925	.649	− 2.8	a	1.0
3513	1925 Sept. 23	4417.726	.855	−22.9	b	1.0
4052	1926 Oct. 19	4808.835	.784	−13.2	b	1.0
4508	1927 Oct. 29	5183.768	.228	−33.7	b	1.0
4926	1928 July 29	5457.939	.414	−19.7	b	1.0
5229	1929 June 23	5786.964	.640	− 9.9	b	1.0
γ 16828	Aug. 19	5843.988	.878	−35.0	b	1.0
C 5285	Aug. 21	5845.868	.051	−43.5	b	1.0
5324	Sept. 18	5873.754	0.613	+ 4.8	b	1.0
RR Lacertae $22^h37^m28^s$, $+55°55'$; 8.7–9.9 pg.						
Max. = JD 2419434.331 + $6^d.416234E$						
Elements and photographic light-curve by Robinson, *Harvard Ann.*, **90**, 50, 57, 1933.						
C 3952	1926 Aug. 16	2424744.956	0.686	−16.4	b	1.0
4132	Dec. 15	4865.635	.494	32.6	b	0.7
4992	1928 Sept. 27	5517.840	.143	41.3	b	1.0
5286	1929 Aug. 21	5845.934	.278	38.6	b	1.0
γ 17723	1930 Sept. 1	6221.900	.874	33.6	b	1.0
C 5628	Dec. 1	6312.635	.016	51.1	b	1.0
γ 18025	Dec. 31	6342.673	.697	28.1	b	0.7
C 5807	1931 Aug. 2	6556.906	.086	47.6	b	1.0
5924	Dec. 19	6695.667	.713	21.0	b	1.0
6056	1932 June 22	6881.983	0.751	−22.3	b	1.0
BG Lacertae $21^h56^m21^s$, $+42°58'$; 8.9–9.6 pg.						
Max. = JD 2420455.051 + $5^d.331847E$						
Elements and photographic light-curve by Robinson, *Harvard Ann.*, **90**, 50, 57, 1933.						
γ 18915	1932 June 23	2426882.944	0.566	−16.0	b	1.0
19029	Aug. 20	6940.861	.428	17.6	b	1.0
C 6117	Aug. 24	6944.826	.172	18.2	b	1.0
6129	Sept. 11	6962.861	.554	5.3	b	0.7
6278	1933 July 14	7268.972	.966	32.3	b	1.0
6287	Aug. 1	7286.941	.336	14.0	b	1.0
6476	1934 July 24	7643.956	.295	34.4	b	1.0
γ 20775	1935 June 13	7967.962	.064	36.0	b	1.0
C 6756	July 9	7993.941	0.936	−25.4	b	1.0

TABLE 1—*Continued*

	Plate	Date	JD	Phase	Vel. Km/Sec	Disp.	Wt.
	RX Librae $15^h36^m12^s$, $-20°27'$; 11.6–13.5 pg.						
	Max. = JD 2425001.0 + $24^d.950E$						
	Elements and photographic light-curve by Parenago, *N.N.V.S.*, **3**, 106, 1931.						
C	6022	1932 May 15	2426843.833	0.861	−54.1	c	0.2
	6235	1933 Apr. 4	7167.955	.852	44.1	c	.4
	6254	June 1	7225.822	.171	53.3	c	.4
	6394	1934 Apr. 19	7547.823	.077	57.7	c	.4
	6418	May 20	7578.778	.318	73.8	c	.4
	6758	1935 July 10	7994.675	0.987	−44.7	c	0.6
	SV Monocerotis $6^h16^m4^s$, $+6°31'$; 8.6–10.2 pg.						
	Max. = JD 2419041.805 + $15^d.230721E$						
	Elements and photographic light-curve by Robinson, *Harvard Ann.*, **90**, 46, 58, 1933.						
C	4136	1926 Dec. 15	2424865.935	0.393	+15.3	b	1.0
	4163	1927 Jan. 12	4893.870	.228	+13.1	b	1.0
	4172	Jan. 16	4897.873	.490	+25.3	b	1.0
	4638	1928 Jan. 9	5255.910	.998	+15.7	b	1.0
	5069	Nov. 21	5572.042	.754	+53.7	b	0.7
	5073	Nov. 22	5573.026	.819	+60.0	b	1.0
γ	16492	1929 Mar. 27	5698.677	.069	− 2.1	b	1.0
C	5405	1930 Mar. 10	6046.681	.918	+28.5	b	0.7
γ	18060	1931 Feb. 25	6398.767	.034	+19.7	b	1.0
C	5852	Sept. 24	6609.010	0.838	+59.4	b	1.0
	TX Monocerotis $6^h45^m48^s$, $-1°19'$; 11.1–12.0 pg.						
	Max. = JD 2423542.51 + $8^d.7019E$						
	Elements by Oosterhoff, *Harvard Bull.*, No. 900, 11, 1935. Photographic light-curve from a letter by Miss H. H. Swope, of the Harvard College Observatory.						
C	6175	1932 Nov. 9	2427021.016	0.741	+47.2	c	0.6
	6194	1933 Jan. 4	7077.910	.279	55.0	c	.4
	6384	1934 Mar. 21	7518.664	.929	42.7	c	.4
γ	20608	Oct. 21	7732.004	.446	68.3	c	.6
C	6616	Dec. 17	7789.885	.097	36.0	c	.4
γ	20903	1936 Jan. 8	8176.817	.563	56.7	c	.2
	20921	Feb. 4	8203.754	0.658	+68.7	c	0.2

TABLE 1—*Continued*

	Plate	Date	JD	Phase	Vel. Km/Sec	Disp.	Wt.
	WW Monocerotis $6^h28^m9^s$, $+9°17'$; 12.8–14.4 pg.						
	Max. = JD 2425298.17 + 4^d.66231 E						
	Elements and photographic light-curve by Parenago, *N.N.V.S.*, **4**, 152, 1933.						
C	6184	1933 Jan. 3	2427076.831	0.498	+64.5	c	0.4
	6380	1934 Mar. 20	7517.688	.055	23.6	c	.2
	6563	Oct. 19	7730.997	.807	80.2	c	.4
	6824	1935 Dec. 5	8142.976	0.171	+38.1	c	0.4
	AC Monocerotis $6^h56^m13^s$, $-8°34'$; 9.4–10.1 vis.						
	Max. = JD 2426687.6 + 8^d.0167 E						
	Elements and visual light-curve by Lause, *A.N.*, **251**, 43, 1934.						
γ	19271	1932 Nov. 10	2427022.969	0.834	+52.5	b	0.7
C	6191	1933 Jan. 4	7077.795	.673	58.8	c	.6
γ	20139	1934 Jan. 7	7445.833	.582	64.6	c	.6
C	6583	Nov. 15	7757.028	.400	47.1	c	.6
γ	20676	Dec. 18	7790.802	.613	72.5	c	.6
	20711	1935 Mar. 19	7881.641	.944	22.7	c	.6
	20746	Apr. 21	7914.684	0.066	+ 9.6	c	0.4
	BF Ophiuchi $16^h59^m54^s$, $-26°27'$; 7.8–8.6 pg.						
	Max. = JD 2420418.868 + 4^d.0680116 E						
	Elements and photographic light-curve by Robinson, *Harvard Ann.*, **90**, 48, 56, 1933.						
C	4776	1928 Apr. 28	2425365.971	0.098	−42.2	b	1.0
	4922	July 29	5457.681	.643	11.5	b	1.0
γ	16572	1929 May 16	5748.850	.218	44.6	b	0.7
C	5253	July 23	5816.674	.890	49.7	b	1.0
γ	17426	1930 May 7	6104.929	.750	23.4	b	1.0
	17485	June 4	6132.842	.611	20.9	b	1.0
C	5473	June 10	6138.892	.098	47.7	b	1.0
	5485	July 6	6164.688	.439	14.8	b	0.7
	5525	Sept. 3	6223.646	0.932	−54.6	b	1.0
	BH Ophiuchi $18^h11^m10^s$, $+12°4'$; 11.1–12.9 vis.						
	Max. = JD 2424385.54 + 11^d.0509 E						
	Elements by Oosterhoff, *Harvard Bull.*, No. 900, 11, 1935. No light-curve available.						
C	6055	1932 June 22	2426881.870	0.894	+53.0	c	0.4
	6103	Aug. 22	6942.704	.399	28.8	c	.6
	6147	Oct. 10	6991.670	.830	59.6	c	.2
	6290	1933 Aug. 29	7314.720	0.063	+19.1	c	0.6

TABLE 1—*Continued*

Plate	Date	JD	Phase	Vel. Km/Sec	Disp.	Wt.
BH Ophiuchi—*Continued*						
C 6685	1935 May 23	2427946.990	0.277	+ 4.3	c	0.2
6759	July 10	7994.750	.599	38.0	c	.6
6899	1936 Apr. 12	8271.990	.686	47.2	c	.6
6918	May 27	8316.828	.744	61.6	c	.2
6949	Aug. 27	8408.764	0.063	+21.1	c	0.4
RS Orionis $6^h16^m31^s$, $+14°44'$; 8.6–9.8 pg.						
Max. = JD 2419045.912 + 7^d.566646 E						
Elements and photographic light-curve by Robinson, *Harvard Ann.*, **90**, 46, 57, 1933.						
C 2531	1923 Nov. 18	2423742.031	0.634	+60.8	b	1.0
2559	Nov. 25	3749.981	.685	63.1	b	1.0
2664	1924 Feb. 11	3827.816	.971	19.8	b	0.7
2713	Mar. 13	3858.701	.053	31.8	b	0.7
2737	Apr. 12	3888.632	.009	23.7	b	1.0
4694	1928 Feb. 28	5305.694	.286	26.5	b	1.0
γ 16260	Oct. 29	5549.014	.443	44.6	b	1.0
C 5397	1930 Feb. 11	6019.715	.650	57.3	b	0.7
γ 17329	Mar. 12	6048.691	.480	48.3	b	1.0
17860	Nov. 4	6285.984	.840	43.3	b	1.0
C 5618	Nov. 29	6310.890	.132	25.0	b	1.0
γ 17942	Dec. 4	6315.925	.797	78.6	b	1.0
18058	1931 Feb. 25	6398.655	0.731	+57.7	b	1.0
CR Orionis $6^h0^m7^s$, $+13°14'$; 12.4–13.1 pg.						
Max. = JD 2425234.1 + 4^d.9143 E						
Elements and photographic light-curve by Hoffmeister, *A.N.*, **238**, 19, 1930.						
C 6166	1932 Nov. 7	2427019.972	0.403	+34.5	c	0.4
6359	1934 Jan. 22	7460.787	.104	28.8	c	.6
6609	Dec. 16	7788.854	.861	56.9	c	.4
6821	1935 Dec. 4	8141.962	.714	50.2	c	.4
6897	1936 Apr. 12	8271.669	0.108	+17.4	c	0.2
CS Orionis $6^h1^m51^s$, $+11°9'$; 11.1–12.0 pg.						
Max. = JD 2422715.94 + 3^d.88946 E						
Elements by Oosterhoff, *Harvard Bull.*, No. 900, 11, 1933. Photographic light-curve by Hoffmeister, *A.N.*, **238**, 20, 1930.						
C 6151	1932 Oct. 10	2426991.983	0.392	+ 2.0	c	0.4
6542	1934 Sept. 20	7701.007	.686	+34.6	c	.4
6546	Sept. 21	7702.000	0.941	+19.5	c	0.4

TABLE 1—*Continued*

Plate	Date	JD	Phase	Vel. Km/Sec	Disp.	Wt.
CS Orionis—*Continued*						
γ 20854	1935 Nov. 6	2428113.033	0.620	+24.1	c	0.4
20866	Nov. 8	8115.915	.361	+ 6.2	c	.6
20902	1936 Jan. 8	8176.712	.992	+12.1	c	.6
20928	Feb. 5	8204.872	.232	+ 8.0	c	.4
C 6893	Apr. 11	8270.736	0.166	− 8.0	c	0.2
SV Persei $4^h42^m46^s$, $+42°7'$; 8.8–9.7 pg.						
Max. = JD 2419611.424 + $11^d128428E$						
Elements and photographic light-curve by Robinson, *Harvard Ann.*, **90**, 46, 58, 1933.						
C 1914	1922 Oct. 1	2423329.959	0.147	−23.3	b	1.0
2580	1923 Dec. 17	3771.896	.860	− 1.2	b	1.0
2622	1924 Jan. 16	3801.792	.546	− 8.5	b	0.7
4055	1926 Oct. 20	4809.007	.054	−20.0	b	1.0
4097	Nov. 14	4834.840	.376	−15.8	b	0.7
4628	1928 Jan. 8	5254.794	.113	−27.2	b	1.0
4693	Feb. 28	5305.643	.682	+ 7.3	b	0.7
5000	Sept. 29	5519.012	.856	− 1.3	b	1.0
5075	Nov. 22	5573.911	.789	+ 8.6	b	1.0
5802	1931 July 31	6554.981	.948	+ 1.9	b	1.0
5805	Aug. 1	6555.979	.037	−12.8	b	1.0
5847	Sept. 22	6607.984	0.710	− 0.6	b	1.0
SX Persei $4^h10^m12^s$, $+41°29'$; 10.9–11.8 vis.						
Max. = JD 2421642.28 + $4^d29007E$						
Elements by Oosterhoff, *Harvard Bull.*, No. 900, 11, 1935. Visual light-curve by Nijland, *Recherches astr. de l'Observatoire d'Utrecht*, **8**, 211, 1923.						
C 5632	1930 Dec. 1	2426312.953	0.717	+10.4	b	0.7
5635	Dec. 2	6313.872	.931	− 0.4	c	.6
6190	1933 Jan. 4	7077.713	.980	−25.1	c	.6
6558	1934 Oct. 18	7729.934	.010	−17.8	c	.4
γ 20920	1936 Feb. 4	8203.677	.438	+21.6	c	.6
21077	Oct. 7	8449.883	0.828	− 9.8	c	0.6
UX Persei $2^h6^m6^s$, $+57°38'$; 11.3–12.4 vis.						
Max. = JD 2425910.82 + $4^d56590E$						
Elements by Oosterhoff, *Harvard Bull.*, No. 900, 11, 1935. Visual light-curve by Kukarkin, *N.N.V.S.*, **4**, 14, 1932.						
C 4662	1928 Jan. 31	2425277.694	0.336	−51.4	b	0.3
5851	1931 Sept. 23	6608.917	.894	30.4	c	.6
6126	1932 Sept. 10	6961.018	0.009	−32.7	c	0.6

TABLE 1—*Continued*

	Plate	Date	JD	Phase	Vel. Km/Sec	Disp.	Wt.
		UX Persei—*Continued*					
C	6143.....	1932 Sept. 21	2426972.991	0.631	−24.2	c	0.6
	6158.....	Nov. 6	7018.856	.676	42.4	c	.4
	6164.....	Nov. 7	7019.845	.893	21.1	c	.6
	6171.....	Nov. 8	7020.771	0.096	−64.1	c	0.6

UY Persei $2^h27^m0^s$, $+58°26'$; 11.1–12.1 vis.

Max. = JD 2423523.073 + 5^d.365069E

Elements and visual light-curve by Kukarkin, *N.N.V.S.*, **4**, 16, 1932.

C	5339.....	1929 Oct. 14	2425899.976	0.033	−73.3	b	0.3
	5670.....	1930 Dec. 30	6341.852	.395	50.4	c	.4
	6119.....	1932 Aug. 24	6944.917	.800	57.5	c	.4
	6313.....	1933 Sept. 29	7345.974	.554	55.7	c	.2
	6608.....	1934 Dec. 16	7788.722	.078	68.7	c	.4
	6979.....	1936 Oct. 24	8466.878	0.480	−53.2	c	0.2

VX Persei $2^h0^m50^s$, $+57°58'$; 9.5–10.4 pg.

Max. = JD 2420438.985 + 10^d.895287E

Elements and photographic light-curve by Robinson, *Harvard Ann.*, **90**, 46, 58, 1933.

C	4161.....	1927 Jan. 12	2424893.682	0.864	−44.7	b	1.0
	4520.....	Nov. 3	5188.885	.959	37.8	b	1.0
	4634.....	1928 Jan. 9	5255.731	.094	42.1	b	1.0
	5362.....	1929 Dec. 10	5956.774	.438	25.0	b	0.7
	5850.....	1931 Sept. 23	6608.812	.284	37.8	b	1.0
γ	19120.....	1932 Sept. 13	6964.979	.974	46.9	b	1.0
C	6142.....	Sept. 21	6972.912	0.702	−19.1	c	0.4

VY Persei $2^h20^m18^s$, $+58°28'$; 11.2–11.7 vis.

Max. = JD 2420273.930 + 5^d.531943E

Elements and visual light-curve by Kukarkin, *N.N.V.S.*, **4**, 48, 1932.

C	5601.....	1930 Nov. 2	2426283.828	0.399	−46.0	c	0.4
	6112.....	1932 Aug. 23	6943.969	.732	20.5	c	.4
	6120.....	Aug. 24	6944.979	.914	36.1	c	.6
γ	19455.....	1933 Feb. 1	7105.693	.966	68.1	c	.4
	20825.....	1935 Oct. 9	8085.974	.170	48.1	c	.4
	20846.....	Oct. 20	8096.960	.156	43.5	c	.6
C	6819.....	Dec. 4	8141.812	.264	58.6	c	.2
	6834.....	1936 Feb. 2	8201.667	.084	61.2	c	.4
γ	20925.....	Feb. 5	8204.679	0.628	−23.9	c	0.2

TABLE 1—*Continued*

Plate	Date	JD	Phase	Vel. Km/Sec	Disp.	Wt.
AS Persei $4^h12^m22^s$, $+48°44'$; 9.4–10.1 vis.						
Max. = JD 2423459.98 + 4^d.97244 E						
Elements by Oosterhoff, *Harvard Bull.*, No. 900, 11, 1935. Visual light-curve by Beyer, *A.N.*, **252**, 186, 1934.						
C 6121	1932 Aug. 25	2426945.023	0.871	−19.1	b	1.0
γ 19197	Oct. 12	6993.901	.700	15.4	b	0.7
19264	Nov. 9	7021.900	.332	25.5	b	1.0
19269	Nov. 10	7022.840	.521	20.2	b	1.0
20826	1935 Oct. 10	8086.019	.336	35.2	c	0.6
C 6826	Dec. 7	8144.780	0.153	−42.9	b	1.0
AW Persei $4^h41^m5^s$, $+36°33'$; 7.2–7.9 vis.						
Max. = JD 2416512.64 + 6^d.46338 E						
Elements by Kukarkin, *N.N.V.S.*, **2**, 49, 1930. Visual light-curve by Jacchia, *A.N.*, **240**, 316, 1930.						
γ 18652	1932 Jan. 18	2426725.771	0.153	+ 6.1	b	0.7
C 5946	Jan. 19	6726.767	.307	+ 8.6	b	1.0
γ 19032	Aug. 21	6941.026	.457	+23.2	b	1.0
C 6113	Aug. 24	6944.016	.920	+ 0.2	b	0.7
γ 19198	Oct. 12	6993.939	.644	+33.0	b	1.0
19265	Nov. 9	7021.936	.975	− 0.2	b	1.0
C 6181	Dec. 10	7052.909	.767	+24.1	b	0.7
6197	1933 Jan. 5	7078.615	.744	+21.5	b	1.0
6319	Oct. 1	7347.028	0.273	+ 8.0	b	1.0
X Puppis $7^h28^m26^s$, $-20°42'$; 8.5–10.3 pg.						
Max. = JD 2419040.869 + 25^d.957789 E						
Elements and photographic light-curve by Robinson, *Harvard Ann.*, **90**, 81, 59, 1933.						
C 768	1920 Nov. 21	2422650.994	0.077	+37.6	a	1.0
4534	1927 Nov. 7	5192.984	.004	80.3	b	1.0
4688	1928 Feb. 27	5304.689	.308	40.5	b	1.0
4734	Apr. 8	5345.656	.886	97.1	b	0.3
5125	1929 Jan. 21	5633.854	.989	91.1	b	0.7
5387	1930 Feb. 9	6017.792	.780	86.5	b	0.7
5411	Mar. 11	6047.761	.934	95.1	b	0.3
5416	Mar. 12	6048.681	.970	79.1	b	0.7
γ 17853	Nov. 3	6284.988	.073	25.2	b	1.0
C 5619	Nov. 29	6310.951	.073	36.0	b	1.0
5902	1931 Nov. 1	6647.057	0.021	+54.4	b	1.0

TABLE 1—*Continued*

	Plate	Date	JD	Phase	Vel. Km/Sec	Disp.	Wt.
	RS Puppis $8^h9^m14^s$, $-34°17'$; 7.4–9.5 pg.						
	Max. = JD 2419186.3 + $41^d.337E$						
	Elements and photographic light-curve by Gerasimovič, *Harvard Bull.*, No. 848, 16, 1927.						
C	3093	1924 Dec. 3	2424123.942	0.448	+15.1	b	0.7
	4137	1926 Dec. 15	4865.981	.399	+23.6	b	1.0
	4535	1927 Nov. 8	5193.035	.311	+ 7.6	b	1.0
	4596	Dec. 31	5246.896	.614	+38.4	b	0.3
	4630	1928 Jan. 8	5254.908	.808	+43.4	b	0.3
	4689	Feb. 27	5304.732	.013	− 7.7	b	1.0
	5132	1929 Feb. 26	5669.726	.843	+55.8	b	0.3
	5598	1930 Nov. 2	6283.026	.680	+31.7	b	1.0
	5659	Dec. 28	6339.901	.056	− 2.7	b	1.0
	5671	Dec. 30	6341.927	.105	− 8.7	b	1.0
	6206	1933 Feb. 4	7108.816	0.657	+33.7	b	0.7
	VZ Puppis $7^h34^m34^s$, $-28°16'$; 9.7–10.9 vis.						
	Max. = JD 2426781.2 + $23^d.17E$						
	Elements and visual light-curve by Florja, *N.N.V.S.*, **4**, 35, 1932.						
C	6214	1933 Mar. 2	2427134.710	0.257	+38.5	c	0.6
	6338	Nov. 4	7381.001	.887	63.9	c	.4
	6388	1934 Apr. 3	7531.649	.389	42.4	c	.4
	6829	1935 Dec. 8	8145.007	.861	69.5	c	.2
	6836	1936 Feb. 2	8201.819	.313	33.2	c	.2
	6841	Feb. 27	8226.767	.390	29.5	c	.2
	7002	1937 Mar. 18	8611.691	.003	45.7	c	.2
	7004	Mar. 19	8612.646	0.044	+52.3	c	0.6
	WW Puppis $7^h37^m35^s$, $-20°54'$; 9.6–10.5 vis.						
	Max. = JD 2424497.73 + $5^d.5159E$						
	Elements by Oosterhoff, *Harvard Bull.*, No. 900, 11, 1935. Visual light-curve by Florja, *N.N.V.S.*, **4**, No. 2, Tafel I, 1932.						
C	6195	1933 Jan. 4	2427077.965	0.781	+98.4	c	0.2
	6232	Apr. 4	7167.638	.038	69.3	c	.4
γ	20067	Dec. 1	7408.007	.616	99.6	c	.4
	20134	1934 Jan. 6	7444.865	0.298	+83.4	c	0.2

TABLE 1—*Continued*

Plate	Date	JD	Phase	Vel. Km/Sec	Disp.	Wt.
WX Puppis $7^h37^m50^s$, $-25°38'$; 9.4–10.0 vis.						
Max. = JD 2426711.65 + 8^d941E						
Elements by Florja, *Tashkent Circ.*, No. 15, 1933. Visual light-curve by Florja, *N.N.V.S.*, **4**, No. 2, Tafel I, 1932.						
C 6215	1933 Mar. 2	2427134.740	0.320	+36.0	c	0.6
γ 20020	Nov. 3	7380.033	.755	74.1	b	1.0
20212	1934 Feb. 24	7493.766	.475	46.9	c	0.6
C 6617	Dec. 17	7789.958	.603	65.0	c	0.4
6622	1935 Feb. 10	7844.771	.733	74.6	c	0.6
γ 20715	Mar. 20	7882.631	.968	49.2	c	0.6
20868	Nov. 9	8116.001	.069	31.2	c	0.6
C 6842	1936 Feb. 27	8226.815	0.462	+41.5	c	0.4
WY Puppis $7^h53^m50^s$, $-23°46'$; 10.6–11.7 pg.						
Max. = JD 2424164.70 + 5^d2509E						
Elements by Oosterhoff, *Harvard Bull.*, No. 900, 11, 1935. Photographic light-curve by Kruytbosch, *B. A. N.*, **8**, 5, 1936.						
C 6185	1933 Jan. 3	2427076.962	0.622	+65.0	b	0.3
6346	Nov. 26	7403.042	.721	56.0	c	.4
6355	Dec. 25	7432.972	.421	50.1	c	.4
γ 20716	1935 Mar. 20	7882.660	.061	21.0	c	.4
20860	Nov. 7	8114.003	0.119	+28.8	c	0.6
WZ Puppis $7^h56^m13^s$, $-23°29'$; 10.9–11.7 vis.						
Max. = JD 2423538.46 + 5^d0270E						
Elements by Oosterhoff, *Harvard Bull.*, No. 900, 12, 1935. Visual light-curve by Florja, *N.N.V.S.*, **4**, No. 2, Tafel I, 1932.						
C 6360	1934 Jan. 22	2427460.868	0.268	+63.6	b	0.3
γ 20153	Jan. 26	7464.868	.064	58.5	c	.6
C 6385	Mar. 21	7518.740	.780	72.0	c	.6
6634	1935 Mar. 17	7879.740	.592	65.6	c	.6
γ 20712	Mar. 19	7881.715	.986	45.0	c	.6
20869	Nov. 9	8116.035	.598	82.0	c	.4
20900	1936 Jan. 7	8175.892	.505	78.1	c	.6
20922	Feb. 4	8203.812	0.059	+39.8	c	0.6

TABLE 1—*Continued*

	Plate	Date	JD	Phase	Vel. Km/Sec	Disp.	Wt.
	AD Puppis $7^h43^m52^s$, $-25°20'$; 9.5–11.5 pg.						
	Max. = JD 2425832.48 + $13^d.595E$						
	Elements and photographic light-curve by Wesselink, *B.A.N.*, **7**, 243, 1935.						
C	6225	1933 Mar. 4	2427136.792	0.940	+60.8	c	0.4
	6327	Oct. 28	7374.004	.389	67.7	c	.4
	6392	1934 Apr. 19	7547.649	.162	38.9	c	.4
	6559	Oct. 19	7730.014	.576	80.8	c	.4
	6605	Dec. 15	7787.922	.835	80.5	c	.4
	6830	1935 Dec. 8	8145.049	0.104	+44.6	c	0.2
	U Sagittarii $18^h26^m0^s$, $-19°12'$; 7.3–8.5 pg.						
	Max. = JD 2420600.325 + $6^d.744917E$						
	Elements and photographic light-curve by Robinson, *Harvard Ann.*, **90**, 49, 57, 1933.						
γ	7144	1918 July 19	2421794.731	0.082	−21.9	a	1.0
	8018	1919 Apr. 9	2058.021	.118	−20.9	a	0.5
	8697	Sept. 11	2213.676	.195	−13.4	a	1.0
C	3954	1926 Aug. 17	4745.747	.599	− 0.2	b	1.0
	5207	1929 June 14	5777.931	.631	+ 9.1	b	1.0
γ	17373	1930 Apr. 9	6076.028	.826	+16.2	b	0.3
	17476	June 2	6130.949	.969	+ 2.3	b	1.0
	17731	Sept. 4	6224.644	0.860	+16.3	b	1.0
	VY Sagittarii $18^h6^m7^s$, $-20°43'$; 11.9–14.0 pg.						
	Max. = JD 2424738.80 + $13^d.5583E$						
	Elements by Oosterhoff, *Harvard Bull.*, No. 900, 12, 1935. Photographic light-curve by Parenago, *N.N.V.S.*, **3**, 108, 1931.						
C	6115	1932 Aug. 24	2426944.709	0.698	+12.4	c	0.2
	6138	Sept. 21	6972.674	.760	+11.1	c	.2
	6294	1933 Aug. 30	7315.717	.062	−22.3	c	.4
	6464	1934 July 21	7640.743	.034	− 4.6	c	.2
	6688	1935 June 8	7962.920	.797	+23.1	c	.2
	6760	July 10	7994.853	.152	−38.6	c	.2
	6931	1936 July 11	8361.781	0.215	−30.5	c	0.2

TABLE 1—*Continued*

	Plate	Date	JD	Phase	Vel. Km/Sec	Disp.	Wt.
	WZ Sagittarii $18^h11^m7^s$, $-19°7'$; 7.9–10.1 pg.						
	Max. = JD 2420889.050+21^d847498E						
	Elements and photographic light-curve by Robinson, *Harvard Ann.*, **90**, 49, 59, 1933.						
C	945	1921 Mar. 18	2422767.035	0.959	− 7.9	b	0.3
	3966	1926 Aug. 20	4748.748	.665	+14.1	b	0.3
	5214	1929 June 17	5780.877	.908	+ 6.0	b	1.0
	5228	June 23	5786.865	.182	−43.2	b	1.0
γ	16698	July 13	5806.853	.097	−39.8	b	1.0
C	5280	Aug. 20	5844.677	.828	+13.7	b	0.7
	5323	Sept. 18	5873.662	.155	−33.8	b	1.0
	5436	1930 Apr. 12	6079.000	.554	+ 0.5	b	0.3
	5457	May 14	6111.925	.060	−41.2	b	1.0
	5844	1931 Sept. 22	6607.657	0.751	+16.3	b	0.7
	XX Sagittarii $18^h18^m57^s$, $-16°51'$; 8.9–10.0 pg.						
	Max. = JD 2419189.730+6^d424264E						
	Elements and photographic light-curve by Robinson, *Harvard Ann.*, **90**, 49, 57, 1933.						
C	3949	1926 Aug. 16	2424744.745	0.693	+16.9	b	0.3
	4895	1928 July 10	5438.868	.740	+19.1	b	0.3
	5202	1929 June 13	5776.892	.357	− 6.3	b	0.3
	5461	1930 June 5	6133.920	.932	+20.8	b	0.7
	5721	1931 Apr. 29	6461.958	.994	−15.7	b	1.0
	5848	Sept. 23	6608.653	.828	+32.3	b	1.0
	6016	1932 May 13	6841.954	.144	−25.7	b	1.0
	6259	1933 June 2	7226.931	.069	− 6.8	b	1.0
	6299	Aug. 31	7316.675	0.039	−17.9	c	0.6
	YZ Sagittarii $18^h43^m42^s$, $-16°50'$; 7.6–8.4 pg.						
	Max. = JD 2419741.300+9^d553151E						
	Elements and photographic light-curve by Robinson, *Harvard Ann.*, **90**, 49, 58, 1933.						
γ	8173	1919 May 13	2422092.993	0.169	+ 5.0	b	1.0
	8711	Sept. 13	2215.679	.012	11.5	a	1.5
	13497	1925 July 1	4333.844	.736	15.8	a	1.5
	15229	1927 Sept. 5	5129.703	.044	8.9	a	1.5
C	5432	1930 Apr. 11	6078.028	.313	26.8	b	1.0
	5458	May 14	6111.988	0.868	+ 2.9	b	1.0

TABLE 1—*Continued*

	Plate	Date	JD	Phase	Vel. Km/Sec	Disp.	Wt.
		YZ Sagittarii—*Continued*					
γ	17543	1930 June 26	2426154.853	0.355	+28.1	b	0.6
	17568	July 9	6167.839	.714	28.6	b	1.0
C	6279	1933 July 31	7285.656	.724	31.6	b	1.0
	6284	Aug. 1	7286.655	.829	7.3	b	1.0
	6298	Aug. 31	7316.651	.969	2.8	c	0.4
	6403	1934 Apr. 22	7550.014	.397	26.5	b	1.0
γ	20402	May 22	7580.844	.624	40.0	b	1.0
C	6469	July 23	7642.717	.100	9.8	b	1.0
	6512	Aug. 23	7673.642	0.338	+10.5	b	1.0

AP Sagittarii $18^h6^m58^s$, $-23°8'$; 7.2–8.2 pg.

Max. = JD 2419491.158 + 5^d.058132 E

Elements and photographic light-curve by Robinson, *Harvard Ann.*, **90**, 49, 57, 1933.

γ	6905	1918 May 18	2421732.927	0.201	−17.5	b	0.7
C	2931	1924 Aug. 13	4011.648	.707	7.8	b	0.4
	3799	1926 May 22	4658.897	.669	3.6	b	1.0
	4843	1928 June 12	5410.867	.335	17.4	b	1.0
γ	17486	1930 June 4	6132.897	.081	20.8	b	1.0
	17567	July 9	6167.792	.980	29.7	b	1.0
	17721	Sept. 1	6221.665	.631	13.3	b	1.0
C	5701	1931 Mar. 30	6431.037	.024	34.9	b	1.0
	5707	Mar. 31	6432.044	.223	28.4	b	1.0
	5745	June 1	6494.844	0.639	− 7.4	b	1.0

AY Sagittarii $18^h17^m26^s$, $-18°37'$; 10.5–11.3 vis.

Max. = JD 2426860.67 + 6^d.56959 E

Elements by Florja, *Tashkent Circ.*, No. 34, 1934. Visual light-curve by Hoffmeister, *A. N.*, **218**, 326, 1923.

C	6044	1932 June 20	2426879.786	0.910	+ 5.8	c	0.2
	6247	1933 May 15	7208.910	.008	−54.3	c	.2
	6271	July 13	7267.707	.958	−25.4	c	.4
	6285	Aug. 1	7286.710	.850	−26.7	c	.4
	6439	1934 June 20	7609.854	.038	−51.7	c	.4
	6465	July 21	7640.814	.751	+12.8	c	.2
	6749	1935 July 8	7992.733	.319	−42.2	c	.4
γ	20818	Oct. 8	8084.625	.306	−31.9	c	.2
C	6896	1936 Apr. 12	8271.004	.676	+ 2.6	c	.2
	6935	July 28	8378.705	0.070	−64.4	c	0.4

TABLE 1—*Continued*

	Plate	Date	JD	Phase	Vel. Km/Sec	Disp.	Wt.
	BB Sagittarii $18^h45^m4^s$, $-20°25'$; 7.1–8.1 pg.						
	Max. = JD 2419282.142 + 6^d.636794 E						
	Elements and photographic light-curve by Robinson, *Harvard Ann.*, **90**, 49, 57, 1933.						
C	4375	1927 July 18	2425080.826	0.718	+31.3	b	1.0
	4935	1928 Aug. 5	5464.833	.578	+26.4	b	1.0
	5232	1929 June 24	5787.910	.258	− 7.3	b	1.0
	5337	Oct. 13	5898.632	.941	− 1.2	b	1.0
γ	17481	1930 June 3	6131.941	.094	− 5.7	b	1.0
C	5527	Sept. 3	6223.735	.926	− 9.5	b	1.0
	5569	Oct. 7	6257.642	.035	−18.9	b	1.0
	5722	1931 Apr. 30	6462.007	.827	+ 6.4	b	1.0
	5746	June 1	6494.906	0.784	+17.3	b	1.0
	V 350 Sagittarii $18^h39^m20^s$, $-20°45'$; 7.5–8.4 pg.						
	Max. = JD 2425885.014 + 5^d.15424 E						
	Elements by Florja, *Tashkent Circ.*, No. 33, 1934. Photographic light-curve by Albitzky, *A. N.*, **238**, 12, 1930.						
γ	17487	1930 June 4	2426132.942	0.102	− 0.7	b	1.0
	17725	Sept. 2	6222.645	.506	+16.0	b	1.0
C	5526	Sept. 3	6223.690	.708	+20.7	b	0.7
	5553	Sept. 19	6239.674	.809	+25.5	b	1.0
γ	17788	Oct. 5	6255.660	.911	+ 5.4	b	0.3
C	5743	1931 May 31	6493.983	.149	− 8.1	b	0.7
γ	18366	July 30	6553.708	.737	+33.0	b	0.7
C	5840	Sept. 21	6606.638	.006	− 5.3	b	1.0
	5845	Sept. 22	6607.720	0.216	− 6.6	b	1.0
	RV Scorpii $16^h51^m47^s$, $-33°27'$; 7.0–8.1 pg.						
	Max. = JD 2420499.353 + 6^d.061428 E						
	Elements and photographic light-curve by Robinson, *Harvard Ann.*, **90**, 48, 57, 1933.						
C	3867	1926 June 27	2424694.769	0.150	−31.7	b	1.0
	4263	1927 May 12	5013.858	.792	− 4.7	b	0.7
	4365	July 16	5078.684	.487	− 9.6	b	1.0
	4369	July 17	5079.672	.650	− 2.0	b	0.7
	4373	July 18	5080.670	.815	+ 6.5	b	0.7
	4782	1928 Apr. 29	5366.962	.046	−39.1	b	1.0
	4842	June 12	5410.809	.280	−19.1	b	1.0
	5162	1929 Apr. 20	5722.938	.774	+ 2.6	b	1.0
	5185	May 21	5753.818	.869	−19.5	b	1.0
	5209	June 16	5779.756	.148	−35.4	b	1.0
	5489	1930 July 7	6165.729	.825	− 3.2	b	0.7
	5741	1931 May 31	6493.828	0.954	−28.9	b	0.7

TABLE 1—*Continued*

	Plate	Date	JD	Phase	Vel. Km/Sec	Disp.	Wt.

RY Scorpii $17^h44^m16^s$, $-33°40'$; 8.3–9.4 pg.

Max. = JD 2419664.594 + $20^d.314133\,E$

Elements and photographic light-curve by Robinson, *Harvard Ann.*, **90**, 48, 59, 1933.

C	1084	1921 June 26	2422867.839	0.685	− 3.4	b	0.3
	4366	1927 July 16	5078.744	.521	− 3.0	b	0.3
	4806	1928 May 13	5380.915	.396	−19.9	b	0.3
	4823	May 27	5394.897	.084	−40.5	b	1.0
	4875	July 4	5432.782	.950	−26.7	b	0.7
	5163	1929 Apr. 21	5723.009	.236	−25.9	b	0.3
	5186	May 21	5753.924	.758	− 5.0	b	0.3
	5272	Aug. 18	5842.666	.127	−25.5	b	0.3
	5994	1932 Apr. 13	6811.992	.844	−11.3	b	0.3
	6269	1933 July 2	7256.785	0.739	+ 2.2	c	0.2

X Scuti $18^h25^m42^s$, $-13°11'$; 9.8–11.0 pg.

Max. = JD 2420934.435 + $4^d.198026\,E$

Elements and photographic light-curve by Robinson, *Harvard Ann.*, **90**, 49, 56, 1933.

C	4367	1927 July 16	2425078.833	0.225	+ 6.4	b	0.7
	4942	1928 Aug. 24	5483.710	.670	+19.4	b	.3
	5326	1929 July 16	5809.809	.349	+ 7.9	b	.3
γ	19026	1932 Aug. 20	6940.694	.734	+25.0	b	.7
C	6401	1934 Apr. 21	7549.913	.854	+ 5.5	c	.4
	6699	1935 June 11	7965.965	.961	− 7.4	c	.6
γ	20839	Oct. 20	8096.616	0.083	−12.6	c	0.6

Y Scuti $18^h32^m36^s$, $-8°27'$; 9.9–10.9 pg.

Max. = JD 2420138.056 + $10^d.341392\,E$

Elements and photographic light-curve by Robinson, *Harvard Ann.*, **90**, 49, 58, 1933.

C	4328	1927 July 6	2425068.869	0.804	+12.2	b	0.3
	4335	July 8	5070.824	.993	+ 3.7	b	.7
	4930	1928 Aug. 4	5463.775	.990	− 0.1	b	.7
	5277	1929 Aug. 19	5843.744	.733	+20.8	b	.3
γ	19766	1933 Aug. 2	7287.705	.362	+12.9	c	.6
	20772	1935 June 13	7967.802	.127	−12.1	c	.4
	20840	Oct. 20	8096.648	.586	+19.3	c	.4
C	6932	1936 July 11	8361.854	.231	−18.8	c	.6
	6942	July 30	8380.667	.050	− 3.0	c	.6
γ	21045	Aug. 1	8382.819	0.258	− 8.5	c	0.6

TABLE 1—*Continued*

Plate	Date	JD	Phase	Vel. Km/Sec	Disp.	Wt.
Z Scuti $18^h37^m36^s$, $-5°55'$; 9.6–11.2 pg.						
Max. = JD 2420133.222 + 12^d.901723 E						
Elements and photographic light-curve by Robinson, *Harvard Ann.*, **90**, 49, 58, 1933.						
C 4332	1927 July 7	2425069.894	0.637	+44.4	b	0.3
4336	July 8	5070.896	.714	50.5	b	0.3
5327	1929 Sept. 20	5875.681	.092	9.8	b	1.0
5565	1930 Oct. 6	6256.677	.623	42.5	c	0.4
γ 19767	1933 Aug. 2	7287.776	.542	34.4	c	0.6
C 6402	1934 Apr. 21	7549.971	.865	39.8	c	0.6
γ 20776	1935 June 14	7968.878	.334	22.8	b	0.7
C 6745	June 22	7976.955	0.960	+25.4	b	0.7
RU Scuti $18^h36^m40^s$, $-4°12'$; 9.5–11.7 pg.						
Max. = JD 2419198.251 + 19^d.696466 E						
Elements and photographic light-curve by Robinson, *Harvard Ann.*, **90**, 49, 59, 1933.						
C 1115	1921 July 11	2422882.894	0.071	−20.7	b	0.3
4831	1928 May 31	5398.916	.811	− 0.3	b	0.3
4876	July 4	5432.861	.534	+ 3.1	b	0.3
5283	1929 Aug. 21	5845.705	.495	+ 4.6	b	0.3
6255	1933 June 1	7225.965	.571	−11.4	c	0.4
γ 19768	Aug. 2	7287.847	.713	+15.1	c	0.4
C 6666	1935 May 10	7933.995	.518	− 6.6	c	0.2
6783	Aug. 7	8022.684	.021	−18.4	b	1.0
6791	Aug. 9	8024.767	.127	−39.3	c	0.6
6901	1936 Apr. 27	8286.922	.437	−23.1	c	0.6
6919	May 27	8316.912	.959	−30.8	c	0.4
6925	May 29	8318.936	.062	−30.2	c	0.4
γ 21010	May 31	8320.880	0.161	−29.2	c	0.6
SS Scuti $18^h38^m18^s$, $-7°50'$; 8.0–8.9 pg.						
Max. = JD 2419984.342 + 3^d.6711843 E						
Elements and photographic light-curve by Robinson, *Harvard Ann.*, **90**, 49, 56, 1933.						
C 3320	1925 June 6	2424308.964	0.991	− 6.4	b	1.0
γ 17542	1930 June 26	6154.787	.778	5.4	b	0.7
C 5532	Sept. 6	6226.670	.358	22.6	b	0.7
γ 18148	1931 Mar. 27	6428.009	.201	23.5	b	1.0
C 5700	Mar. 29	6430.997	.015	16.6	b	1.0
5753	June 22	6515.773	.107	19.0	b	0.3
6015	1932 May 13	6841.894	.940	5.0	b	1.0
γ 19027	Aug. 20	6940.771	0.873	− 2.4	b	1.0

TABLE 1—*Continued*

Plate	Date	JD	Phase	Vel. Km/Sec	Disp.	Wt.
TY Scuti $18^h36^m49^s$, $-4°24'$; 12.1–13.2 pg.						
Max. = JD 2425903.518 + 11^d0515E						
Elements by Harwood, *Harvard Bull.*, No. 893, 22, 1933. Photographic light-curve by Parenago, *N.N.V.S.*, **3**, 110, 1932.						
C 6045	1932 June 20	2426879.892	0.348	+24.2	c	0.2
6104	Aug. 22	6942.773	.037	−29.5	c	.6
6280	1933 July 31	7285.729	.070	−14.8	c	.2
6691	1935 June 9	7963.934	.438	+15.5	c	.6
6784	Aug. 7	8022.790	.763	+12.6	c	.6
6891	1936 Apr. 11	8270.021	0.134	+ 1.1	c	0.4
UZ Scuti $18^h25^m44^s$, $-13°0'$; 12.0–12.9 pg.						
Max. = JD 2424790.95 + 14^d749E						
Elements by Oosterhoff, *Harvard Bull.*, No. 900, 12, 1935. Unpublished photographic light-curve kindly supplied by Miss H. H. Swope, of the Harvard College Observatory.						
C 6088	1932 July 25	2426914.756	0.997	+11.7	c	0.4
6277	1933 July 14	7268.891	.007	− 3.1	c	.4
6281	July 31	7285.823	.155	− 5.7	c	.2
γ 20769	1935 June 12	7966.891	.333	+ 4.2	c	.4
C 6890	1936 Apr. 10	8269.970	0.882	+31.3	c	0.4
BX Scuti $18^h44^m52^s$, $-4°29'$; 13.3–14.5 pg.						
Max. = JD 2425388.43 + 6^d4099E						
Elements by Oosterhoff, *Harvard Bull.*, No. 900, 12, 1935. Unpublished photographic light-curve kindly supplied by Miss Margaret Harwood, of the Maria Mitchell Observatory.						
C 6098	1932 Aug. 21	2426941.736	0.329	−13.5	c	0.4
6430	1934 May 23	7581.896	.200	25.4	c	.2
6509	Aug. 22	7672.767	.376	7.5	c	.4
6741	1935 June 21	7975.875	.664	3.3	c	.2
6788	Aug. 8	8023.833	0.146	−31.6	c	0.4
ST Tauri $5^h39^m24^s$, $+13°32'$; 8.3–9.2 pg.						
Max. = JD 2419718.565 + $4^d034229E$						
Elements and photographic light-curves by Robinson, *Harvard Ann.*, **90**, 46, 56, 1933.						
C 4183	1927 Feb. 8	2424920.698	0.499	+12.9	b	0.7
4503	Oct. 28	5182.998	.517	14.0	b	1.0
4512	Oct. 30	5184.045	0.777	+ 9.3	b	1.0

TABLE 1—*Continued*

	Plate	Date	JD	Phase	Vel. Km/Sec	Disp.	Wt.
		ST Tauri—*Continued*					
C	4629	1928 Jan. 8	2425254.854	0.329	+ 3.1	b	1.0
	4643	Jan. 11	5257.828	.066	−22.3	b	1.0
	5064	Nov. 4	5555.951	.964	−11.6	b	1.0
γ	17852	1930 Nov. 3	6284.917	.660	+12.0	b	1.0
	17859	Nov. 4	6285.937	.912	+ 3.6	b	1.0
C	5660	Dec. 28	6339.955	.302	− 1.6	b	1.0
γ	18028	Dec. 31	6342.903	.033	−20.9	b	1.0
C	5907	1931 Nov. 3	6649.022	.914	+ 0.3	b	1.0
	5956	1932 Feb. 18	6756.793	0.628	+18.0	b	0.7

SW Tauri $4^h19^m17^s$, $+3°54'$; 9.0–10.0 pg.

Max. = JD 2419730.9036 + 1^d.5836468E

Elements and photographic light-curve by Robinson, *Harvard Ann.*, **90**, 46, 56, 1933. 0.55 day has been added to the epoch given to reduce it to maximum.

C	4162	1927 Jan. 12	2424893.783	0.121	+11.0	b	1.0
	4170	Jan. 15	4896.807	.030	+ 8.9	b	0.3
	4188	Feb. 11	4923.747	.041	+ 8.4	b	1.0
	4635	1928 Jan. 9	5255.794	.714	+14.2	b	0.7
γ	19191	1932 Oct. 12	6993.031	.699	+35.8	b	0.7
	20019	1933 Nov. 2	7379.980	.039	+ 3.1	b	0.7
C	6337	Nov. 3	7380.906	.624	+44.0	b	0.7
γ	20065	Nov. 30	7407.832	.626	+33.5	b	1.0
	20105	Dec. 27	7434.750	.624	+34.9	b	0.7
	20148	1934 Jan. 25	7463.642	.868	− 5.8	c	1.0
	20836	1935 Oct. 19	8095.917	.120	+ 3.7	b	1.0
C	6820	Dec. 4	8141.874	.140	+16.7	b	0.7
γ	20895	1936 Jan. 6	8174.767	.911	+ 3.4	b	1.0
	20938	Mar. 3	8231.628	.816	+ 3.1	b	1.0
	20944	Mar. 4	8232.610	0.436	+25.4	c	1.0

W Virginis $13^h20^m52^s$, $-2°52'$; 9.8–11.1 pg.

Max. = JD 2414848.19 + 17^d.27169E

Elements by Güssow, *A.N.*, **244**, 301, 1932. 6.2 days have been added to the epoch to reduce it to maximum. Photographic light-curve by Chant, *Harvard Ann.*, **80**, 225, 1917.

Bright hydrogen lines are present on 11 plates taken during the increase in the star's light from phase 0.594 to maximum, but the emission shows no certain variation of velocity with phase. The mean velocity given by measures of $H\gamma$ and $H\delta$ is −108.8 km/sec. The large proper motion and high galactic latitude of this star are notable.

C	877	1921 Feb. 15	2422736.988	0.747	−34.9	b	0.7
	981	Apr. 10	2790.800	.863	51.6	b	1.0
	1041	June 9	2850.712	0.332	−78.1	b	1.0

TABLE 1—*Continued*

Plate	Date	JD	Phase	Vel. Km/Sec	Disp.	Wt.
W Virginis—*Continued*						
C 1599	1922 Mar. 9	2423123.919	0.150	−94.0	b	0.7
2669	1924 Feb. 13	3829.015	.974	71.3	b	0.7
3285	1925 May 6	4277.705	.952	77.3	b	1.0
3290	May 7	4278.771	.014	88.2	b	1.0
3293	May 8	4279.807	.074	92.3	b	1.0
3733	1926 Mar. 24	4599.906	.607	43.4	b	0.3
3763	Apr. 24	4630.880	.400	70.5	b	0.7
4173	1927 Jan. 17	4898.000	.866	47.7	b	1.0
4223	Apr. 13	4984.816	.892	69.2	b	1.0
4250	May 9	5010.835	.399	61.8	b	0.3
4253	May 10	5011.729	.451	66.1	b	0.3
4307	June 16	5048.747	.594	47.7	b	0.7
4802	1928 May 12	5379.778	.760	43.7	b	0.7
4824	May 28	5395.724	0.683	−33.4	b	1.0

AL Virginis $14^h5^m45^s$, $-12°50'$; 9.3–10.4 pg.

Max. = JD 2425624.8 + 10^d.2974 E

Elements from Prager, *Kleinere Veröff. Berlin-Babelsberg*, No. 15, 150, 1936. No light-curve available.

C 5975	1932 Mar. 15	2426782.910	0.466	+29.2	b	0.7
5993	Apr. 13	6811.876	.279	11.5	b	0.7
6043	June 20	6879.679	.864	26.8	b	0.7
6077	July 23	6912.678	.068	22.6	b	1.0
γ 19525	1933 Mar. 5	7137.920	.942	21.7	b	0.7
19569	Apr. 2	7165.922	.661	42.5	b	0.3
C 6253	June 1	7225.681	.464	28.2	b	0.3
γ 19711	July 3	7257.712	.575	26.8	b	0.7
C 6400	1934 Apr. 21	7549.862	.946	17.3	b	1.0
γ 20377	May 2	7560.826	.011	12.1	b	1.0
20380	May 3	7561.802	.106	0.2	c	0.6
C 6417	May 20	7578.674	.744	30.0	b	1.0
6431	May 24	7582.665	.132	9.8	b	0.7
6434	June 19	7608.693	0.660	+48.9	b	0.7

X Vulpeculae $19^h53^m19^s$, $+26°17'$; 8.8–9.5 pg.

Max. = JD 2420636.248 + 6^d.319490 E

Elements and photographic light-curve by Robinson, *Harvard Ann.*, **90**, 49, 57, 1933.

C 3955	1926 Aug. 17	2424745.866	0.308	−18.0	b	0.3
3956	Aug. 18	4746.722	.444	5.8	b	1.0
3967	Aug. 20	4748.826	0.777	− 5.1	b	1.0

TABLE 1—*Continued*

	Plate	Date	JD	Phase	Vel. Km/Sec	Disp.	Wt.
		X Vulpeculae—*Continued*					
C	3975.....	1926 Aug. 21	2424749.862	0.941	−25.0	b	1.0
	4530.....	1927 Nov. 7	5192.693	.015	−30.5	b	1.0
	4924.....	1928 July 29	5457.823	.969	−24.3	b	1.0
	5062.....	Nov. 4	5555.660	.451	− 4.4	b	0.7
	5183.....	1929 May 20	5752.976	0.674	+12.8	b	0.3

SV Vulpeculae $19^h47^m30^s$, $+27°12'$; 8.0–9.6 pg.

Max. = JD 2423561.26 + $45^d.212E$

Elements by Zacharov, *Tashkent Obs. Pub.*, **1**, 84, 1929. Photographic light-curve by Gerasimovič, *N.N.V.S.*, **3**, 80, 1931.

γ	14457.....	1926 Aug. 23	2424751.859	0.334	− 5.6	a	1.0
	14518.....	Sept. 19	4778.653	.926	+13.9	a	1.5
	14587.....	Oct. 16	4805.646	.523	− 1.0	a	1.0
C	4283.....	1927 June 7	5039.984	.706	+ 9.4	b	1.0
γ	15144.....	Aug. 5	5098.906	.010	−23.1	a	1.5
C	4505.....	Oct. 29	5183.632	.884	+23.5	b	1.0
	4529.....	Nov. 7	5192.642	.083	−27.6	a	1.5
γ	15714.....	1928 Apr. 28	5365.922	.916	+11.1	a	1.5
	15722.....	Apr. 29	5366.951	.938	+ 4.6	a	1.5
	15730.....	Apr. 30	5367.984	.961	− 7.9	a	1.5
C	4808.....	May 13	5380.994	0.249	−13.0	b	1.5

TABLE 2

OBSERVATIONS OF ADDITIONAL CEPHEIDS

Plate	Date	JD	Phase	Vel. Km/Sec	Disp.	Wt.
KL Aquilae $19^h56^m35^s$, $+15°32'$; 8.5–9.5 vis.						
Max. = JD 2425857.84 + $6^d.0989E$						
Elements by Nabokov, *A.N.*, **241**, 192, 1931.						
C 6339	1933 Nov. 4	2427381.653	0.850	+ 3.1	c	0.6
γ 20061	Nov. 27	7404.646	.620	− 6.7	b	0.7
C 6420	1934 May 20	7578.984	.206	+17.8	b	1.0
γ 20399	May 21	7579.965	.366	−16.3	b	1.0
C 6442	June 21	7610.983	.452	−17.2	b	1.0
6536	Sept. 18	7699.760	.009	+ 7.8	b	1.0
γ 20842	1935 Oct. 20	8096.731	0.097	+ 3.7	c	0.6
AS Aurigae $5^h59^m4^s$, $+28°48'$; 11.5–12 pg.						
C 6333	1933 Oct. 29	2427375.006	.....	+26.9	c	0.6
C 6352	Dec. 25	7432.771	.....	+35.8	c	.6
γ 20949	1936 Mar. 4	8232.833	.....	−14.6	c	.2
21088	Nov. 6	8479.910	.....	+22.6	c	.6
21113	1937 Feb. 1	8566.885	.....	+ 1.9	c	0.4
176.1932 Canis Majoris $6^h15^m33^s$, $-21°37'$; 9–10 pg.						
C 6224	1933 Mar. 4	2427136.683	.....	+47.9	c	0.6
6632	1935 Mar. 17	7879.630	.....	72.4	c	.6
γ 20867	Nov. 8	8115.972	.....	66.7	c	.6
20889	Dec. 8	8145.869	.....	40.7	c	.6
C 6833	1936 Jan. 3	8171.840	.....	+57.1	c	0.6
BP Cassiopeiae $1^h8^m25^s$, $+65°5'$; 10.8–12.3 pg.						
Max. = JD 2426034.25 + $1^d.5064E$						
Elements by Beljawsky, *Pulkowa Obs. Circ.*, No. 6, 22, 1933.						
γ 20606	1934 Oct. 20	2427731.828	0.911	−48.5	c	0.2
20637	Nov. 14	7756.802	.489	11.6	c	.4
20821	1935 Oct. 8	8084.903	.294	65.1	c	.6
20835	Oct. 19	8095.837	.552	25.8	c	.4
20844	Oct. 20	8096.833	.214	35.0	c	.6
20904	1936 Jan. 9	8177.663	.871	43.8	c	.4
20934	Mar. 2	8230.637	.037	65.7	c	.2
21079	Oct. 8	8450.958	.294	40.7	c	.6
21087	Nov. 6	8479.796	.437	63.9	c	.6
21105	1937 Jan. 4	8538.769	0.586	−51.4	c	0.6

TABLE 2—*Continued*

	Plate	Date	JD	Phase	Vel. Km/Sec	Disp.	Wt.
	AK Cephei $22^h25^m11^s$, $+57°42'$; 11.6–12.6 pg.						
	Max. = JD 2427273.26 + $7^d.2399E$						
	Elements by Zonn, *Beob. Zirk.*, No. 22, 1935.						
γ	20849	1935 Nov. 5	2428112.736	0.689	−71.0	c	0.6
	20865	Nov. 8	8115.819	.377	53.0	c	.6
C	6934	1936 July 11	8361.974	.377	29.3	c	.4
	6950	Aug. 27	8408.936	.864	58.5	c	.6
	6959	Sept. 8	8420.873	.512	30.0	c	.4
	6962	Sept. 9	8421.917	.656	33.6	c	.6
γ	21104	1937 Jan. 4	8538.667	0.782	−62.0	c	0.6
	GH Cygni $19^h55^m6^s$, $+29°11'$; 10.1–11.5 pg.						
	Max. = JD 2424738.76 + $7^d.8176E$						
	Elements by Oosterhoff, *Harvard Bull.*, No. 900, 10, 1935.						
C	6083	1932 July 24	2426913.868	0.232	− 7.3	c	0.4
γ	19025	Aug. 19	6939.872	.558	−33.9	b	0.3
C	6128	Sept. 11	6962.785	.489	−34.0	b	0.3
γ	19260	Nov. 9	7021.626	.016	−11.2	b	1.0
	19273	Nov. 11	7023.618	.271	−10.3	b	0.7
	20855	1935 Nov. 6	8113.685	.708	−23.1	c	0.6
	21011	1936 May 31	8320.939	.220	−28.3	c	0.6
	21035	July 7	8357.819	.937	+ 3.4	c	0.6
C	6946	July 30	8380.958	.897	− 7.4	c	0.4
γ	21046	Aug. 1	8382.865	0.141	− 8.9	c	0.4
	GL Cygni $20^h0^m1^s$, $+38°53'$; 14.0–15.2 pg.						
	Max. = JD 2427312.0260 + $3^d.37040E$						
	Unpublished elements by Baade.						
C	6295	1933 Aug. 30	2427315.861	0.138	−40.5	c	0.4
	6560	1934 Oct. 19	7730.708	.223	93.3	c	.6
	6747	1935 July 7	7991.901	.719	59.9	c	.6
	6751	July 8	7992.943	0.028	−23.3	c	0.6
	V 343 Cygni $20^h0^m30^s$, $+38°49'$; 14.1–15.4 pg.						
	Max. = JD 2427313.1890 + $11^d.9290E$						
	Unpublished elements by Baade.						
C	6291	1933 Aug. 29	2427314.875	0.141	−107.5	c	0.2
	6502	1934 Aug. 20	7670.806	.979	117.5	c	.6
	6964	1936 Sept. 10	8422.792	0.017	−105.2	c	0.4

TABLE 2—*Continued*

Plate	Date	JD	Phase	Vel. Km/Sec	Disp.	Wt.
V 386 Cygni $21^h10^m52^s$, $+41°18'$; 10–11 pg.						
Max. = JD 2427977.09 + $5^d.238E$						
Elements by Seliwanow, *Beob. Zirk.*, No. 12, 1936.						
γ 21083	1936 Nov. 5	2428478.706	0.765	−14.7	c	0.6
21098	Dec. 5	8508.677	.487	−38.8	c	.6
21128	1937 Apr. 23	8647.988	.083	−14.2	c	.6
21134	Apr. 24	8648.988	0.274	+ 6.9	c	0.6
CN Lyrae $18^h37^m21^s$, $+28°38'$; 11.0–11.6 pg.						
Max. = JD 2427770.31 + $2^d.33596E$						
Elements by Florja, *N.N.V.S.*, **5**, 109, 1937.						
C 6665	1935 May 10	2427933.860	0.014	+36.3	c	0.6
6687	June 8	7962.319	.411	− 5.3	c	0.6
6753	July 9	7993.700	.631	+26.4	b	1.0
γ 20833	Oct. 19	8095.649	.274	− 9.1	c	0.6
20848	Nov. 5	8112.648	.551	+15.4	c	0.6
21032	1936 July 1	8351.793	.927	+26.9	c	0.6
C 6933	July 11	8361.899	.253	+29.3	c	0.4
6936	July 28	8378.774	.477	− 0.8	c	0.6
γ 21050	Aug. 2	8383.774	0.618	+41.9	c	0.6
SZ Monocerotis $6^h46^m25^s$, $-1°15'$; 10.4–11.4 vis.						
Max. = JD 2425232.4 + $16^d.382E$						
Elements by Dubiago, *A.N.*, **239**, 16, 1930.						
C 6152	1932 Oct. 11	2426992.034	0.413	+66.0	c	0.4
6176	Nov. 9	7021.045	.184	+37.4	c	0.6
6193	1933 Jan. 4	7077.860	.652	+70.3	c	0.4
6594	1934 Dec. 14	7786.983	.938	− 5.4	c	0.4
γ 20739	1935 Apr. 20	7913.665	.671	+29.5	c	0.6
20861	Nov. 7	8114.040	.903	+ 2.1	c	0.6
20906	1936 Jan. 9	8177.768	.793	+ 6.4	c	0.6
20927	Feb. 5	8204.806	.443	+20.1	c	0.4
20970	Mar. 28	8256.674	.610	+28.6	c	0.4
21085	Nov. 5	8478.913	.176	+16.9	c	0.6
21096	Dec. 4	8507.870	.943	+27.7	c	0.6
21101	Dec. 5	8508.889	.005	+34.3	b	1.0
21106	1937 Jan. 4	8538.894	.837	+31.7	b	0.7
21107	Jan. 31	8565.702	.473	+56.0	c	0.6
21112	Feb. 1	8566.783	0.539	+66.6	c	0.6

TABLE 2—*Continued*

Plate	Date	JD	Phase	Vel. Km/Sec	Disp.	Wt.
TZ Monocerotis $6^h52^m54^s$, $-0°15'$; 11.0–12.2 pg.						
Max. = JD 2425615.36 + $7^d.4284E$						
Elements by Oosterhoff, *Harvard Bull.*, No. 900, 11, 1935.						
γ 19266	1932 Nov. 10	2427022.002	0.360	+37.4	b	0.7
19278	Nov. 12	7024.006	.630	52.8	b	.3
C 6192	1933 Jan. 4	7077.828	.875	50.6	c	.6
6606	1934 Dec. 16	7788.000	.478	23.5	c	.4
γ 20702	1935 Feb. 14	7848.774	.659	40.7	c	.2
20907	1936 Jan. 9	8177.801	.952	27.3	c	.6
20923	Feb. 4	8203.860	.460	36.1	c	.4
21108	1937 Jan. 31	8565.781	0.189	+47.7	c	0.6
XX Monocerotis $6^h47^m11^s$, $-2°41'$; 11–12 pg.						
C 6202	1933 Jan. 5	2427078.885	.....	+85.0	c	0.2
6652	1935 Apr. 12	7905.684	.....	44.9	c	.2
γ 20908	1936 Jan. 9	8177.832	.....	43.9	c	.6
C 6980	Oct. 24	8466.974	.....	67.2	c	.2
γ 21086	Nov. 6	8479.008	.....	+63.3	c	0.4
VW Puppis $7^h27^m25^s$, $-19°56'$; 11.2–12.1 vis.						
Max. = JD 2425184.67 + $4^d.28405E$						
Elements by Oosterhoff, *Harvard Bull.*, No. 900, 11, 1935.						
C 6237	1933 Apr. 5	2427168.694	0.119	− 3.0	c	0.2
6353	Dec. 25	7432.875	.785	+43.9	c	.4
6367	1934 Feb. 20	7489.740	.058	+16.0	c	.2
6626	1935 Mar. 16	7878.667	.843	+29.5	c	.4
γ 20909	1936 Jan. 9	8177.890	.689	+34.0	c	.4
C 6892	Apr. 11	8270.663	0.345	+29.5	c	0.4
VX Puppis $7^h28^m19^s$, $-21°43'$; 7.8–9.4 pg.						
Max. = JD 2426961.2 + $3^d.012E$						
Elements by O'Connell, *Riverview Pub.*, **1**, 15, 1935.						
γ 19401	1933 Jan. 3	2427076.875	0.405	+32.1	b	1.0
C 6236	Apr. 5	7168.628	.867	− 1.5	c	0.6
γ 20066	Nov. 30	7407.927	.316	+ 7.7	b	1.0
20107	Dec. 27	7434.936	.283	− 4.0	b	1.0
20152	1934 Jan. 26	7464.795	0.196	− 4.3	c	0.6

TABLE 2—*Continued*

	Plate	Date	JD	Phase	Vel. Km/Sec	Disp.	Wt.
		VX Puppis—*Continued*					
C	6633.....	1935 Mar. 17	7879.689	0.943	+12.6	b	1.0
γ	20897.....	1936 Jan. 6	8174.896	.954	− 5.3	b	1.0
C	6837.....	Feb. 2	8201.862	.906	− 5.3	c	0.6
γ	20948.....	Mar. 4	8232.766	.167	+ 8.5	b	1.0
	20969.....	Mar. 28	8256.626	.088	+ 2.0	b	1.0
	21097.....	Dec. 4	8507.955	.531	+25.1	c	0.6
	21102.....	Dec. 5	8508.956	0.863	+ 2.4	b	1.0
		AP Puppis $7^h54^m18^s$, $-39°51'$; 7.6–8.7 pg.					
		Max. = JD 2427341.25+5^{d}084E					
		Elements by O'Leary, *A.N.*, **257**, 391, 1935.					
C	6985.....	1937 Feb. 17	2428582.773	0.196	+41.2	c	0.2
	7005.....	Mar. 19	8612.684	.079	37.4	c	.2
	7010.....	Mar. 20	8613.661	.272	25.1	c	.4
	7023.....	Apr. 21	8645.656	.565	49.4	c	.2
	7027.....	Apr. 22	8646.653	0.761	+52.4	c	0.2
		AQ Puppis $7^h54^m20^s$, $-28°52'$; 9.0–10.9 pg.					
		Max. = JD 2427519.14+22^{d}92E					
		Elements by O'Leary and O'Connell, *A.N.*, **259**, 399, 1936.					
C	6216.....	1933 Mar. 2	2427134.772	0.153	+15.5	c	0.4
	6623.....	1935 Feb. 10	7844.847	.886	56.5	c	.4
	6627.....	Mar. 16	7878.729	.018	35.5	c	.6
	6981.....	1936 Oct. 25	8467.024	.681	63.6	c	.6
	6984.....	1937 Feb. 17	8582.729	0.548	+37.0	c	0.2
		AT Puppis $8^h8^m40^s$, $-36°39'$; 8.0–9.4 pg.					
		Max. = JD 2426758.205+6^{d}66481E					
		Elements by O'Connell, *A.N.*, **257**, 391, 1935.					
C	6986.....	1937 Feb. 17	2428582.830	0.770	+33.7	c	0.4
	7006.....	Mar. 19	8612.719	.254	12.3	c	.6
	7011.....	Mar. 20	8613.701	.402	33.8	c	.6
	7020.....	Apr. 20	8644.685	0.051	+ 9.7	c	0.4

TABLE 2—*Continued*

	Plate	Date	JD	Phase	Vel. Km/Sec	Disp.	Wt.
	V 377 Sagittarii $18^h42^m14^s$, $-20°14'$; 13.6–15.0 pg.						
	Max. = JD 2426077.535 + $16^d.17076E$						
	Elements by Martin, *B.A.N.*, **6**, 232, 1932.						
C	6270.....	1933 July 2	2427256.903	0.932	+29.4	c	0.2
	6539.....	1934 Sept. 19	7700.685	.376	−22.4	c	.2
	6543.....	Sept. 20	7701.688	0.438	−29.1	c	0.2
	V 410 Sagittarii $19^h0^m13^s$, $-18°33'$; 12.6–14.1 pg.						
	Max. = JD 2426082.83 + $13^d.7835E$						
	Elements by Martin, *B.A.N.*, **6**, 232, 1932.						
C	6078.....	1932 July 23	2426912.809	0.216	−29.4	c	0.2
	6110.....	Aug. 23	6943.740	.460	0.0	c	.2
	6272.....	1933 July 13	7267.835	.973	+19.5	c	.6
	6447.....	1934 June 23	7612.885	0.006	+15.7	c	0.4
	BW Scuti $18^h42^m3^s$, $-4°52'$; 11.8–13.6 pg.						
	Max. = JD 2413752.67 + $3^d.8823E$						
	Elements by Harwood, *Harvard Bull.*, No. 880, 12, 1930.						
C	6262.....	1933 June 30	2427254.924	0.848	+20.6	c	0.4
	6286.....	Aug. 1	7286.823	.192	− 1.3	c	.2
	6300.....	Aug. 31	7316.750	.020	+ 4.5	c	.2
	6761.....	1935 July 10	7994.927	.414	− 8.8	c	.2
	6944.....	July 30	8380.823	.354	−19.7	c	.4
	6958.....	Sept. 8	8420.760	0.801	+14.5	c	0.4
	AA Serpentis $18^h36^m11^s$, $-1°12'$; 13.8–15.4 pg.						
	Max. = JD 2425475.68 + $17^d.155E$						
	Elements by Oosterhoff, *Harvard Bull.*, No. 900, 12, 1935.						
C	6132.....	1932 Sept. 12	2426963.722	0.741	−56.7	c	0.4
	6470.....	1934 July 23	7642.844	.328	+25.0	c	.2
	6698.....	1935 June 11	7965.844	.157	+24.9	c	.2
	6755.....	July 9	7993.872	.790	−46.7	c	.4
	6960.....	1936 Sept. 9	8421.712	0.720	−28.8	c	0.4

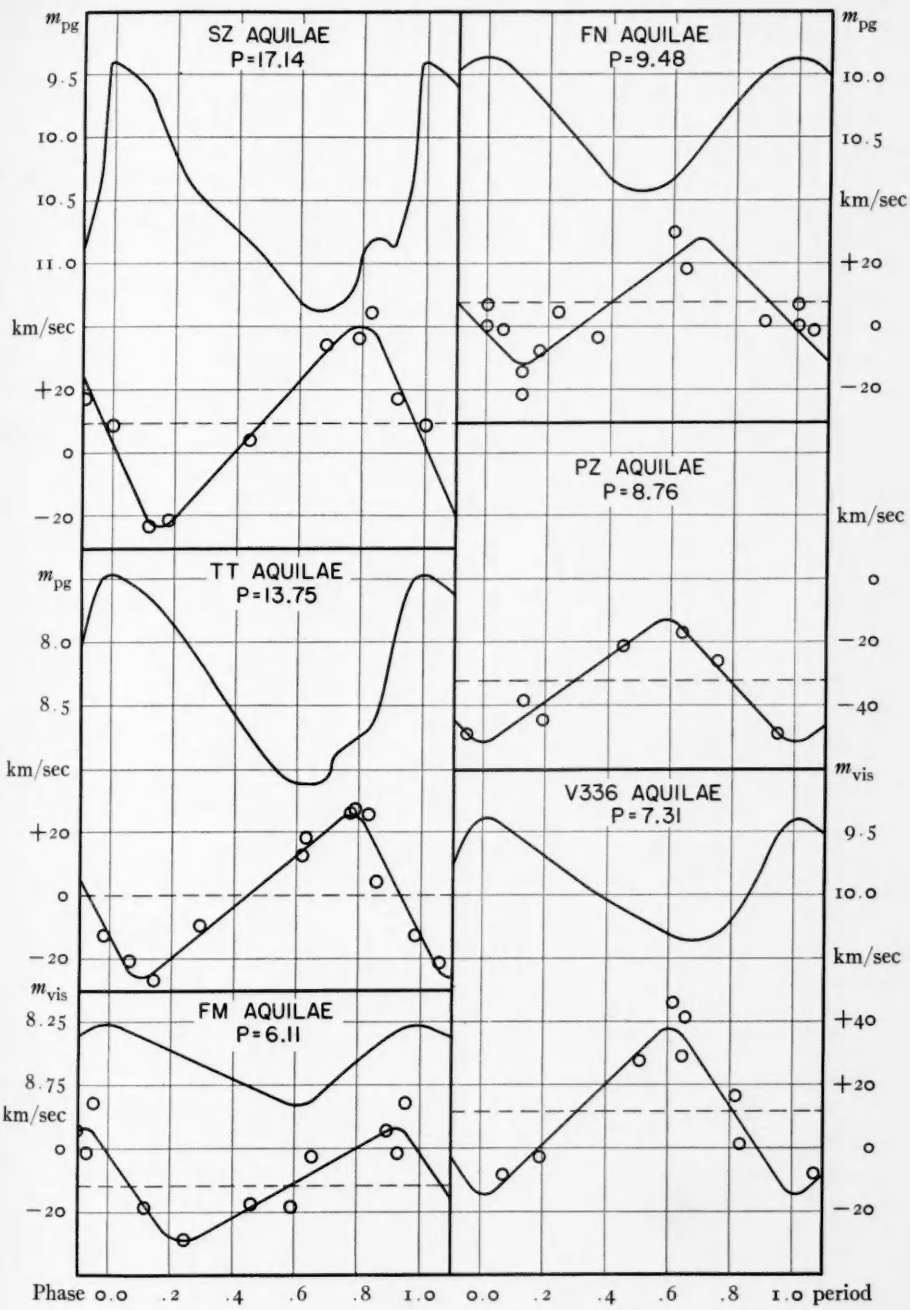

FIG. 1.—Light- and velocity-curves

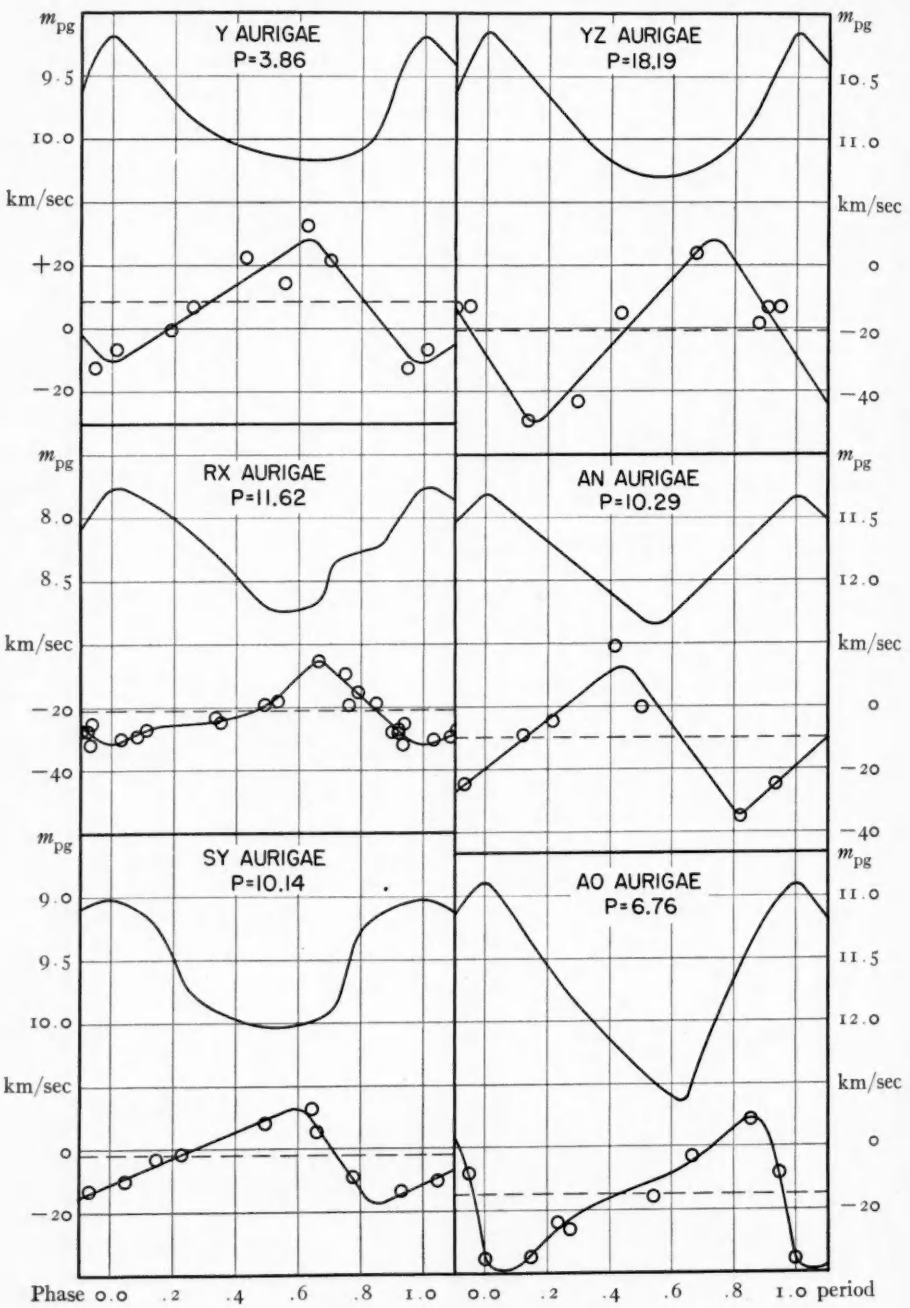

FIG. 2.—Light- and velocity-curves

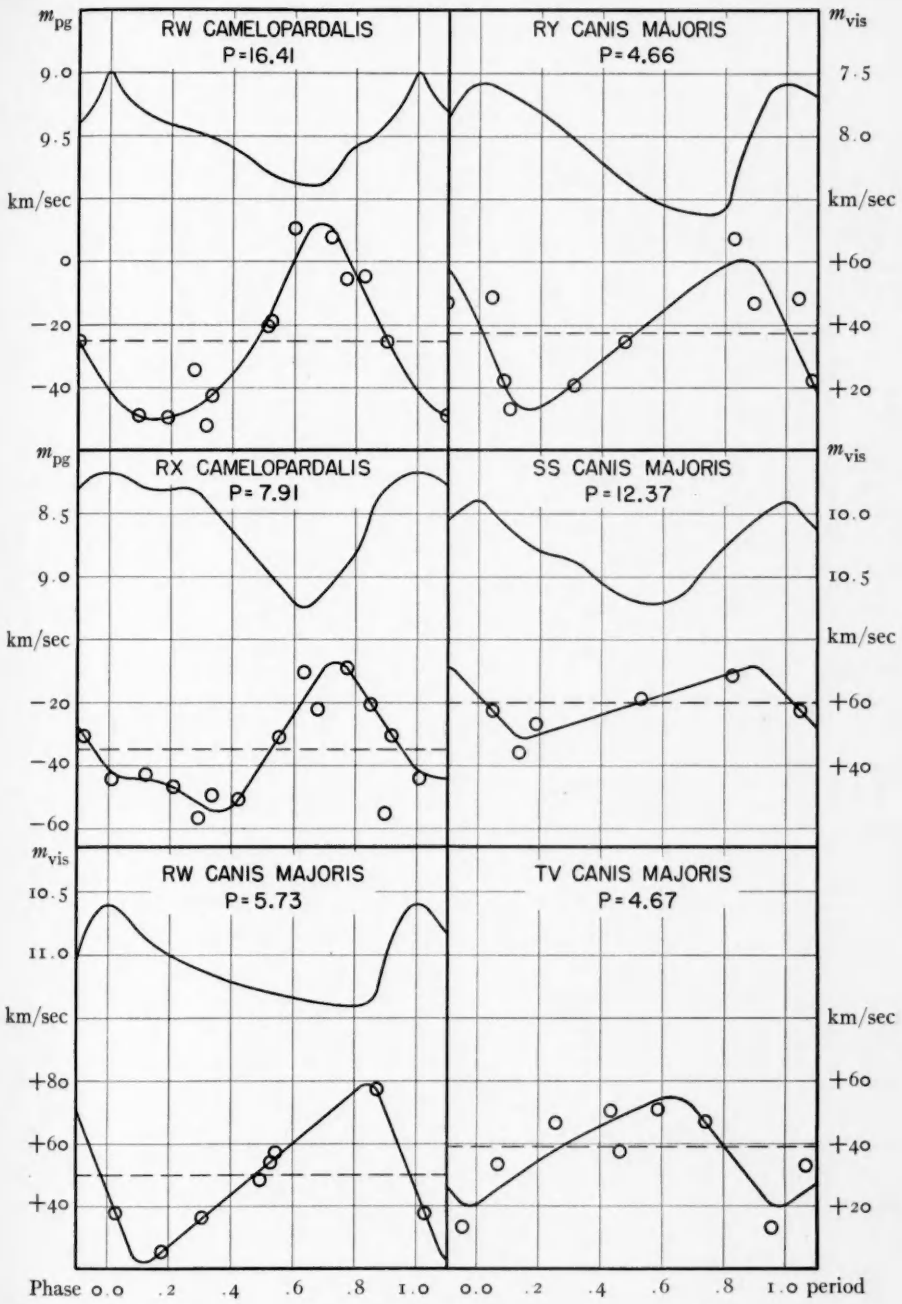

FIG. 3.—Light- and velocity-curves

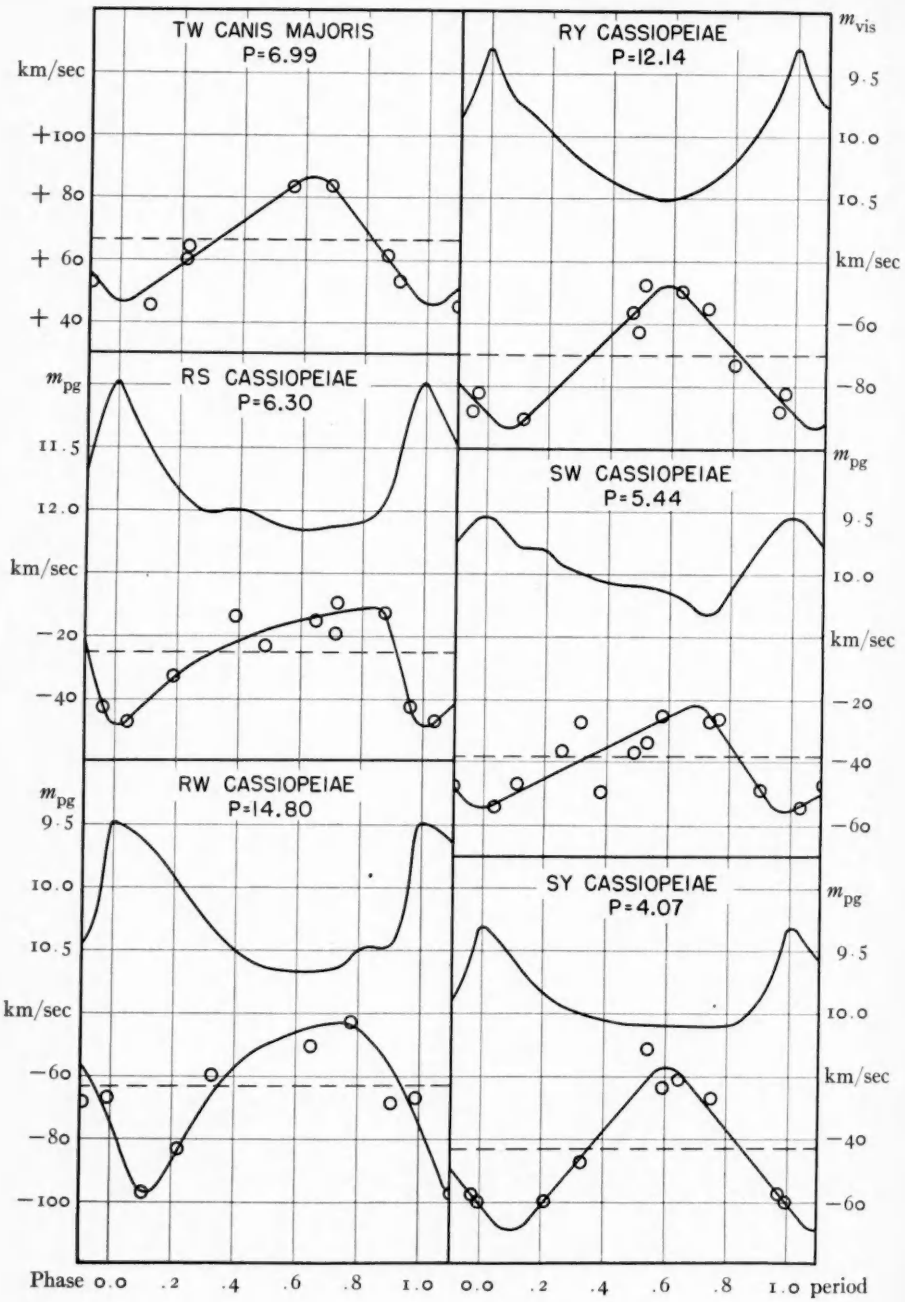

FIG. 4.—Light- and velocity-curves

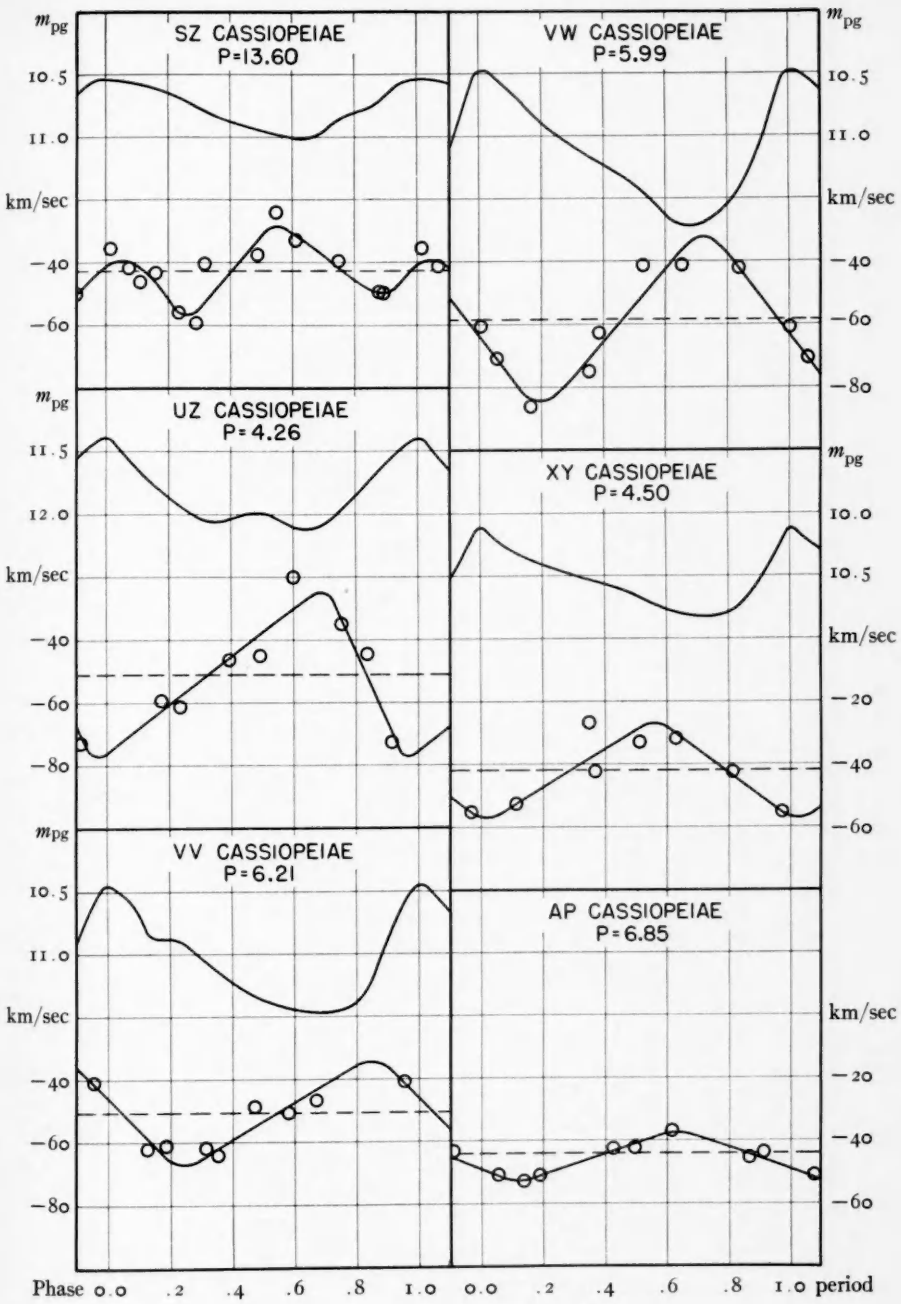

FIG. 5.—Light- and velocity-curves

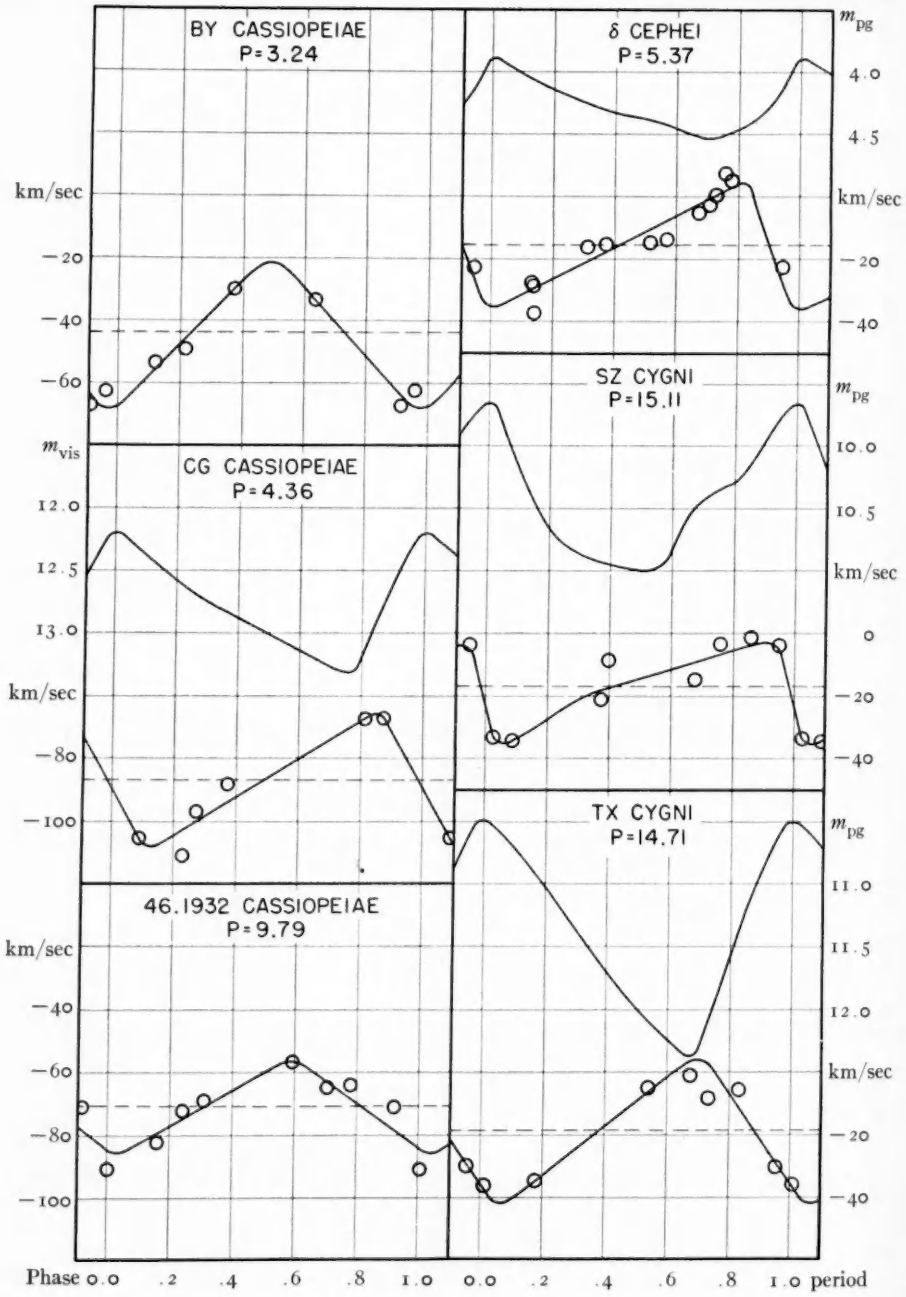

FIG. 6.—Light- and velocity-curves

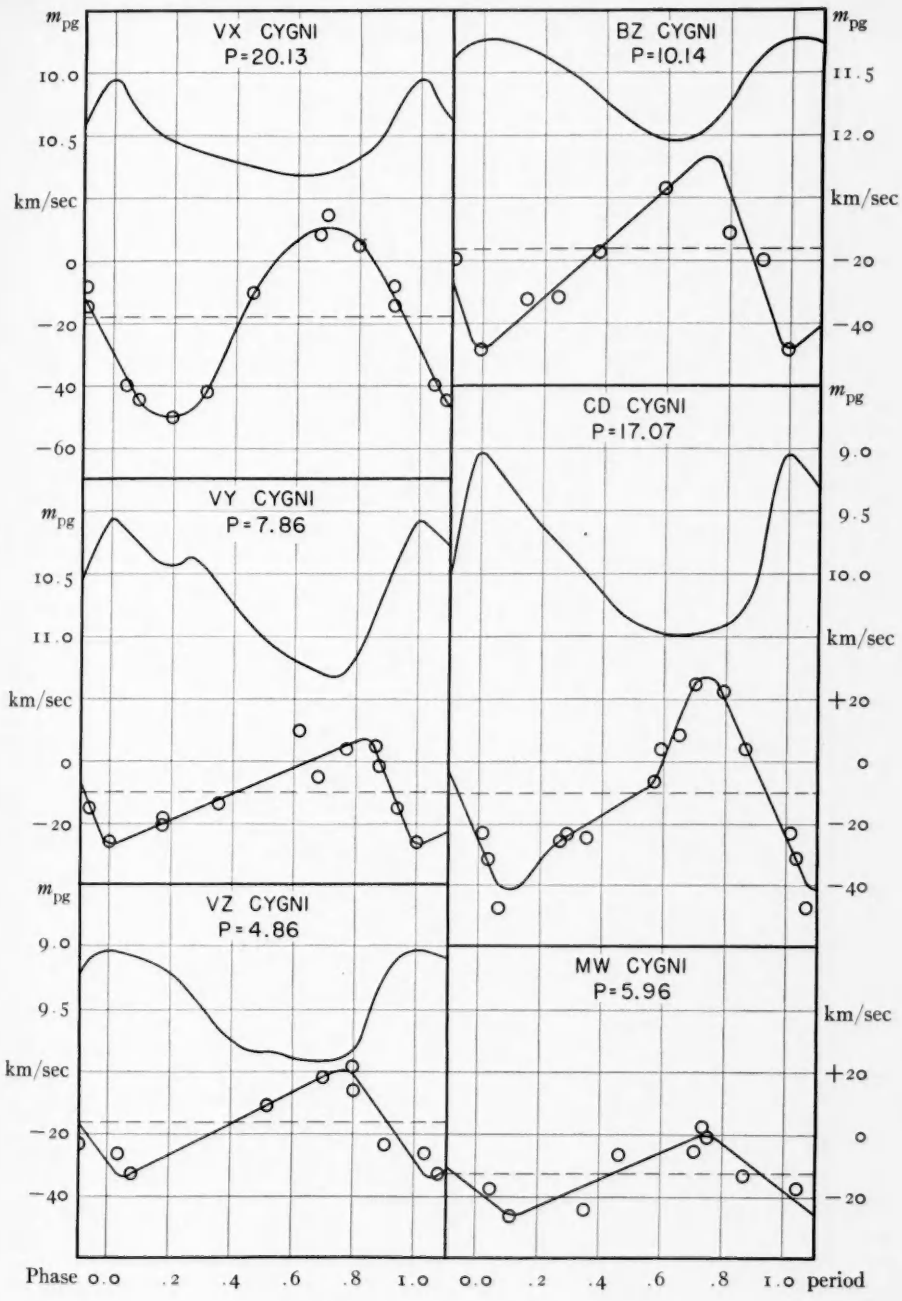

FIG. 7.—Light- and velocity-curves

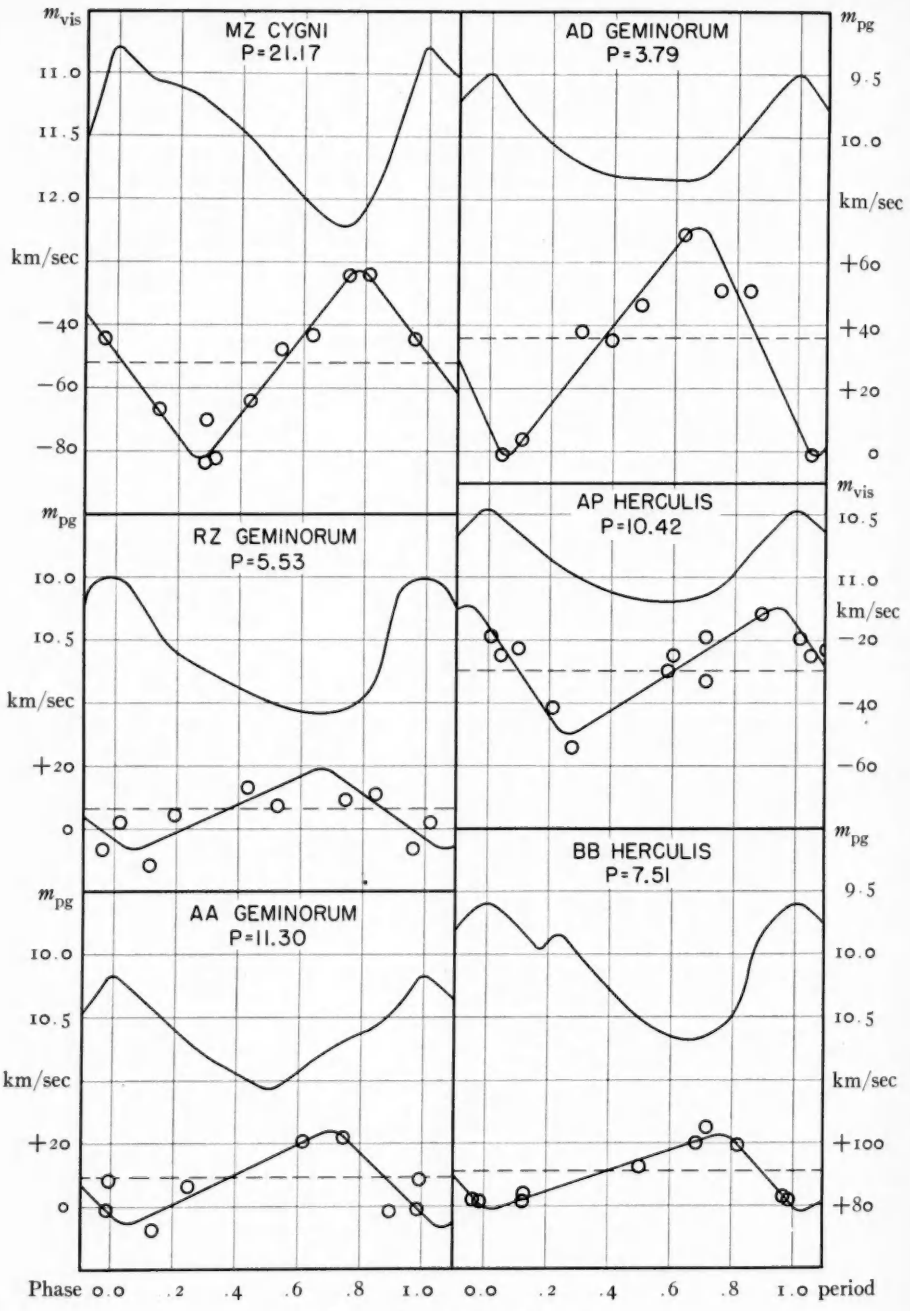

FIG. 8.—Light- and velocity-curves

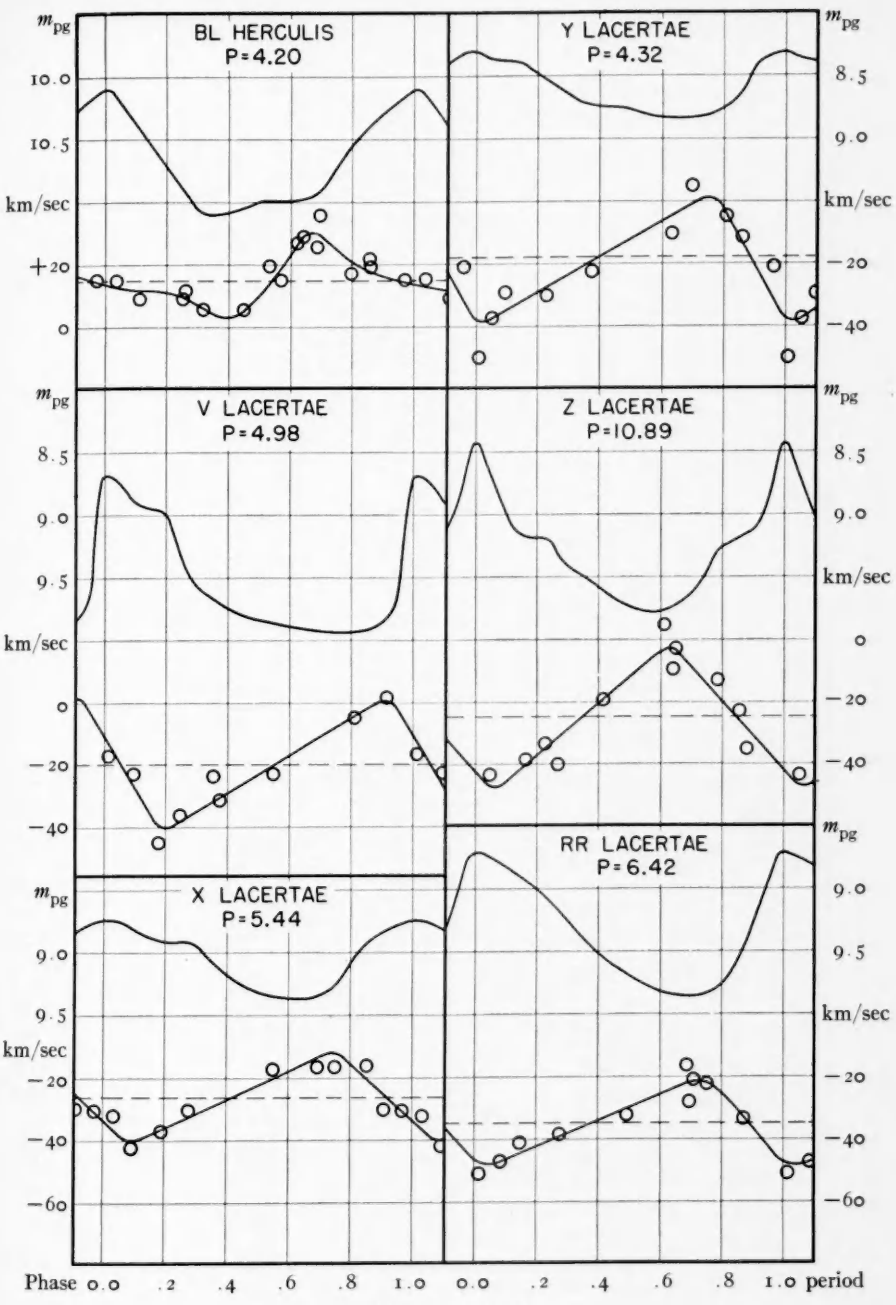

FIG. 9.—Light- and velocity-curves

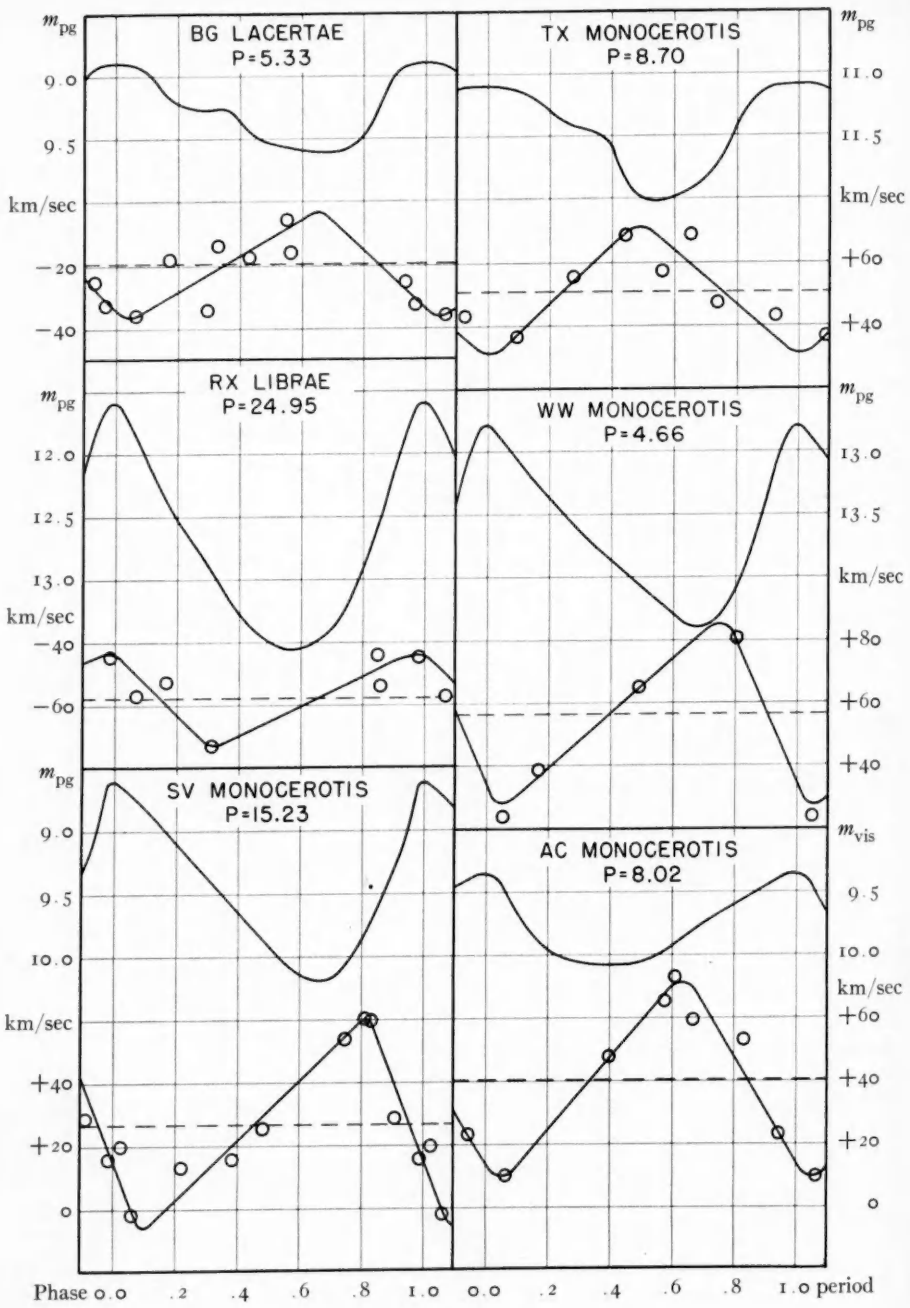

FIG. 10.—Light- and velocity-curves

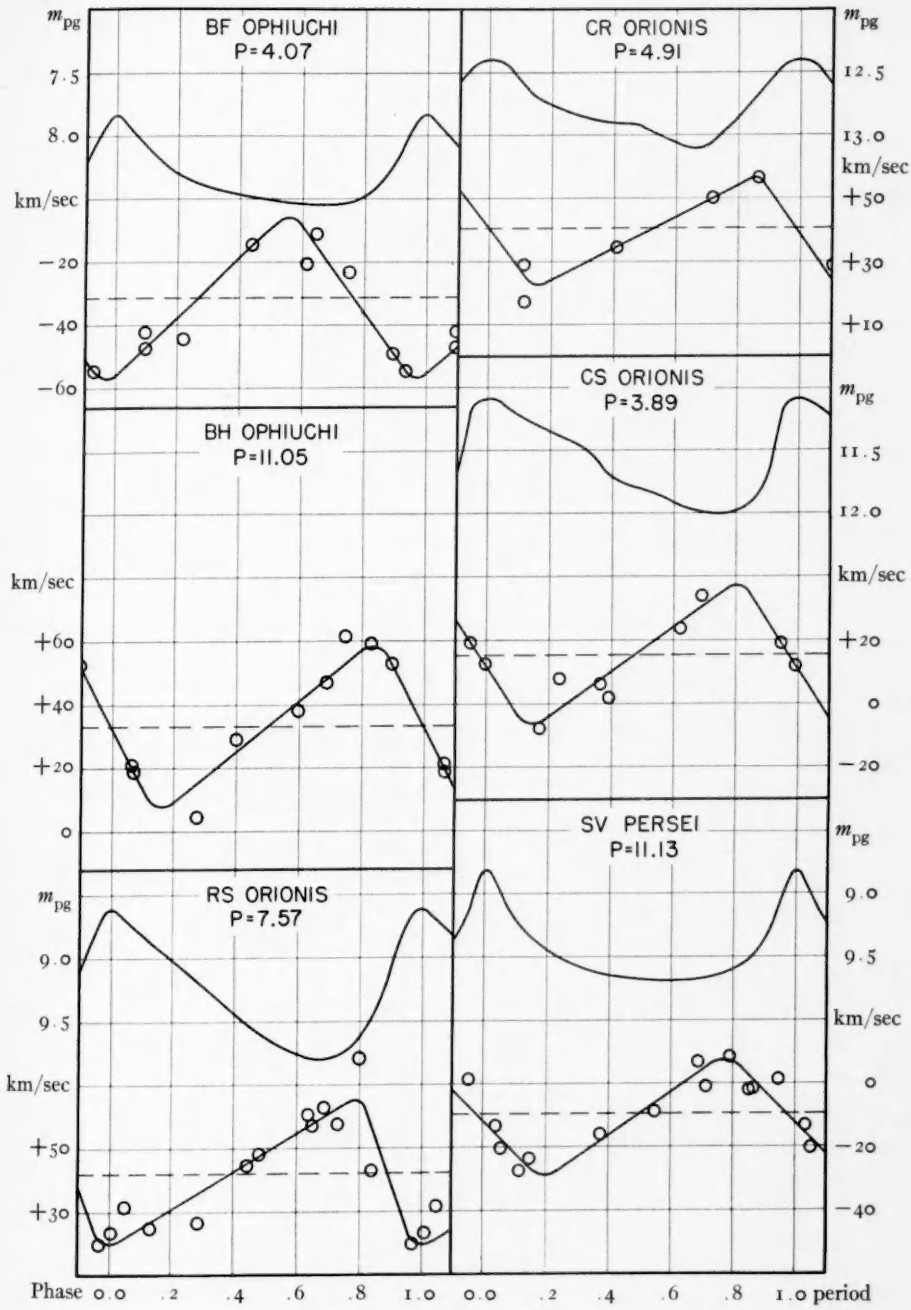

FIG. 11.—Light- and velocity-curves

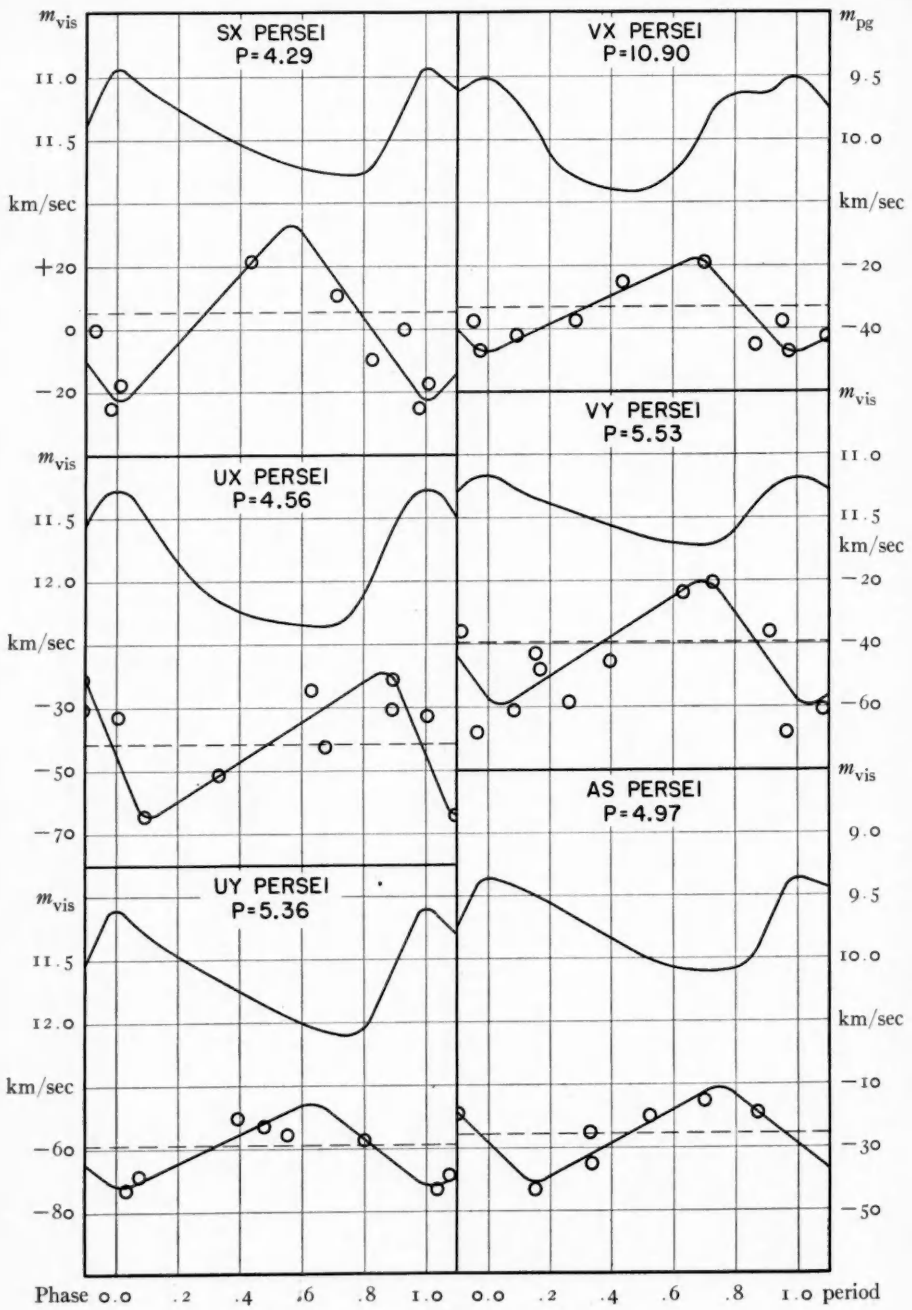

FIG. 12.—Light- and velocity-curves

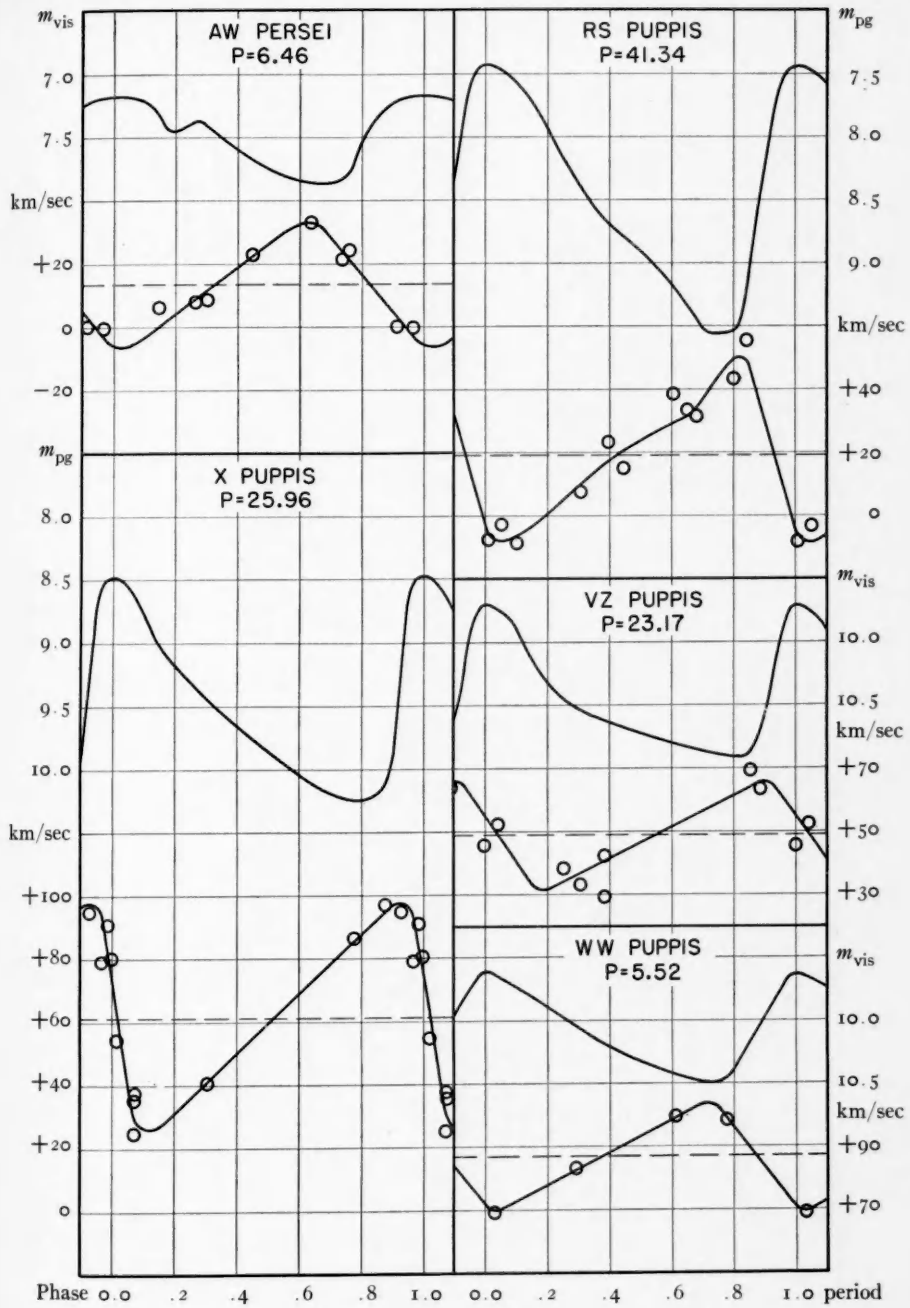

FIG. 13.—Light- and velocity-curves

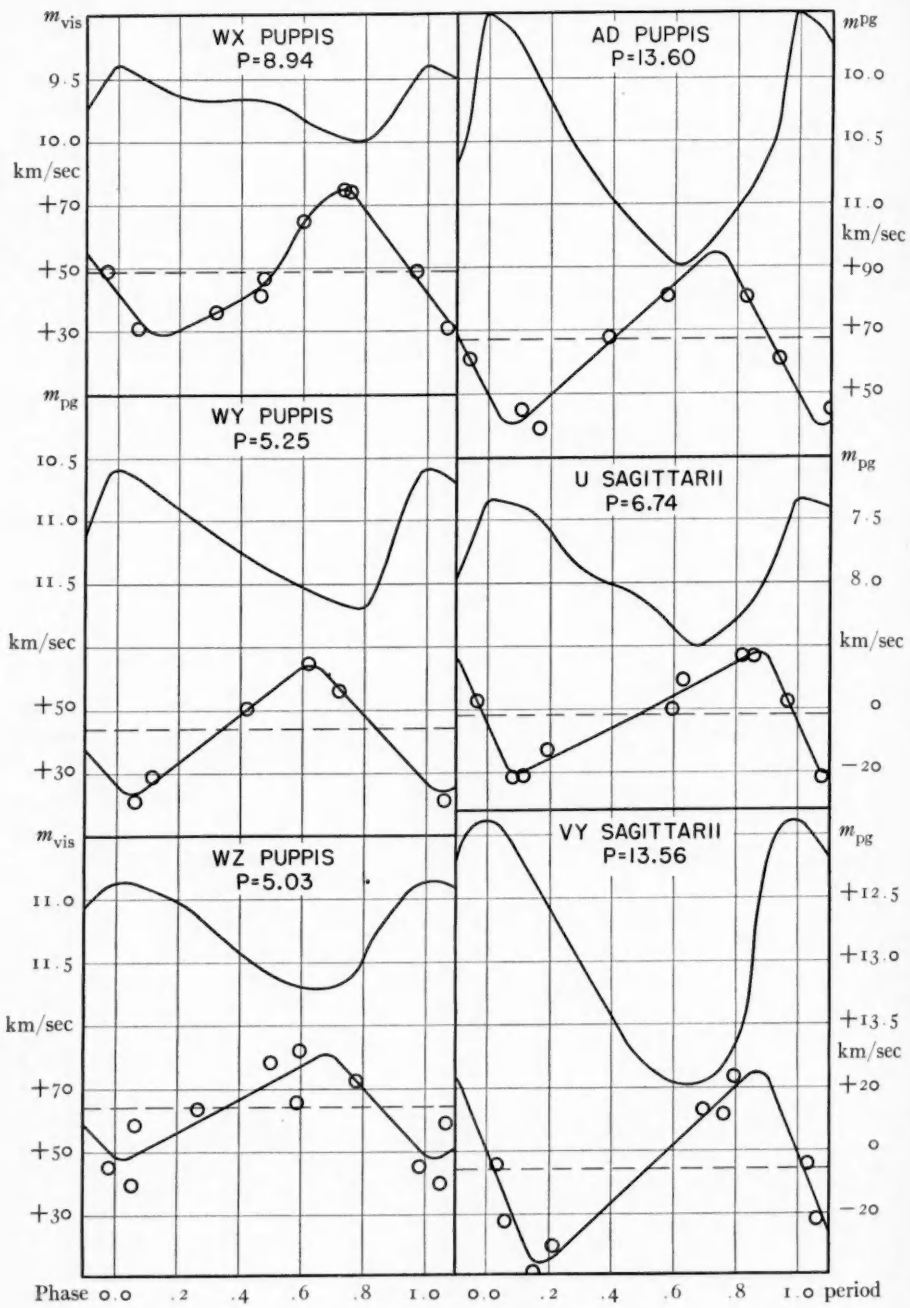

FIG. 14.—Light- and velocity-curves

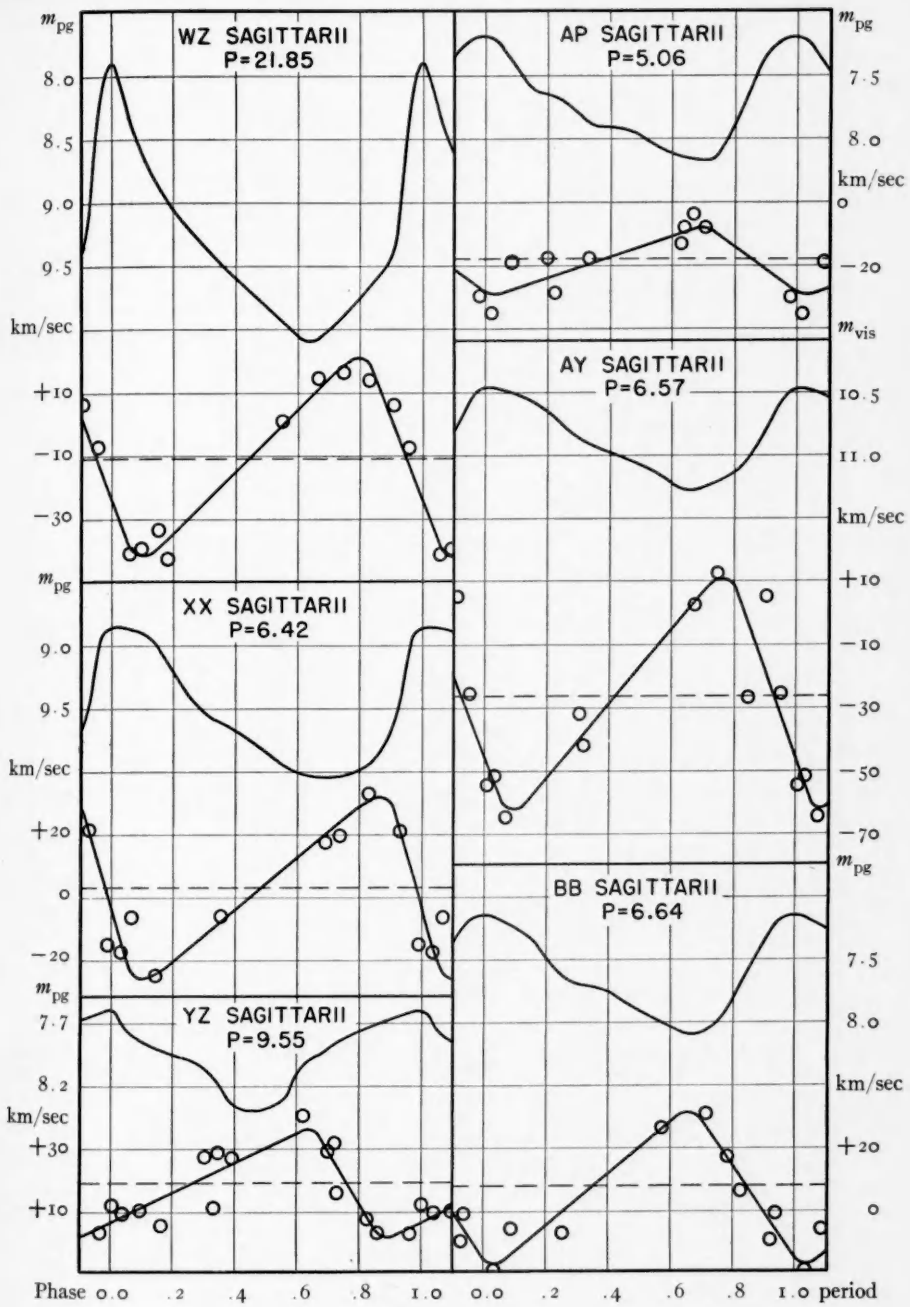

FIG. 15.—Light- and velocity-curves

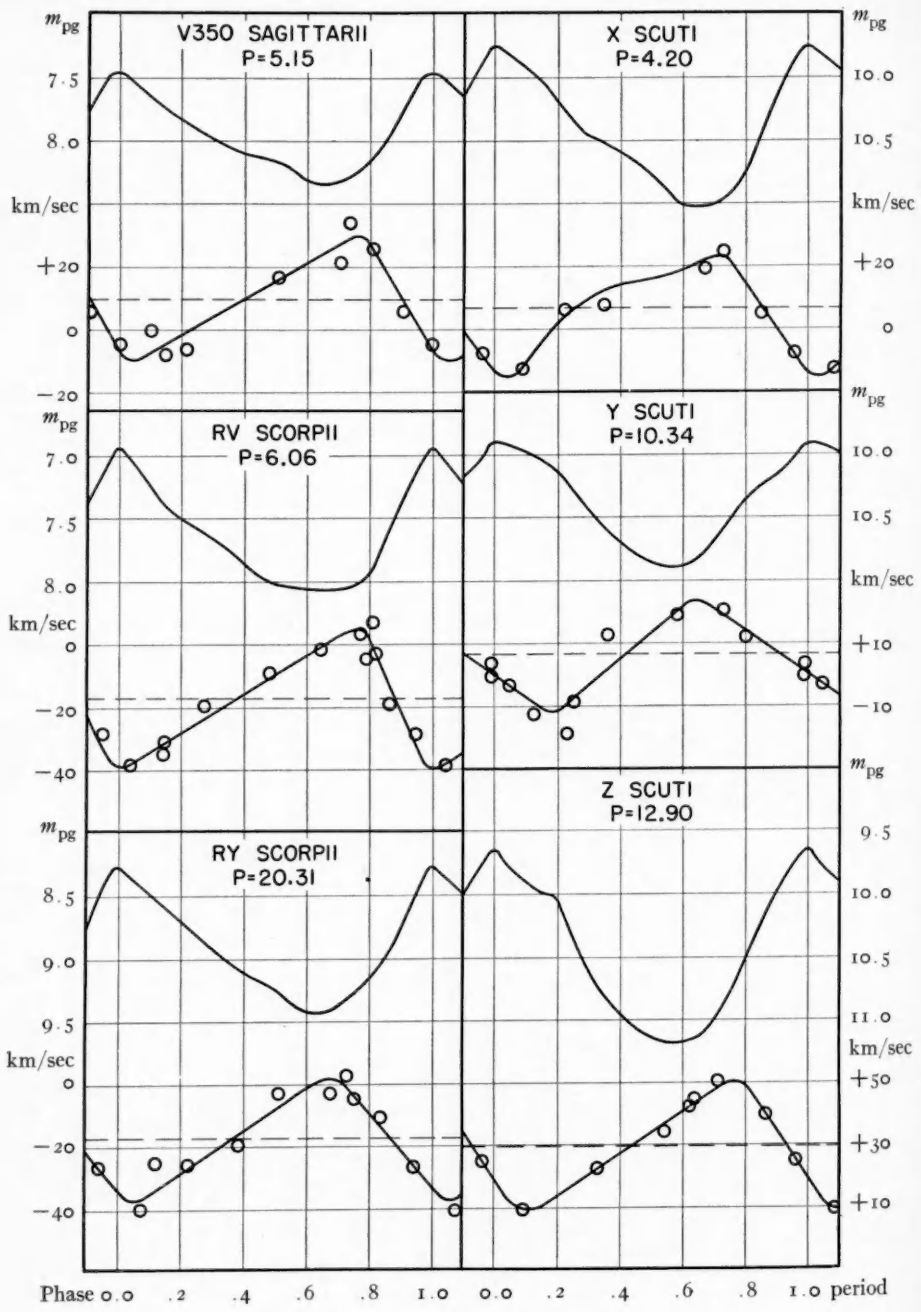

FIG. 16.—Light- and velocity-curves

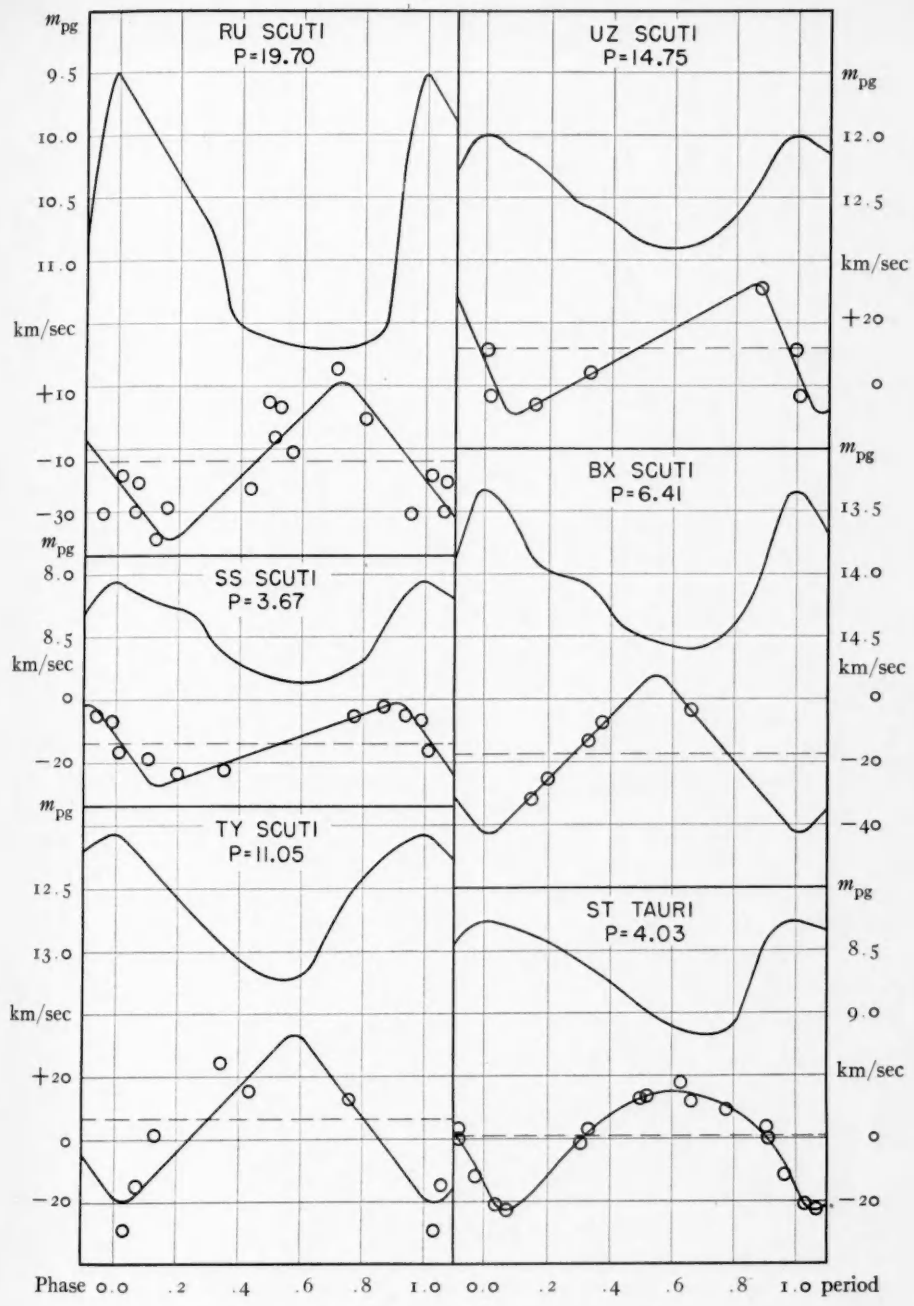

FIG. 17.—Light- and velocity-curves

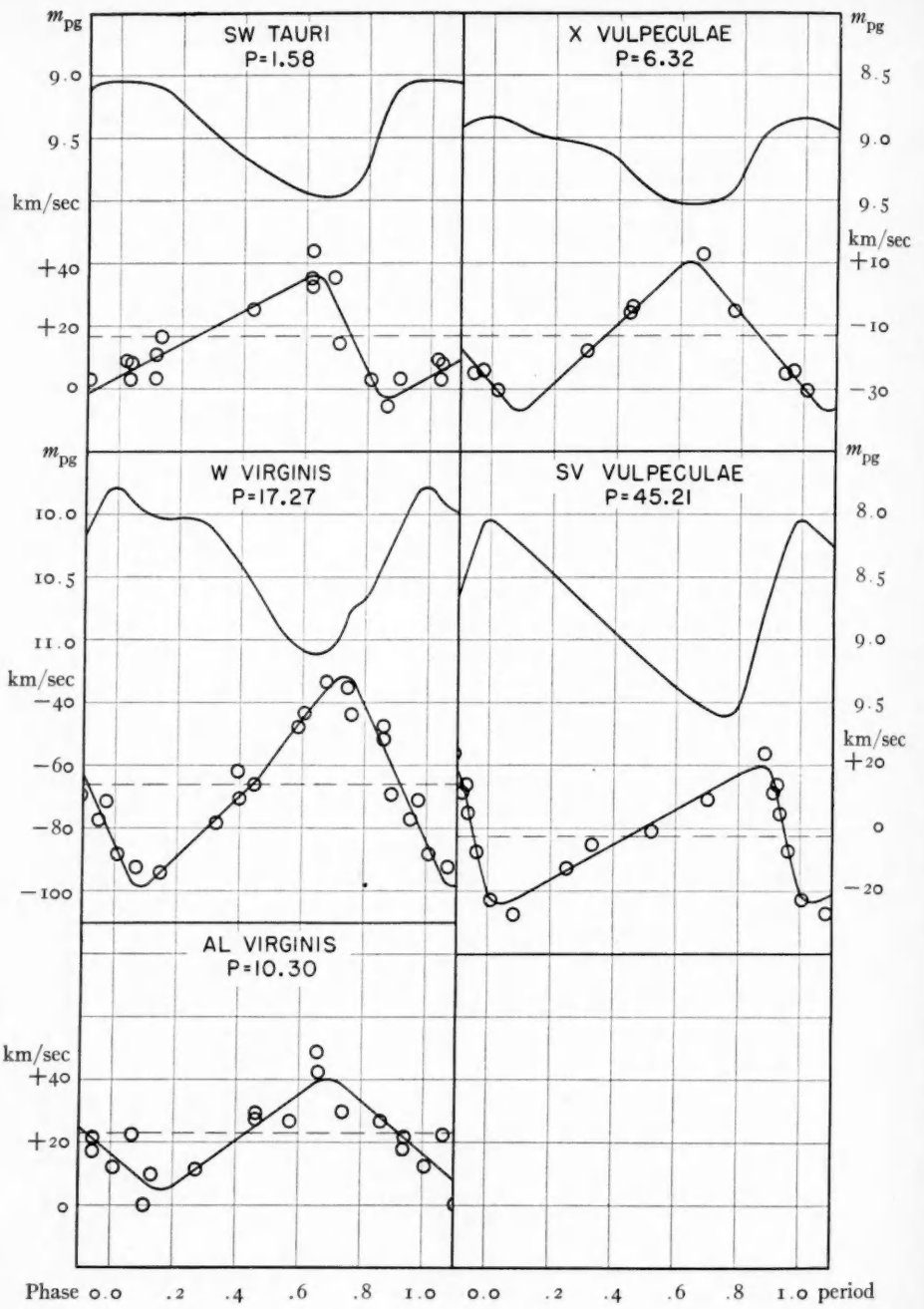

FIG. 18.—Light- and velocity-curves

In Table 4 the various data available for 155 Cepheids observed here and elsewhere are collected. Most of the columns need no explanation. The fifth and tenth give, in percentage of the period, the time from minimum to maximum light and from greatest velocity of recession to greatest velocity of approach, respectively. The eighth

TABLE 3

COMPARISON OF LICK AND MOUNT WILSON VELOCITIES

Star	Mag.	Spec.	Lick Vel.	Mt. W. Vel.	Diff.	No. of Plates
			km/sec	km/sec		
Boss 772	1.9	cF4	− 2.1	− 1.4	+0.7	4
1806	5.2	cG2	− 8.1	− 6.9	+1.2	6
4443	3.0	cG2	−20.9	−20.1	+0.8	13
4707	5.0	cF8	−11.3	− 9.8	+1.5	14
5229	2.3	cF7	− 5.4	− 1.3	+4.1	1
5255	4.1	cF4	−18.6	−14.6	+4.0	2
5676	3.2	cG1	+ 7.6	+ 3.3	−4.3	4
6135	4.8	cG0	−42.5	−46.5	−4.0	11

and ninth show the lag of the velocity-curve at maximum and minimum of light, respectively, also in percentage of the period. Positive signs indicate that the extreme values of the velocity-curve occur later than the corresponding extremes of the light-curve. The values in these four columns were read directly from the curves of light and velocity when plotted according to decimal fractions of the period.

TABLE 4

CHARACTERISTIC DATA OF CEPHEID LIGHT- AND VELOCITY-CURVES

Star	Period	Median m_{pg}	Light Range	Light $M-m$	Normal Vel.	Vel. Range	Vel. Lag at Max. Light	Vel. Lag at Min. Light	Vel. ϵ
	days		mag. pg.	% per.	km/ sec	km/ sec	% per.	% per.	% per.
U Aql	7.02	7.3	0.7	33	− 7.0	41.6	+ 2	+ 5	30
SZ Aql	17.14	10.4	2.0	34	+ 9.5	64	+15	+13	35
TT Aql	13.75	8.3	1.7	36	0.0	52	+10	+14	32
FF Aql	4.47	6.0	0.6	45	−14.4	14.2	+ 7	+ 6	36
FM Aql	6.11	9.6	1.2	39	−12.0	35	+24	+31	31
FN Aql	9.48	10.4	1.0	50	+ 8.0	40	+12	+17	44
KL Aql	6.10	10.0	1.6	33	− 2.5	32	.....	.....	.....
PZ Aql	8.76	13.0	1.1	40	−32.0	39	0	− 2	42
V 336 Aql	7.31	10.8	1.1	32	+11.5	53	+ 1	− 8	41
η Aql	7.18	5.0	1.6	32	−15.1	41.7	+ 6	+14	24
Y Aur	3.86	9.7	1.0	34	+ 8.5	39	0	− 3	36
RT Aur	3.73	6.0	1.3	27	+21.4	.....	+ 7	+14	20
RX Aur	11.62	8.3	1.0	43	−21.0	27	0	+ 9	33
SY Aur	10.14	9.5	1.0	46	− 2.0	30	−14	+ 6	26
YZ Aur	18.19	10.8	1.2	43	−20.5	58	+16	+16	43
AN Aur	10.29	11.8	1.0	46	− 9.5	37	−18	−10	38
AO Aur	6.76	11.7	1.7	37	−14.5	49	+ 5	+23	19
AS Aur	.....	11.8	.....	.....	+10.5	.....	.....	.....	.....
RW Cam	16.41	9.4	0.9	33	−25.5	62	+15	+ 2	46
RX Cam	7.92	8.7	1.1	36	−35.0	48	.....	+10	.....
RW CMa	5.73	12.0	1.3	21	+50.0	57	+12	+ 5	27
RY CMa	4.66	9.0	1.5	26	+37.5	48	+17	+12	31
SS CMa	12.37	11.4	1.4	43	+60.0	22	+15	+32	25
TV CMa	4.67	11.9	1.1	20	+39.0	35	− 2	−17	35
TW CMa	7.00	10.6	1.0	35	+66.5	40	+ 1	− 2	38
176.1932 CMa	.....	9.5	1.0	.....	+56.5	.....	.....	.....	.....
l Car	35.52	4.8	1.4	37	+ 4.1	40.3	0	+10	27
RS Cas	6.30	11.6	1.2	37	−25.0	38	+ 1	+20	17
RW Cas	14.80	10.1	1.2	36	−63.0	53	+12	+10	37
RY Cas	12.14	11.0	1.8	43	−70.0	46	+ 7	+ 2	48
SU Cas	1.95	6.8	0.2	46	− 7.0	22.0	− 3	− 5	48
SW Cas	5.44	9.9	0.7	27	−38.0	32	− 1	− 4	29
SY Cas	4.07	9.7	0.8	28	−43.0	52	+10	−11	49
SZ Cas	13.60	10.8	0.5	36	−42.5	28	.....	.....	.....
TU Cas	2.14	8.3	0.7	39	−22.2	35.1	+ 2	+ 8	33
UZ Cas	4.26	11.9	1.3	35	−51.0	52	− 3	+ 4	27
VV Cas	6.21	11.0	1.0	31	−50.5	33	+24	+15	39
VW Cas	5.99	11.1	1.2	33	−58.5	52	+20	+ 5	48
XY Cas	4.50	10.5	0.6	29	−42.0	30	+ 2	−16	46
AP Cas	6.85	12.5	1.1	31	−44.5	16	+13	.....	49

TABLE 4—*Continued*

Star	Period	Median m_{pg}	Light Range	Light $M-m$	Normal Vel.	Vel. Range	Vel. Lag at Max. Light	Vel. Lag at Min. Light	Vel. ϵ
	days		mag. pg.	% per.	km/ sec	km/ sec	% per.	% per.	% per.
BP Cas	1.51	11.6	1.5	.....	−41.0	48	.....	.....	.....
BY Cas	3.24	12.0	0.9	46	−44.0	44	− 3	− 6	49
CG Cas	4.36	12.6	0.9	25	−87.0	42	+13	+ 9	28
46.1932 Cas	9.79	11.0	1.0	.....	−71.0	29	.....	.....	46
AK Cep	7.24	12.1	1.0	33	−52.5	53	0	− 9	24
δ Cep	5.37	4.2	0.6	29	−15.6	39.5	0	+10	21
X Cyg	16.39	7.4	1.4	34	+ 9.3	56.1	+ 4	+ 4	34
SU Cyg	3.85	7.3	1.0	29	−35.8	47.0	+ 7	+13	23
SZ Cyg	15.11	10.3	1.3	50	−17.0	32	+ 6	+40	15
TX Cyg	14.71	11.4	1.9	33	−19.0	46	+ 7	+ 3	37
VX Cyg	20.13	10.4	0.8	37	−18.5	61	+18	+ 6	50
VY Cyg	7.86	10.7	1.2	27	−10.5	34	0	+ 9	18
VZ Cyg	4.86	9.5	0.9	33	−16.5	34	+ 5	+10	28
BZ Cyg	10.14	11.6	0.8	37	−17.0	61	0	+10	27
CD Cyg	17.07	9.8	1.5	33	−11.0	68	+10	+ 7	36
DT Cyg	2.50	5.9	0.4	48	− 0.5	17.0	0	− 3	51
GH Cyg	7.82	10.8	1.4	27	−16.5	37	.....	.....	.....
GL Cyg	3.37	14.6	1.2	.....	−58.5	.....	.....	.....	.....
MW Cyg	5.96	10.5	1.0	29	−13.0	26	+12	+ 3	39
MZ Cyg	21.17	12.8	2.0	26	−52.0	59	+27	+ 4	49
V 343 Cyg	11.93	14.8	1.3	.....	−93.0	.....	.....	.....	.....
V 386 Cyg	5.24	10.5	1.0	.....	−16.5	.....	.....	.....	.....
β Dor	9.84	5.0	1.4	49	+ 5.8	37.0	0	+ 6	43
W Gem	7.91	7.4	1.1	32	− 0.7	33.4	− 8	+ 5	19
RZ Gem	5.53	10.6	1.1	33	+ 6.5	25	+ 6	0	40
AA Gem	11.30	10.6	0.9	49	+ 9.5	30	+ 6	+20	35
AD Gem	3.79	9.9	0.8	36	+36.0	72	+ 6	+ 3	38
ζ Gem	10.15	4.5	0.6	50	+ 6.8	28.5	0	− 5	55
AP Her	10.42	11.9	1.4	42	−29.5	40	+27	+36	33
BB Her	7.51	10.1	1.0	34	+91.0	24	+ 2	+11	27
BL Her	4.20	10.6	0.9	.....	+14.5	27	.....	.....	.....
V Lac	4.98	9.3	1.2	23	−20.0	40	+19	+13	29
X Lac	5.44	9.1	0.6	38	−26.5	29	+ 9	+12	34
Y Lac	4.32	8.6	0.5	33	−18.0	39	+ 2	+ 8	27
Z Lac	10.89	9.1	1.4	42	−25.0	44	+ 7	+ 5	43
RR Lac	6.42	9.3	1.2	30	−35.0	26	+ 5	+ 3	32
BG Lac	5.33	9.2	0.7	31	−19.5	34	+ 4	− 4	40
RX Lib	24.95	12.6	1.9	42	−58.0	29	+32	+40	33
CN Lyr	2.34	11.3	0.6	34	+22.0	40	.....	.....	.....
T Mon	27.01	7.3	1.6	32	+32.0	50.5	0	0	32

TABLE 4—*Continued*

Star	Period	Median m_{pg}	Light Range	Light $M-m$	Normal Vel.	Vel. Range	Vel. Lag at Max. Light	Vel. Lag at Min. Light	Vel. ϵ
	days		mag. pg.	% per.	km/ sec	km/ sec	% per.	% per.	% per.
SV Mon	15.23	9.4	1.6	32	+26.5	66	+10	+14	29
SZ Mon	16.38	12.1	1.6	33	+35.0	60	.....	.....	.....
TX Mon	8.70	11.5	0.9	46	+51.0	40	+ 1	− 5	51
TZ Mon	7.43	11.6	1.2	35	+34.0	.....	.....	.....	.....
WW Mon	4.66	13.6	1.6	31	+56.5	57	+ 5	+ 6	30
XX Mon	.....	11.5	1.0	.....	+64.5	.....	.....	.....	.....
AC Mon	8.02	10.8	1.3	60	+40.5	62	+ 5	+24	41
S Mus	9.66	6.9	1.0	45	0.0	48	.....	+14	.....
S Nor	9.75	7.1	0.8	50	− 6.5	37.0	0	+14	36
Y Oph	17.12	7.3	0.9	47	− 6.1	19.8	+20	+ 3	64
BF Oph	4.07	8.2	0.7	32	−31.5	51	− 3	−13	41
BH Oph	11.05	13.0	2.3	.....	+33.0	50	+16	.....	32
RS Ori	7.57	9.2	1.2	31	+42.0	45	0	+10	21
CR Ori	4.91	12.8	0.7	34	+40.5	34	+15	+19	29
CS Ori	3.89	11.5	0.9	27	+15.5	43	+14	+ 7	34
κ Pav	9.11	5.1	0.8	48	+36.5	31.0	+ 9	+39	18
SV Per	11.13	9.3	0.9	40	− 9.5	36	+19	+17	41
SX Per	4.29	12.2	1.3	25	+ 5.5	56	+ 1	−19	45
UX Per	4.57	12.6	1.6	33	−41.5	46	+11	+10	24
UY Per	5.37	12.4	1.5	26	−59.0	26	+ 3	−11	39
VX Per	10.90	10.0	0.9	53	−33.0	30	0	+21	32
VY Per	5.53	12.3	1.0	32	−39.5	39	+ 4	+ 1	34
AS Per	4.97	10.6	1.2	27	−25.5	30	+15	+ 2	41
AW Per	6.46	8.8	1.2	32	+13.5	40	+ 3	− 5	40
X Pup	25.96	9.4	1.8	20	+61.5	71	+12	+14	19
RS Pup	41.34	8.4	2.1	23	+19.0	58	+ 5	+ 5	22
VW Pup	4.28	12.5	1.4	25	+24.0	41	+14	.....	.....
VX Pup	3.01	8.6	1.6	45	+12.0	40	.....	.....	.....
VZ Pup	23.17	11.6	1.8	18	+49.0	34	+19	+ 8	29
WW Pup	5.52	10.9	1.4	25	+87.0	34	+ 4	− 3	31
WX Pup	8.94	10.7	1.1	20	+49.0	46	+15	− 7	42
WY Pup	5.25	11.1	1.1	21	+44.0	41	+ 6	−16	42
WZ Pup	5.03	12.1	1.3	34	+64.0	34	+ 3	+ 3	34
AD Pup	13.60	10.5	2.0	38	+67.5	54	+ 8	+11	34
AP Pup	5.08	8.1	1.1	26	+42.5	.....	.....	.....	.....
AQ Pup	29.92	10.0	1.9	.....	+41.0	52	+17	− 5	38
AT Pup	6.66	8.7	1.5	26	+24.5	.....	.....	.....	.....
S Sge	8.38	6.3	1.0	34	−10.3	41.1	+ 3	+ 8	29
U Sgr	6.74	7.9	1.2	32	− 2.0	38	+ 9	+20	21
W Sgr	7.59	5.2	1.8	32	−25.0	41.7	− 2	0	21

TABLE 4—*Continued*

Star	Period	Median m_{pg}	Light Range	Light $M-m$	Normal Vel.	Vel. Range	Vel. Lag at Max. Light	Vel. Lag at Min. Light	Vel. ϵ
	days		mag. pg.	% per.	km/ sec	km/ sec	% per.	% per.	% per.
X Sgr	7.01	5.1	1.2	35	−13.5	30.4	+ 1	+10	26
Y Sgr	5.77	6.2	1.1	30	− 3.2	36.6	.....	.....	.....
VY Sgr	13.56	13.0	2.1	35	− 6.0	60	+17	+22	29
WZ Sgr	21.85	9.0	2.2	36	−11.0	62	+11	+16	30
XX Sgr	6.42	9.5	1.2	31	+ 2.5	57	+11	+18	24
YZ Sgr	9.55	8.0	0.8	36	+18.5	34	0	+17	19
AP Sgr	5.06	7.7	1.0	30	−18.0	21	+ 3	0	33
AY Sgr	6.57	12.0	1.4	34	−26.5	73	+ 9	+10	33
BB Sgr	6.64	7.6	1.0	32	+ 7.5	48	+ 4	− 2	38
V 350 Sgr	5.15	8.0	0.9	34	+ 9.5	39	+ 5	+10	29
V 377 Sgr	16.17	14.3	1.4	41	− 5.0	.....	.....	.....	.....
V 410 Sgr	13.78	13.3	1.5	41	+ 5.0	.....	.....	.....	.....
RV Sco	6.06	7.6	1.1	33	−17.5	43	+ 1	+10	25
RY Sco	20.31	8.9	1.1	36	−17.5	39	+ 6	+ 4	38
X Sct	4.20	10.4	1.2	36	+ 7.0	38	+ 4	+ 8	32
Y Sct	10.34	10.4	1.0	44	+ 6.5	36	+18	+ 8	54
Z Sct	12.90	10.4	1.6	42	+29.5	40	+10	+19	33
RU Sct	19.70	10.6	2.2	28	−14.0	50	+18	+ 1	44
SS Sct	3.67	8.4	0.9	38	−14.0	26	+14	+30	22
TY Sct	11.05	12.6	1.1	45	+ 6.5	53	+ 4	+ 3	46
UZ Sct	14.75	12.4	0.9	14	+12.0	41	+ 9	+25	23
BW Sct	3.82	12.7	1.6	.....	+ 1.5	37	.....	.....	.....
BX Sct	6.41	13.9	1.3	28	−17.5	50	.....	.....	.....
AA Ser	17.13	14.6	1.6	45	− 5.5	.....	.....	.....	.....
ST Tau	4.03	8.7	0.9	29	+ 1.0	38	+ 7	−10	46
SW Tau	1.58	9.5	0.9	32	+17.0	38	− 3	− 5	23
SZ Tau	3.15	7.0	0.6	63	− 3.2	21.9	+10	+25	48
R TrA	3.39	7.1	1.0	33	−18.9	32.0	+13	+ 5	41
S TrA	6.32	6.9	1.2	34	+ 2.0	38.0	+ 3	+ 6	31
W Vir	17.27	10.4	1.3	35	−66.0	67	+ 8	+ 9	35
AL Vir	10.30	9.9	1.1	40	+23.0	35	+16	+10	46
T Vul	4.44	6.4	0.9	30	− 1.4	35.3	+ 2	+ 4	28
U Vul	7.99	8.2	1.0	42	−11.7	37.6	.....	.....	.....
X Vul	6.32	9.2	0.7	34	−13.0	47	+ 9	− 4	46
SV Vul	45.21	8.8	1.6	24	− 2.5	44	+ 4	+11	16

DISCUSSION

In any statistical use of the data presented it should be kept in mind that the observations are too few to determine unique curves and that, in many cases, their features have been purposely adapted to preconceived notions obtained from well-determined curves previously published and by experience in drawing other curves in this present series. It is rather surprising to find that for 90 stars of the list the simple form of the δ Cephei curve, which is practically made up of two straight lines, represents the observations as well as any other. There are 16 stars, however, for which departures from the simple form seem to be required. RW Cam, RW Cas, and VX Cyg have rounded curves but no irregularities. For RX Aur, AO Aur, TV CMa, RS Cas, SZ Cyg, CD Cyg, RS Pup, and X Sct the curves have been drawn with humps on the ascending branch of the velocity-curve, while for WX Pup and W Vir there is a dip on this branch. The curve of RX Cam shows a striking double minimum which corresponds to the double maximum of the light-curve. A very similar irregularity may be noted on the curve of β Dor as drawn by Miss Applegate.[2] RS Pup, WX Pup, X Sct, and W Vir also show a marked resemblance to the mirror image of their light-curves. The curves of SZ Cas and BL Her are most irregular. Both have small ranges in light and velocity and probably should be classed as peculiar, although their spectra are typical for their respective periods.

FM Aql, AP Her, and RX Lib are peculiar in that the maximum velocity of recession occurs close to the time of maximum light. The photometric elements may need adjustment.

Hertzsprung[3] has studied the forms of light-curves of Cepheids in relation to period and has suggested that certain irregularities are characteristic of certain definite periods. Robinson,[4] who had at hand a much larger collection of photometric material, states that for periods less than about seven days the relation between light-curve and period is slight, but that for periods between 8.5 and 30 days a relationship certainly exists which has but few exceptions. The ve-

[2] *Ibid.*, **13**, 12, 1927.

[3] *B.A.N.*, **3**, 115, 1926.

[4] *Harvard Ann.*, **90**, 82, 1933.

locity-curves, as drawn in Figures 1–18, show little or no tendency to conform to set rules. In most cases the number of observations is not sufficient to show irregularities, but there is apparently a larger percentage of irregular curves among the stars with longer periods. Half the curves showing peculiarities have periods greater than 13 days, while of 36 stars with periods between 7 and 11 days only two have irregular velocity-curves.

The period is the fundamental characteristic of Cepheid variation. Numerous investigators have shown the relation of various physical properties of these stars to the period of the light-variation. The

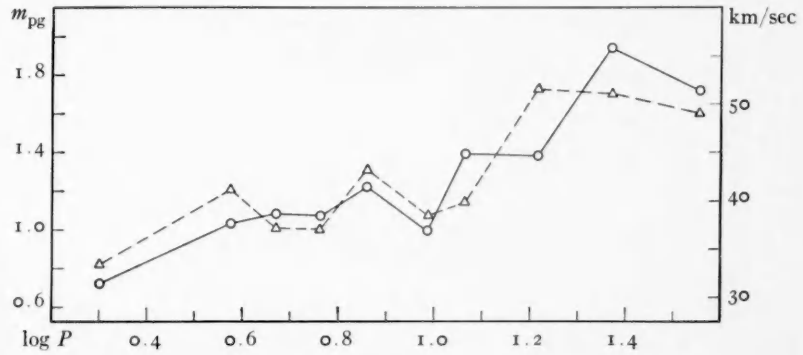

FIG. 19.—Relation of period to magnitude- and velocity-range. Normal points of magnitude-range, circles; velocity-range, triangles.

most striking relationships are those correlating period with luminosity, spectrum, light-range, and velocity-range.

In view of the large increase in the amount of data now available, it will be worth while to reconsider the relation of period to range and eccentricity of light-and velocity-curves, and the lag of velocity extremes.

In Figure 19 the photographic magnitude-range and the velocity-range have been plotted as ordinates and the logarithms of the periods as abscissae. The points represent normal places for ten groups taken according to the logarithm of the period. The numbers of stars in each group from left to right are: 6, 18, 18, 24, 24, 18, 12, 22, 5, 5. With the exception of a drop at about 10 days, there is, in the mean, a fairly steady increase in range, with increasing period,

from 0.7 to 1.9 mags. in light and from 33 to 50 km/sec in velocity. The decrease in range shown by the last group may or may not be real. It is based on only 5 stars and is considerably influenced by the small range of l Carinae both in light and velocity.

In statistical studies of stars of this kind a large dispersion is found when individual stars are considered. The scatter diagram (Fig. 20) showing the correlation between magnitude range-and velocity-range will serve to illustrate the amount of spread which may be expected.

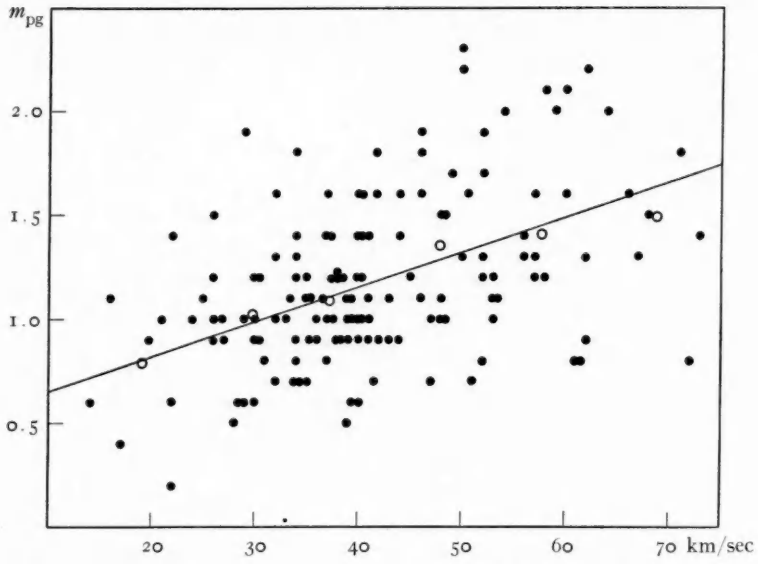

FIG. 20.—Magnitude- and velocity-range. The circles are normal points for groups taken according to velocity-range.

The dots represent individual stars, and the circles are the normal points for groups chosen according to velocity-range.

The same groups which were used in Figure 19 have been employed in Figure 21 to show the relation between period and steepness or eccentricity of the light- and velocity-curves. The mean values of the time elapsing between minimum and maximum light ($M-m$), and between maximum velocity of recession and approach (ϵ), expressed in percentage of the period, are plotted as ordinates. The well-known symmetry of the light-curves of stars of the ζ Geminorum type causes the notable drop in the curve of $M-m$ in the region

of phase 10 days, but this drop is not so prominent in the diagram showing the steepness of the velocity-curves. In general, there is an increase of eccentricity with period in both curves.

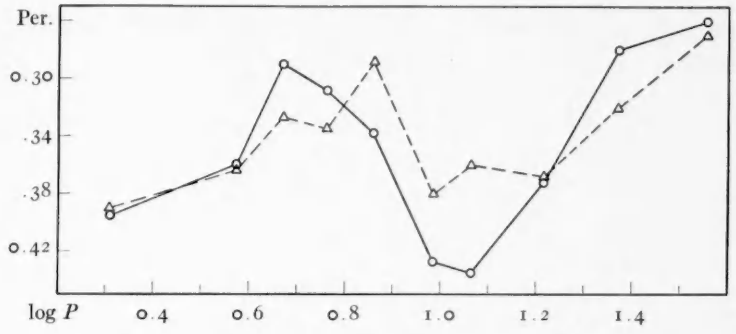

FIG. 21.—Relation of period to asymmetry of light- $(M-m)$ and velocity- (ϵ) curves. Normal points of $M-m$, circles; of ϵ, triangles.

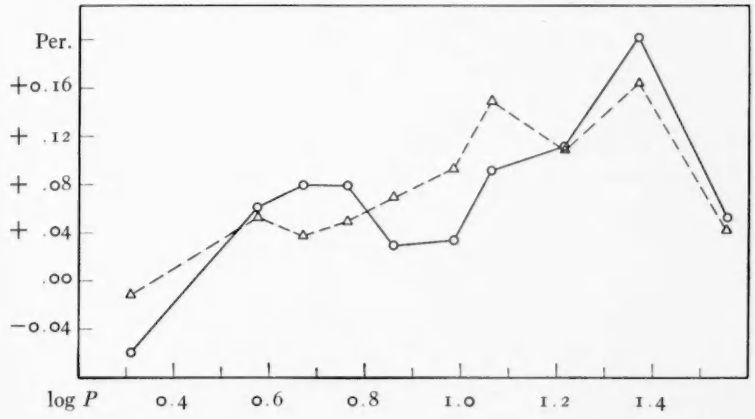

FIG. 22.—Relation of period to lag of velocity extremes at maximum and minimum light. Normal points of lag at maximum light, circles; at minimum light, triangles.

The curves of Figure 22 show the relation of period to the lag of the velocity extremes at maximum and minimum light. The same groups are used as for the preceding figures, and the lags are given in percentages of the period. The differences between the curves are, of course, related to the differences in eccentricity shown in Figure 21. There is apparently an increase of lag with lengthening period

up to periods of about 30 days, beyond which it falls off considerably. The lag varies up to about 20 per cent of the period and averages 6.9 at maximum light and 7.4 per cent at minimum light. These values may be affected by inaccuracy of the photometric elements used in drawing the velocity-curves and also to some extent by the arbitrary manner in which the curves are drawn.

The writer is greatly indebted to Miss Ada Margaret Brayton for much assistance in plotting the light- and velocity-curves and in preparing the material of this paper for publication.

CARNEGIE INSTITUTION OF WASHINGTON
MOUNT WILSON OBSERVATORY
July 1937

THE TESTING OF DIFFRACTION GRATINGS BY KNIFE EDGE AND BY INTERFEROMETER

HENRY G. GALE

ABSTRACT

Knife-edge and interference tests for an optical surface are compared and are shown to be of about equal sensitiveness. Both methods may be used to test periodic errors and error of run, in either plane or concave gratings. The use of knife-edge tests for error of run in the case of concave gratings is discussed, and quantitative results are deduced for the case of a slanting slit. The use of interference for testing the periodic error in a plane grating is illustrated. The effect of lack of straightness in the ruled lines of the grating is discussed briefly.

The testing of lenses and mirrors by viewing them with the eye close behind a knife edge set to interrupt the image of a point is well known and has often been described. It seemed worth while to attempt to secure a comparison of the sensitiveness of this method with interferometer tests.

Two surfaces of glass, one convex and the other concave, were prepared and polished as nearly as possible to perfectly spherical forms of equal curvature. The diameters were about 6 inches, and the radius of curvature about 21 feet. When placed in contact and illuminated with monochromatic light, the interference fringes, as viewed from directly above, were straight to within about one-twentieth of a fringe and were of uniform width, as is shown in Figure 1 (Pl. X). The knife-edge test showed nearly uniform illumination over the concave surface when the image of a point source was partially intercepted, as is shown in the photograph of Figure 2 (Pl. X).

When various errors were intentionally introduced into the concave surface, the fringes were distorted, and the knife-edge tests showed the corresponding irregularities. Thus, in Figures 3 and 4 (Pl. X) the extreme edge of the mirror is decidedly flattened and the center is high; the fringes bend in the direction indicating a thicker air film between the two test surfaces at the edge and a thinner air film in the center. The knife-edge test indicates a longer radius of curvature for the outer zone and a shorter radius at the

center. Figures 5 and 6 (Pl. X) indicate two photographs taken when an irregular error of about one fringe had been intentionally introduced.

With a spherical surface of diameter $2a$ and of radius of curvature r, the depth d of the center below the edges is given by $d = a^2/(2r - d)$, or, if we neglect d in comparison with $2r$,

$$d = \frac{a^2}{2r}$$

and

$$\Delta d = \frac{a^2}{2r^2}\,\Delta r,$$

which gives the relation between small changes in d and the corresponding changes in r. It is interesting to compute the change in r corresponding to a change of $\lambda/20$ in d in the case of a mirror $6''$ (15 cm) in diameter and of radius $21'$ (640 cm). This gives

$$\frac{0.00005}{20} = \frac{(7.5)^2}{2(640)^2}\,\Delta r\ ;$$

$$\Delta r = \frac{2 \times 409600 \times 0.00005}{20 \times 56.25} = 0.036 \text{ cm}\ .$$

This indicates that an error in depth of the mirror corresponding to $\lambda/20$ would cause a change of focus of about $1/3$ mm if the difference in level occurs between center and edge. This is about the limit for errors easily detected by interference; and, while it is near the limit for actual setting of the knife edge for radius, this departure would be indicated by the unequal rate of darkening at center and edge. If the change is more abrupt, occurring, for example, in half the distance from center to edge, the change in radius would be four times as great, or 1.4 mm, an amount which could be detected perhaps more easily by the knife edge than by the interferometer, as the central and outer portions would not be cut off exactly together. These considerations, as well as a study of the conditions represented by the figures, indicate that interferometer tests and knife-edge tests are of the same order of sensitiveness. It seems more convenient to test flat surfaces by interference when suitable standard

PLATE X

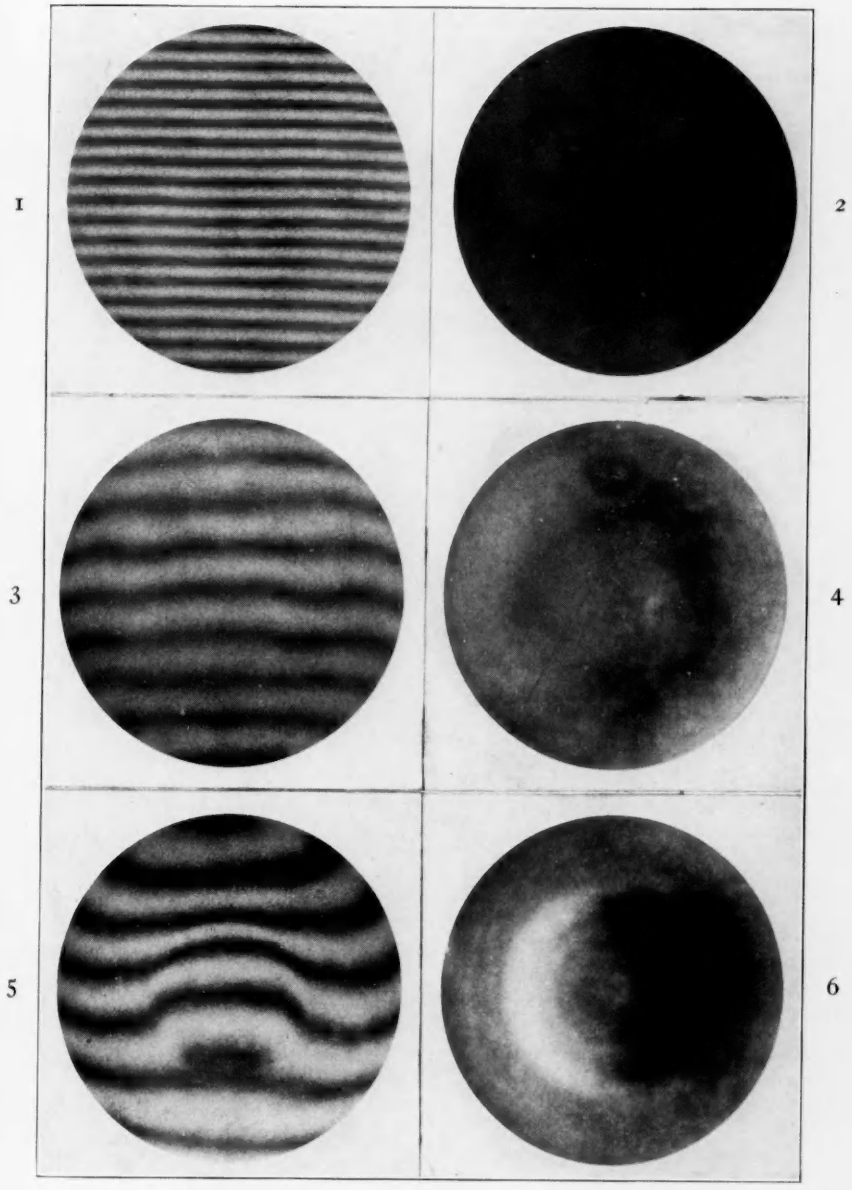

INTERFEROMETER AND KNIFE-EDGE TESTS OF CONCAVE SURFACES

UNIV. OF MICH.

flats are available, and to test concave surfaces by the knife-edge test. It is, of course, entirely feasible to reverse the process and test a flat surface (in combination with an accurate spherical surface) by the knife-edge test, and to test concave surfaces by interference as suggested above or by the well-known method of the Twyman interferometer, using a point source of light.

It is a fairly common practice to test the accuracy of the rulings of a diffraction grating by using a knife edge held in the focal plane. The image of a monochromatic line in the focal plane receives light from all parts of the ruled surface. If the grating is perfect and if the line is gradually intercepted, the light fades out evenly over the entire ruled surface when observed by an eye placed close behind the knife edge. If, however, there are inequalities in ruling, the regions of larger and shorter spacing send light slightly to one side or the other of the image produced by the average spacing. If, for example, in an Eagle mounting the incident and refracted rays are at the left of the normal, the region of smaller spacing throws the light to the left of the proper position and those of longer spacing throw the light to the right. If the knife edge is introduced from the left, therefore, the region of the grating ruled with less than average spacing will darken first. If the knife edge is introduced from the right, the region ruled with larger than average spacing will darken first. If a pinhole or a narrow slit is used instead of a knife edge at the proper setting, the portions of the grating which are correctly ruled will remain bright, while those which are incorrectly ruled will appear dark.

If a point source is used instead of a slit, and if the grating is viewed through a pinhole placed on the image of a spectral line in the focal plane, a single bright strip will be observed across the grating, uniformly illuminated if the grating is perfect, but interrupted by dark portions whenever the grating space is too large or too small. If the point source is raised or lowered, the bright strip is raised or lowered. If the point source is moved to the right, the light will disappear except for such portions of the grating as are ruled with an appropriately greater spacing; and, similarly, if the point source is moved to the left, light will come to the pinhole only from parts of the grating ruled with appropriately shorter spacing.

In testing the gratings ruled at the Ryerson Physical Laboratory recently, Mr. O'Donnell suggested setting the slit at a slight angle (1° or 2°) with the grating lines. This gives, in effect, a continuous set of point sources displaced vertically from one another, and horizontally as well. If the slit is rotated, for example, in a counter-clockwise direction, top to the left, each point on the slit will be slightly nearer to the spectrum line than the points below it. The grating, as viewed through a pinhole in the focal plane, may now be considered to be illuminated by a series of horizontal strips, each illuminated by a point on the slit. The adjustment of the pinhole is made so that a bright strip crosses the middle of a grating for the correct or average spacing. The upper and lower edges of the bright strip will now no longer be straight, however, if the spacing is not uniform. If the slit had been vertical, a bright strip of width two or three times the length of the slit, depending upon the angle of diffraction, would appear across the grating, which would be interrupted at all places where the spacing is too wide or too narrow. But if a slanting slit is used, points along the upper edge of the strip observed before will send light to the pinhole from points higher on the slit wherever the spacing is slightly less than the average, and light will again appear through the pinhole for points correspondingly higher on the grating. Points lower down on the slit will send light to the pinhole from points lower down on the grating, wherever the grating space is slightly too wide. The band of light will now be continuous, instead of interrupted as with a vertical slit; but instead of a straight band, as in the case of a perfect grating, the band will be curved, moving up where the grating spaces are narrowing, and moving down where the grating spaces are widening. A short periodic error will give rise to vertical strips superposed on the general curve, which indicates errors of run. The amount of error between two points of the ruling detected by this arrangement is easily calculated. A grating recently ruled on the new dividing-engine at Ryerson Laboratory was tested in this way. It was placed in an Eagle mounting and was adjusted for λ 5461 in the third order. The grating was ruled with 6000 lines per centimeter. If m represents the order, a the grating space, λ the wave-length, and θ_1 and θ_2 the an-

gles of incidence and refraction, and if $\theta_1 = \theta_2 = \theta$ in the Eagle mounting,

$$m\lambda = 2a \sin \theta$$

(for m and λ constant); and

$$0 = 2\, da \sin \theta + a \cos \theta\, d\theta ,$$

since the angle of diffraction alone changes, while the angle of incidence remains constant.

$$da = -\frac{a}{2 \tan \theta}\, d\theta .$$

The negative sign means merely that θ decreases as a increases, i.e., $d\theta$ positive corresponds to da negative and vice versa. For a change da in grating space, there will be a change dp in the position of the spectrum line, and $dp = r\, d\theta$, where r is the distance from the slit or spectrum line to the grating. But $r = R \cos \theta$, where R is the radius of curvature of the grating. Therefore $dp = R \cos \theta\, d\theta$. A lateral displacement dp of the spectrum line corresponds to a lateral displacement $-dx$ at the slit ($\pm d\theta_1 = \mp d\theta_2$), and $dx = \alpha dy$ where α is the angle of inclination of the slit and dy is the vertical distance between two points which have a horizontal displacement dx with respect to each other.

$$\alpha\, dy = -R \cos \theta\, d\theta .$$

But since $d\theta = -(2 \tan \theta\, da/a)$ and $m\lambda = 2a \sin \theta$, we have

$$\alpha\, dy = R \cos \theta \frac{2 \tan \theta}{a}\, da = \frac{2R \sin \theta\, da}{a} = \frac{R\, m\lambda\, da}{a^2}, \quad da = \frac{\alpha a^2}{mR\lambda}\, dy .$$

This equation means that two portions of the grating show maximum (or minimum) brightness through the observing pinhole when two points on the slit at a distance dy from each other are illuminated. To determine this distance, the slit is covered first from above and then from below, or a narrow opening is moved up and down on the slit to locate the position y_1 on the slit corresponding to the edge of

maximum brightness of a portion, A, on the grating. The position of y_2 is determined in the same way for a position B on the grating.

Instead of locating the points A and B with reference to y_1 and y_2 at the slit, it is often more convenient to get them as fractions of the length z of the rulings. In general, two points separated a distance y on the slit will appear to be a distance y apart at the image, and the light from them will appear to come from two points a distance z apart, vertically on the surface of the grating.

In the third order of an Eagle mounting for green light, this reduces nearly to $dy = d(z/2)$, that is, a point in the focal plane illuminated by a slit of length dy will receive light from a portion of the rulings of length dz, where $dz = 2\,dy$ and

$$da = \frac{\alpha a^2 dz}{2mR\lambda}.$$

It is usually more convenient in testing and in photographing to use a knife edge in the focal plane instead of a pinhole. The upper (or lower) ends of the astigmatic images of the slit then vary in vertical position across the surface of the grating, as in Figure 7 (Pl. XI), just as the narrower band from a pinhole would vary. In the case of Figure 7, $\alpha = (1/60)$, $a = (1/6000)$, $dz = 0.5$ cm between the positions A and B, which are 5 cm apart, $\lambda = 0.00005461$, $m = 3$, and $R = 640$. The difference in width of the rulings at A and B is then

$$da = \frac{\alpha a^2 dz}{2mR\lambda} = \frac{\frac{1}{60} \times (\frac{1}{6000})^2 \times 0.5}{2 \times 3 \times 640 \times 0.00005461} = \frac{1}{900{,}000{,}000}\ \text{cm},$$

that is, the difference in grating space at the two points A and B, 5 cm apart, for which $dz = 0.5$ cm, is 1/900,000,000 cm or 1/150,000 of a grating space, or 1/25,000 fringe.

If the change had varied uniformly between the two points, the error in position of the spacings would have been the average error times the number of spacings, N, or

$$N\left[\left(\frac{a + a + da}{2}\right) - a\right] = \frac{N da}{2}.$$

PLATE XI

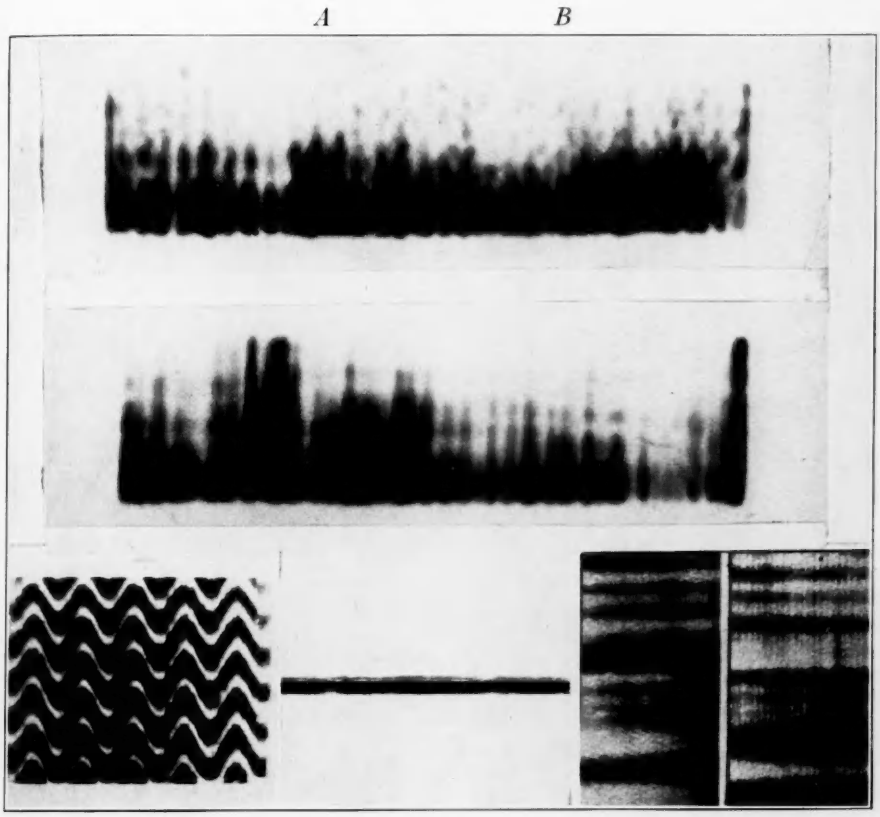

7 AND 8, KNIFE-EDGE TESTS OF ERROR OF RIM, WITH INCLINED SLIT; 10, PERIODIC ERROR AS SHOWN BY INTERFEROMETER; 11, IMAGE OF HORIZONTAL SLIT WHEN RULINGS ARE NOT STRAIGHT; 12, APPEARANCE OF GRATING WHEN KNIFE-EDGE IS INTRODUCED FROM BELOW AND ABOVE

UNIV. OF MICH.

In this case, $N = 5 \times 6000$, and ϵ, the error in position of the spacings at B with reference to those at A as a fraction of the grating space, is

$$\epsilon = \frac{5 \times 6000}{2} \times \frac{a}{150{,}000} = \frac{a}{10}.$$

The average error, that is, the average difference in spacing from the mean spacing, would have been one-half of this, or

$$\bar{\epsilon} = \frac{a}{20},$$

which would not affect the definition seriously. In fact, the definition of this grating is about 95 per cent of the full theoretical value. The larger departures from the correct spacing, indicated by the longer lines at the very beginning and end of the grating, would send only a negligible amount of light to the image and would produce only an undetectable broadening of the spectrum lines.

In the case of the grating used in Figure 8 (Pl. XI), the departures are obviously considerably greater than in the case of Figure 7. This grating was not satisfactory. The resolving power was only about 75 per cent of the full theoretical value, and there was an undue amount of scattered light.

Mention has already been made of the fact that a periodic error causes the light to be broken up into vertical strips. These strips can be used to measure the periodic error. They have been studied by R. W. Wood.[1] The number of them occurring in the length of the grating gives the period of the error. As in any case of systematic variation in grating space, a focusing effect is produced, in front of and behind the grating; and the strip may be photographed by merely placing a photographic plate at the proper distance in front of the grating. The positions may also be found not only by focusing an observing telescope on the surface of the grating, as was done in this case, but by focusing it for the proper planes in front of and behind the grating.

[1] *Phil. Mag.*, **48**, 497, 1924.

Instead of the knife-edge method of investigating the periodic error, it is perhaps more convenient to use an interference method.

The arrangement of Figure 9 gives an immediate and simple test for periodic error. The two gratings used as back mirrors diffract monochromatic light of any order back to the separating plate. If the instrument is adjusted for horizontal fringes, and if one of the gratings is without periodic error, the periodic error of the other grating will be shown at once by periodic curvature of the fringes.

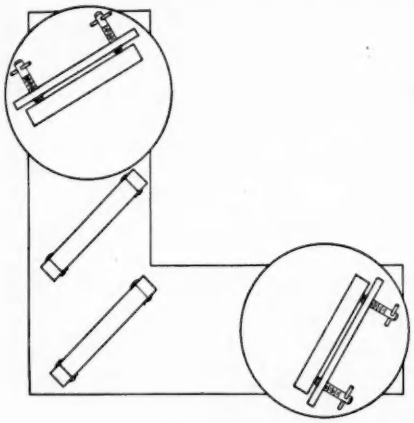

FIG. 9

The fringes of Figure 10 (Pl. XI) were photographed when a single periodic error of about one fringe had been arbitrarily introduced in one grating. More complicated errors give the fringes the corresponding curves, and these curves indicate the amount and nature of the errors. As a matter of fact, it is usually sufficient, when the errors are small, to deduce the nature and amount of periodic errors from the positions and intensities of the Rowland ghosts. Since, however, the intensities are periodic functions of the amount of error, considerable care must be exercised in interpretation, unless the errors are minute.

If the lines of the grating are not perfectly straight, certain aberrations will result. If a portion of the rulings slants to the right going up, light will be thrown too high in the spectral image. If the slant is in the opposite direction, light will be thrown too low. While the effect may be too small to affect the definition, it may produce the faint dots above the lines noticeable in Figures 7 and 8. This disturbance is of no importance for ordinary spectroscopic work but may cause serious difficulty if, for example, good images of a short horizontal slit are desired. If the ruled lines of the grating are not straight, the image of a horizontal slit will not be sharp, and if the changes of direction in the rulings are sudden, the main image of the slit will be accompanied by fainter false images above and below the

main image. If the grating surface is viewed by an eye placed just behind the focal plane, a horizontal knife edge moved down from above will first cut off light from all portions of the ruling which are slanted in a clockwise direction to the average direction of the rulings, and a knife edge moved up from below will first cut off light from portions of the rulings slanted in the opposite direction.

The photograph in Figure 11 (Pl. XI) shows the image of a horizontal slit, greatly overexposed to show the false images and scattered light from a horizontal slit. Figure 12 (Pl. XI) shows the appearance of the surface when viewed from behind the knife edge introduced from above and from below. As was to be expected, the light places in one correspond to the dark places in the other, and vice versa.

RYERSON PHYSICAL LABORATORY
UNIVERSITY OF CHICAGO
August 1937

THE BEHAVIOR OF FORBIDDEN OXYGEN LINES IN NOVAE

N. T. BOBROVNIKOFF AND J. M. MACQUEEN

ABSTRACT

The ratios of total intensities of the nebular pair of *O* I have been determined for eleven spectrograms of Nova Herculis, 1934. The mean for the seven more reliable spectrograms is 2.75 ± 0.14, but the individual values range from 2.11 to 3.71. A comparison with the data published by other investigators indicates that this variation may be real. Differences in the behavior of nebular forbidden lines in nebulae and novae are briefly discussed.

Among many forbidden lines occurring in celestial sources the analogous groups of *O* I and *O* III are of particular interest. Following Menzel, Boyce, and Payne,[1] we shall refer to the lines resulting from the D–P transition as nebular, and from the S–D transition as auroral, regardless of whether they actually occur in terrestrial aurorae or not.

The theory of these lines has been developed by Condon.[2] The transition probabilities are found to be:

Line	O III	O I
First nebular	180×10^{-4} sec^{-1}	75×10^{-4} sec^{-1}
Second nebular	60×10^{-4} sec^{-1}	25×10^{-4} sec^{-1}
Auroral	$18{,}000 \times 10^{-4}$ sec^{-1}	$20{,}000 \times 10^{-4}$ sec^{-1}

These figures indicate that the auroral lines should be from one to two hundred times as strong as the strongest line in one corresponding nebular pair. It is known that in the spectra of terrestrial aurorae the green line of *O* I is much stronger than the nebular line λ 6300. In a recent photometric investigation[3] the intensities of the nebular pair were given as 38 and 21 (i.e., in the ratio not of 3.0 but rather of 1.8), but the green line was so overexposed that its intensity on the

[1] *Proc. Nat. Acad.*, **19**, 581, 1933; *Harvard Reprint No. 93*.

[2] *Ap. J.*, **79**, 217, 1934. Similar results were derived by Stevenson, *Proc. R. Soc.*, A, **137**, 298, 1932.

[3] Vegard and Harang, *Geofys. Pub.*, **11**, 8, 1937.

same scale was indicated as (1080), making it approximately thirty times as strong as λ 6300. However, in nebulae the auroral lines are generally fainter than the nebular pairs, whereas in novae at certain stages of their development the auroral lines may equal in strength, or may even exceed, the corresponding nebular lines.[4]

This circumstance shows that the number of atoms in the S and D states cannot be calculated on the basis of inherent probability only and that physical conditions in the source should be taken into account. Indeed, this point has been brought up before.[5] However, the lines of the nebular pair have the upper metastable level, D, in common, and their ratio of intensity should depend only on the weight of the P-levels regardless of physical conditions in the nebulae or novae. The present paper deals with the observational material in regard to the ratio of intensities of the nebular pairs of *O* III and *O* I.

The behavior of the nebular pair of *O* III has been discussed by one of the writers.[6] No conclusive evidence that these two lines might behave differently in different sources has been found. Since that time several new investigations relevant to the problem have been published. Pearson[7] has found in the spectrum of Nova Aquilae, 1918, that the average displacement of various features of N_1 and N_2 was not the same. Thus for one feature (maximum *a*) the difference in the velocity factor between these two lines amounts to 0.33, or 10 km/sec. These figures represent means over long periods of time, and a claim is made that the upper limit of the probable error in the velocity factor at this wave-length is 0.10 for a sharp marking and 0.19 for a vague marking, for a single plate.

As far as the relative intensities of nebular lines of either *O* III or *O* I are concerned, there are few reliable data for discussion. Eye-estimates are uncertain and can at most give only an idea of the ratios. Wright's[8] ratios N_1/N_2 for twenty-seven nebulae vary from 1.3 to 2.5, with a mean of 1.7. It is evident that, since N_1 and N_2 are often the strongest lines in the nebular spectrum, visual estimates

[4] See Table 4 in Menzel, Boyce, and Payne, *loc. cit.*

[5] See, e.g., Grotrian, *Zs. f. Ap.*, **2**, 78, 1931.

[6] *Perkins Obs. Contr.* No. 4, 1936.

[7] *Ann. Solar Phys. Obs.*, **4**, Part III, 1936.

[8] *Lick Obs. Pub.*, **13**, 193, 1918.

are much affected by overexposure, which would reduce the ratio of intensities. A comparison of Wright's values with those by Berman (photometric study)[9] is available for the nebulae NGC 6543, 6572, and 7009. The ratio of intensities N_1/N_2 by Wright are 1.59, 1.60, and 1.53, whereas those by Berman are 2.65, 2.65, and 2.70, respectively. The ratio N_1/N_2 in NGC 7027 is given by Wright as 2.00 and by H. H. Plaskett[10] (photometric study) as 2.81. A large systematic difference between eye-estimates and spectrophotometric determinations of line intensities in Wolf-Rayet stars was found by Beals.[11]

It appears also that estimates of the ratios N_1/N_2 are strongly affected by instrumental factors. Thus, for the six nebulae for which Wright[12] gives estimates of N_1/N_2 both for the slit glass spectrograph (I_g) and the slitless quartz spectrograph (I_q), the mean values are 2.24 for I_g and 1.78 for I_q, with the extreme values (for the same nebula, NGC 7027) I_g 4.0 and I_q 2.0. It is clear that eye-estimates are not precise enough to settle the question whether the relative intensities of the nebular lines remain constant from nebula to nebula.

At the present time the spectrophotometric data on the ratio of intensities N_1/N_2 in nebulae consist of five nebulae investigated by Berman, two by Plaskett, and the Orion nebula by Minkowski. Berman obtains the mean ratio 2.62 with the extreme values of 2.42 and 2.70. Plaskett's values are 2.59 and 2.81, and Minkowski's[13] are 2.99. Thus there is some evidence that the ratio of intensities of the nebular pair of *O* III may change from nebula to nebula, but the amount of change involved is hardly greater than the uncertainty of measurement.

Eye-estimates for the intensities of the nebular pair of *O* I for five nebulae are given by Stoy.[14] The ratios vary from 1.3 to 3.0,

[9] *Lick Obs. Bull.*, **15**, 86, 1930.

[10] *Dom. Ap. Obs.*, **4**, 187, 1928.

[11] *Ibid.*, **6**, 127, 1934.

[12] *Loc. cit.*, Table II.

[13] *Zs. f. Ap.*, **9**, 202, 1934. A previous investigation (*ibid.*, **6**, 355, 1933) indicates a variation from 2.5 to 4.0, depending on the place in the nebula. Scheiner and Wilsing's results indicate a variation from 2.36 to 2.73 (*Ap. J.*, **16**, 234, 1902).

[14] *Lick Obs. Bull.*, **17**, 179, 1935. The author is conscious of the uncertainty of his estimates.

with a mean of 1.83. Of course these estimates are as likely to be affected by large systematic errors as are those of the nebular pair of *O* III.

The problem of the ratio of intensities in the nebular pair seemed worthy of investigation, as it was apparent from the visual inspection and photometric tracings of our plates of Nova Herculis, 1934, that there was a considerable difference in the behavior of the nebular lines of *O* I.

Eleven plates were selected for a photometric study. These were Y 170, Y 173, P 482, P 488, Y 176, P 491, Y 180, Y 184, Y 185, Y 187, and Y 189. All of them were taken on the Eastman Spectroscopic Emulsion IF with the autocollimating grating spectrograph in conjunction with the 69-inch reflector.[15]

The procedure adopted for the conversion of photographic densities into light-intensities was as follows. A series of six photometric squares was impressed on the plates just before the exposures. As a source of light in the densitometer a lamp was employed, with appropriate regulation of the current flowing through the filament. The light from the lamp passed through an Eastman filter No. 8, which transmits light uniformly between λ 5000 and λ 7000, with complete opacity to the violet of λ 4600.

The use of a filter of such a wide transmission range obviously eliminates the possibility of studying the variation of absolute intensity, or even of relative intensity of various features in widely separated spectral regions. This is the reason why no attempt has been made to study the behavior of the green auroral line as compared with the nebular pair. As far as the nebular lines λ 6300 and λ 6363 are concerned, it is thought that the material is suitable for discovering any large variation in their relative intensities. Owing to the use of the filter, an average gamma for the whole photographic plates was used rather than the gamma for λ 6300. No data are available on the IF plates, but from a study of similar emulsions[16] it appears that the true gamma for the nebular pair is considerably greater than the average gamma. This would make the ratio 6300/6363 systematically too large. This is an important point, as the

[15] Details are given in *Perkins Obs. Contr.* No. 2, Table 1, 1935.

[16] Webb, *J. Opt. Soc. Amer.*, **26**, 12, 1936.

average value found for the intensity ratio of these two lines is considerably below the theoretical ratio.

Among other factors to be considered in exact spectrophotometry, the following should be mentioned: (*a*) the difference in the exposure time for the star and for the photometric squares; (*b*) the difference in the temperature of exposure and development; (*c*) the variation of the temperature and the time of development; (*d*) the relative humidity in the spectrograph and in the darkroom; (*e*) the age of the developer, etc. Needless to say, all these factors must be taken into account if precise results are to be expected. None of them was considered when exposures on the nova were made, except that the temperature of the developer (Eastman D–11) was kept approximately constant (65° F) and the plates were developed five minutes. However, exact spectrophotometry is a thing of the future, and our methods, inadequate as they are, are those generally adopted in astronomical practice. A comparison of our data with those of other observatories does not show any marked systematic difference. The spectrograms were run through a Moll registering microphotometer, and galvanometer deflections at the interval of 1 A were converted into light-ratios in terms of stellar magnitudes.

The profiles of the lines are given in Figure 1. The general development of the nebular pair is clearly seen. The gradual increase in width of λ 6300 from 12.1 A on January 5 to 16.4 A on March 30 can be noticed at a glance. It is evident that the elimination of the continuous spectrum on the first four days is very difficult, owing to the presence of numerous absorption and emission lines, so that all the values of intensities of various features on these dates can be only a rough approximation.

From the very beginning of the emergence of the nebular lines, they were very sharply defined on either side. On the diagrams of Figure 1 the flanks are almost perpendicular. Considering that the width of the slit of the spectrograph, 0.05 mm, corresponds to about 1 A on the plate, we must conclude that there was almost no dispersion of velocity in the *O* 1 shell ejected from the nova, although the velocity of the shell increased from 290 km/sec to 390 km/sec between January 5 and March 30. This is the more remarkable because the increase in velocity was not constant, that is, the width of the

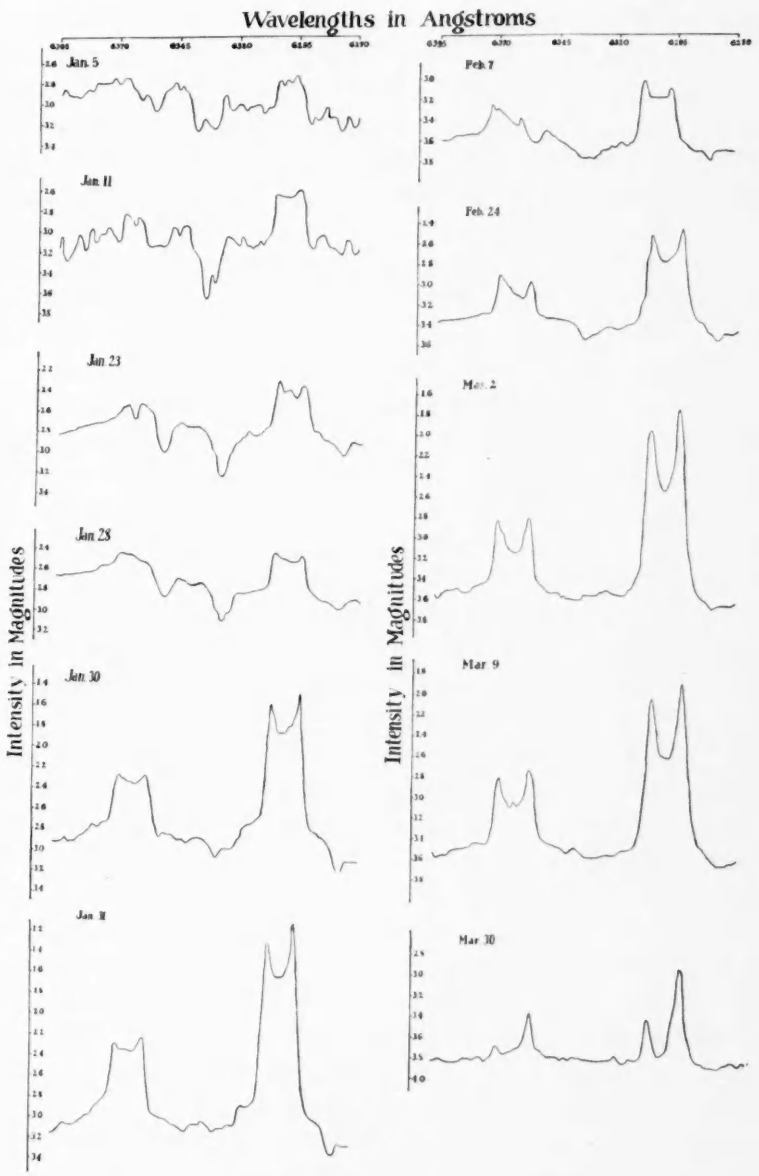

FIG. 1.—Photometric curves of the spectrum of Nova Herculis in the neighborhood of the nebular pair of *O* 1.

lines as a function of the time could not be represented by a straight line but rather by a sinusoid superimposed on a straight line.[17] It would seem that the *O* I shell (or prominence) was entirely separated from the rest of the nova ejections, otherwise we should expect some interference on the part of other atoms moving with different and often with much greater velocities. There is no evidence of a thermal distribution of velocities among the *O* I atoms which would have resulted in inclined flanks of the profiles, as shown by hydrogen lines on the same dates. From the similarity of the curves of increase in width of both the nebular lines of *O* I, we must infer that they originated in exactly the same volume of space.

One of the most interesting features of the profiles of the nebular lines is the presence of faint flanks on either side of the main emission lines. These flanks are noticeable on practically every tracing. In fact, on some dates they were strong enough to be measured.[18] Their width was in the neighborhood of 40 A, so that the maximum velocity of this outward shell was about 960 km/sec. The similar flanks in the *O* III nebulium lines of Nova Lacertae, 1936, were much more conspicuous.[19]

The general development of the profiles of the nebular pair is in accordance with the suggestion made by Menzel and Payne.[20] They postulate an emission of symmetrical jets with material more abundant along the line of symmetry. The profile is determined by the angle made by this line with the line of sight to the star. The middle of the resulting profile will be lower and lower with respect to its edges as the angle between these two directions changes from 90° to 180° (or to 0°). Since during the three months of observations the profiles underwent the change from the flat-topped structure to the middle without emission, we should infer that during this period the jets rotated through about 90°. This is in accordance with the shape of the curve correlating the time with the width of the lines mentioned above. It would seem also that the jets were not quite sym-

[17] *Perkins Obs. Contr.* No. 2, Fig. 1, 1935.

[18] *Ibid.*, Table 3.

[19] *Ibid.*, No. 6, 1937.

[20] *Proc. Nat. Acad.*, **19**, 641, 1933. Harvard Reprint No. 95.

metrical, as the red sides of the lines were getting progressively fainter. Needless to say, this picture of the *O* I jets is at variance with the profiles of other lines produced by atoms which must have moved through the *O* I jets without in the least affecting their development. The coexistence of different profiles is, indeed, one of the most baffling features of the nova spectrum.

Even if we confine our attention to the material producing *O* I forbidden transitions, the existence of the two jets is not sufficient to account for the faint diffuse flanks betraying the presence of *O* I atoms in a diffuse shell rather than in definite jets.

As to the difference in the profiles of the nebular lines, nothing can be said about the first four dates, owing to the presence of numerous absorption and emission lines belonging to other elements. On January 30 and 31 the dip in λ 6300 is much more pronounced than in λ 6363. The ratios of intensity (Table 1) of the middle of the lines for the two dates are 2.50 and 3.05, whereas the same ratios for the violet components are 3.45 and 4.05, and for the red components 3.04 and 3.83. On February 7 and 24 the profiles are quite different. On February 24 the red edge of λ 6363 is stronger than the violet (intensity ratio 1.18), but the situation is reversed for λ 6300 (intensity ratio 0.89). For the rest of the tracings the depression in the middle is more pronounced in λ 6300. It is evident, however, that the differences in the profiles are not very great and may conceivably be due to some instrumental factors or to the presence of faint absorption and emission lines.

For the study of the ratio of intensities of various features of the lines, the microphotometer tracings were reduced from stellar magnitudes to light ratios. Figure 2 gives an example of the resulting profiles for three dates. The total intensity of the line is defined as the area bounded on one side by the line of the continuous spectrum and on all other sides by the profile of the line. Whereas the profile of the line is influenced by the width of the slit and the length of the exposure, the total intensity should remain constant, and it is therefore considered more reliable than any other data. The difficulty lies in drawing the line of the continuous spectrum, especially so on the first four dates. The ratio of intensities for these dates, given in

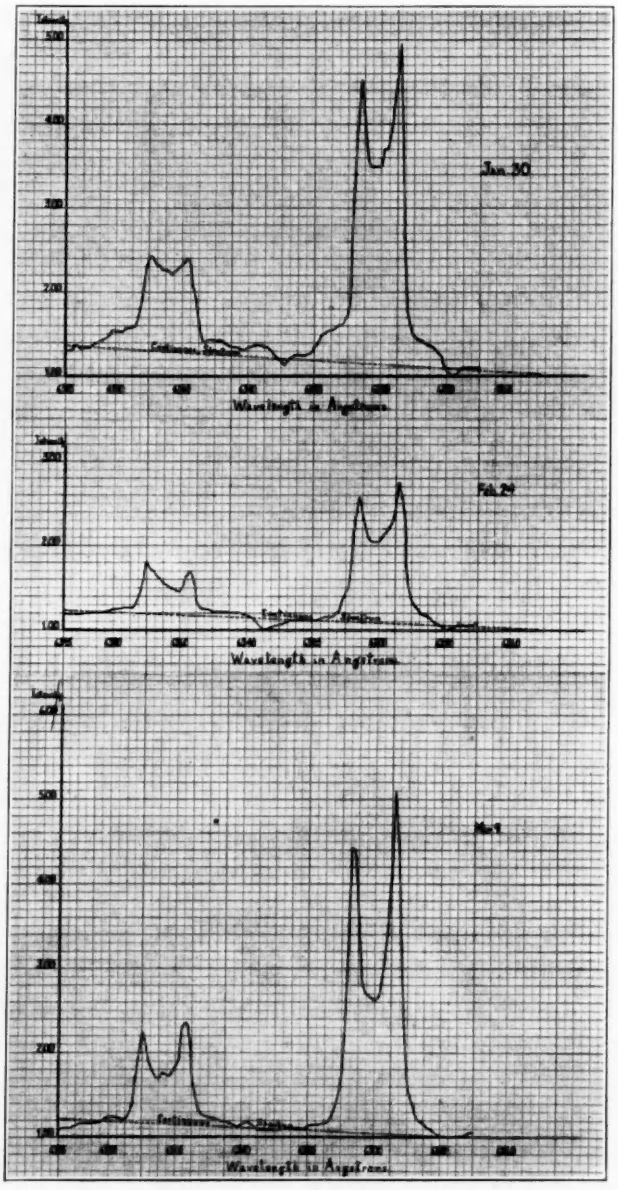

FIG. 2.—Profiles of the nebular lines *O* I on selected dates

Table 1, is considered to be near maximum possible value, as the line of the continuous spectrum was drawn rather high, going near the emission peaks of other lines. The continuous spectrum for other dates was easy to eliminate. By intensities of other features—for instance, violet components—are meant the ratios of their ordinates above the line of the continuous spectrum. These data have no immediate physical meaning, as they evidently depend on the width of the slit and on other instrumental factors. They are introduced here

TABLE 1

RELATIVE INTENSITIES OF THE NEBULAR PAIR OF *O* I

DATE	*R*/*V*		*C*/*V*		$\frac{R\ 6300}{R\ 6363}$	$\frac{C\ 6300}{C\ 6363}$	$\frac{V\ 6300}{V\ 6363}$	$\frac{T\ 6300}{T\ 6363}$
	6300	6363	6300	6363				
Jan. 5	0.82	.....	.....	.....	.....	.....	1.89	2.60
11	0.88	1.14	.....	.....	1.92	.....	2.47	3.48
23	1.02	0.88	.....	.....	2.50	.....	2.16	2.22
28	1.07	1.36	.....	.....	1.58	.....	2.00	1.46
30	0.88	1.00	0.58	0.82	3.04	2.50	3.45	2.48
31	0.85	0.90	.58	.78	3.83	3.05	4.05	2.99
Feb. 7	1.19	1.68	.82	.67	2.08	3.58	2.90	2.11
24	0.89	1.18	.57	.54	2.43	3.39	3.21	2.81
Mar. 2	0.76	0.92	.36	.44	3.78	3.81	4.59	3.71
9	0.83	0.88	.39	.45	3.15	2.95	3.35	2.97
30	0.34	0.23	0.04	0.05	4.15	2.28	2.64	2.18
Mean	0.87	1.02	.....	.....	2.85	.....	2.97	2.64
Mean Jan. 30–Mar. 30	0.82	0.97	0.48	0.54	3.21	3.08	3.46	2.75

to make a comparison with published results by other investigators.

Table 1 gives the relative intensities of various features. Letters *R*, *V*, *C*, and *T* refer, respectively, to the red peaks, the violet peaks, the centers (i.e., the lowest points between the peaks), and the total intensities.

The most significant data in Table 1 are the relative total intensities between January 30 and March 30. If we consider the variation in the ratios of total intensities to be due to accidental errors, the probable error of the mean is 0.14 and the probable error of a single observation is 0.37. The mean 2.75 ± 0.14 is very close to the mean ratio of intensities N_1/N_2 obtained by Berman (2.62) and by

Plaskett (2.70) mentioned previously, although it is somewhat below the required theoretical ratio 3.00.

The question is whether the variation in the ratio of intensities should be considered real or merely accidental, owing to the imperfection of the method of reduction. As far as our plates are concerned, the fact of variation is beyond doubt. Repeated microphotometer tracings gave practically identical results. The elimination of the continuous spectrum did not present any great difficulties. For instance, for the extreme values of the ratios on February 7 and March 2, five independent measures of intensities gave the values 2.11 ± 0.03 and 3.71 ± 0.09. The most important defect of our method—the use of an average reduction curve for converting microphotometer deflections into light intensities—would tend to increase the observed ratio but should not introduce large variations. However, many other factors entering into photographic spectrophotometry have been neglected by us. Their influence is presumably small, but no exact data exist on this point. It would perhaps be wiser to consider the variation in the intensity ratio of the nebular lines to be strongly indicated by the existing material but not established beyond doubt.

Intensities of various lines in the spectrum of Nova Herculis were derived photometrically by Greaves and Martin.[21] Their method seems to be substantially the same as that used in the present investigation. Table 2 gives the relative total intensities of the nebular pair of *O* I derived from the published Greenwich data, and their comparison with the Perkins results.

The means of the two determinations differ considerably, but, if the fact of the variation is conceded, the means are not comparable unless we deal with a large number of data. Moreover, if we neglect the clearly exceptional values 1.27 in the Greenwich series and 3.71 in the Perkins series, we obtain for the means 2.37 and 2.59, which are in fair agreement.

The total intensities of the two lines were estimated by MacLaughlin[22] for the period from December 27 to March 27 (sixteen dates). His ratios vary from 1.8 to 3.4, with an average of 2.35, un-

[21] *M.N.*, **96**, 425, 1936. [22] *Pub. Obs. U. of Michigan*, **6**, 157, 1937.

expectedly close to the values of Table 2. Intensity ratios based on visual estimates are usually considerably below the spectrophotometric determinations, as was pointed out earlier in this paper.

Among other visual estimates of the intensities of nebular lines there should be mentioned those by Dufay and Bloch.[23] They give forty-seven estimates arranged in seven groups. The ratios of the nebular pair of *O* III in these groups vary from 1.15 to 1.67.

In order to ascertain the presence of systematic errors in our determinations of intensities of various spectral features, a comparison

TABLE 2

RELATIVE INTENSITIES OF λ 6300 AND λ 6363

Date	Greenwich	Perkins
Jan. 30	.....	2.48
31	.....	2.99
Feb. 7	.....	2.11
9	2.50	.....
24	.....	2.81
Mar. 2	.....	3.71
8	2.50	.....
9	.....	2.97
26	1.27	.....
30	.....	2.18
Apr. 6	2.10	.....
Mean	2.09	2.75

of our results with those by Merrill[24] may be of interest. Table 3 gives the necessary data.

Although the means of the Perkins series differ somewhat from the means of the Mount Wilson series, the values are in good agreement. It is evident that the values of R/V decreased toward the end of the observing period. Therefore, the means are determined by the distribution of the observations during this period. For one date common to both series, January 31, the agreement is almost perfect.

The Mount Wilson mean for the ratios of the violet components is considerably higher than the Perkins mean. With the few data available, the effect of selection is necessarily great. For instance,

[23] *Zs. f. Ap.*, **13**, 36, 1936. [24] *Ap. J.*, **85**, 62, 1937.

neglecting the exceptionally high value 4.54 of the Mount Wilson series and the exceptionally low value 2.64 of the Perkins series, the means become 3.60 and 3.62, respectively.

We conclude, therefore, that a comparison of our spectrophotometric data with those of other observers indicates as good an agreement as might be expected under the circumstances.

There are some interesting features in Table 1 that perhaps might be emphasized. The means (January 30 to March 30) for the ratios

TABLE 3

RELATIVE INTENSITIES OF VARIOUS FEATURES IN [O I] LINES

DATE	$V\,6300 / V\,6363$		R/V			
			Mt. Wilson		Perkins	
	Mt. Wilson	Perkins	6300	6363	6300	6363
Jan. 30	.....	3.45	.....	.....	0.88	1.00
31	.....	4.05	0.81	0.90	0.85	0.90
Feb. 7	.....	2.90	.....	.....	1.19	1.68
11	3.55	.....	0.93	0.91	.....	.....
17	4.00	.....	1.09	1.21	.....	.....
24	.....	3.21	.....	.....	0.89	1.18
Mar. 2	.....	4.59	.....	.....	0.76	0.92
9	.....	3.35	.....	.....	0.83	0.88
16	3.71	.....	0.76	0.73	.....	.....
24	4.54	.....	0.58	0.54	.....	.....
30	.....	2.64	.....	.....	0.34	0.23
Apr. 2	3.15	.....	0.28	0.28	.....	.....
Mean	3.79	3.46	0.74	0.76	0.82	0.97

of the red components, centers, and violet components are all above the theoretical value 3.00. The difference between these means, in itself, speaks for the difference in the structure of the two lines. The mean for the ratios of total intensities, on the other hand, is considerably below the theoretical value. The explanation lies in the fact that the fainter line, λ 6363, was wider than the stronger line, λ 6300. The average width of the first line[25] for the dates of Table 1 was 15.92 A, as compared with 15.59 A for the other line. This increase in width is wholly accounted for by the difference in the wave-

[25] Given in Table 3, *Perkins Obs. Contr.*, No. 2, 1935.

length, on the hypothesis of the Doppler effect. The spreading of the fainter line over a larger area naturally decreased the intensities of its peaks in comparison with the peaks of the stronger line. The other reason for the smaller ratio of total intensities is the presence of faint flanks in both lines. Since these flanks were of approximately equal intensity, they undoubtedly tended to make the fainter line appear stronger than it was.

Although the material at our disposal is hardly sufficient to establish the difference in the behavior of the forbidden lines of *O* I beyond any doubt, there are strong indications that the variation is real. The problem is of such interest from the theoretical viewpoint that we have considered it desirable to draw to it the attention of other investigators, who might possess better material. Considerations of physical conditions in the nebulae and novae allowing two lines from the same metastable level to differ in behavior should be postponed until the fact of the variation is proved by applying more efficient methods of spectrophotometry.

PERKINS OBSERVATORY
July 7, 1937

PHOTOMETRY OF THE G BAND IN REPRESENTATIVE STELLAR SPECTRA

W. A. RENSE AND J. A. HYNEK

ABSTRACT

The total absorptions between the limits λλ 4236–4292, λλ 4293–4317 (G band), and λλ 4318–4383, designated as *V*, *G*, and *R*, respectively, have been measured for twenty-five giant and dwarf stars of spectral classes F to M. The accuracy of the measures is shown to be better than 8 per cent. The variation of the intensity of the G band and of *S*, the sum of *V*, *G*, and *R*, with spectral class and luminosity is discussed.

An attempt is made to evaluate the relative contribution of the *CH* molecule to the absorption in the G band region by the use of the comparison regions *V* and *R*, the measure being designated as *B*. It is found that whereas *G* increases somewhat in intensity in passing from dwarfs to giants, *B* decreases in the same range, as is predicted by theory. A flatter maximum than that given by theory for *CH* is observed.

By means of Russell's formulae, the mean degree of association into molecules in an F8 dwarf is found to be 4.5 times greater than in a Go giant, while the partial pressure of *CH* in the dwarf is, similarly, found to be some 80 times that in the giant.

The use of the quantity *S* as an absorption index is considered.

The marked absorption in the region of λ 4300 in later-type spectra, first called the G band by Fraunhofer, and its availability to spectrographs of high and low dispersion have long established its usefulness as a criterion of spectral classification. It is known to be composite in character, being a mixture of strong neutral and ionized atomic lines and a large part of the (0, 0) and (1, 1) bands of the $^2\Delta - {}^2\Pi$ system of the *CH* molecule.[1] Because of this, visual estimates of the G band are likely to be largely a function of the dispersion employed, for with low dispersions the atomic and molecular components are indistinguishable.

Accordingly, there is a point in measuring the equivalent widths in this region in typical dwarf and giant spectra and, since considerable theoretical work has been done on the *CH* absorption in stellar spectra, in attempting an evaluation of the relative contribution of atomic and molecular absorption to the total absorption of this region.

Previous work on the G band in stellar spectra has been largely visual or has employed very low dispersions. Lindblad[2] studied the

[1] W. Jevons, *Report on Band Spectra of Diatomic Molecules*, p. 178.

[2] *Medd. A. Obs., Upsala*, No. 11, p. 3.

absorption of *CN* and the G band as a function of absolute magnitude, using a dispersion of but 1.4 mm between $H\gamma$ and $H\epsilon$ which was too small to give a measure of the true *CH* absorption. Swings and Struve,[3] using a much higher dispersion, made a visual study of the *CN* and *CH* bands in relation to spectral type by the examination of single pure lines of the bands. For *CH*, the lines at λ 4293.12 and λ 4303.94 were used, and for *CN*, λ 4192.57 and λ 4197.10. Rufus[4] has examined the behavior of the G band in the principal spectral classes and has given a curve for the same, and Shane[5] has reported its behavior in R and N stars. Wildt[6] and Russell[7] have given a comprehensive treatment of the theoretical behavior of the *CH* and *CN* molecules for the entire spectral sequence. The present note, it is hoped, will give the necessary quantitative data for a discussion of the previous work in terms of the relative contributions of atomic and molecular absorption.

We have adopted for the G band the rather narrow limits λ 4293 and λ 4317. While it is true that the twelve main branches of the $^2\Delta - {}^2\Pi$ band of *CH* have detectable lines considerably beyond these limits, an examination of a laboratory spectrogram[8] of the λ 4300 band of *CH* shows clearly a very high concentration of lines in the region adopted. Clearly, it is this group which forms the stellar band.

Within this region in the solar spectrum there are forty-five neutral and ten ionized lines of Rowland intensity two or greater. Since the atomic lines are so numerous, a strict evaluation of the *CH* absorption is impossible with ordinary stellar dispersions, but a rough measure of it can be obtained by measuring the equivalent atomic absorption adjacent to the G band and subtracting this from the total absorption of the band.

OBSERVATIONAL MATERIAL

From large-scale microphotometric tracings of homochromatically calibrated prism spectrograms (30 A/mm at $H\gamma$) of representative

[3] *Phys. Rev.*, **39**, 142, 1932.

[4] *Pub. Obs. U. of Mich.*, **3**, 258, 1923.

[5] *Lick Obs. Bull.*, **10**, 79, 1919.

[6] *Zs. f. Phys.*, **54**, 856, 1929.

[7] *Ap. J.*, **79**, 317, 1934.

[8] Jevons, *op. cit.*, p. 83.

stars of spectral types F to M selected from the files of the Yerkes and Perkins observatories, total absorptions, expressed in angstrom units, of the following regions were measured: $G \equiv \lambda 4293 - \lambda 4317$; $V \equiv \lambda 4236 - \lambda 4292$; $R \equiv \lambda 4318 - \lambda 4383$. The tracings of each region were reduced to the usual plots of percentage absorption and were then integrated by means of a planimeter. No approximations were used, measures being made at short intervals along the tracing. From this point on, G, V, and R will be taken to mean the equivalent widths of those respective regions. Twenty-five stars (Table 2) were used, distributed as well as possible both in spectral class and luminosity. Only plates of nearly equal density, having no guiding errors, and for which complete and very well-defined H and D curves were available, were used.

ACCURACY OF THE MEASURES

The data in Table 2 are meaningless unless the order of their accuracy is known. To check the general accuracy, three spectrograms of α Persei (two Perkins plates and one Yerkes plate), two of the sun (sky), two of o^2 Eridani, and two of η Coronae were reduced independently. To check the microphotometer in particular, two plates of the sun were reduced twice each and on different days. The results appear in Table 1 and are very gratifying. The largest scatter is seen to be 13 per cent and the mean error is but 5 per cent. The final result, which is a simple function of these observed quantities, will have a slightly higher mean error. It is actually observed to be about 8 per cent. We can, therefore, be reasonably sure of the variations in equivalent widths given in Table 2.

THE METHOD OF REDUCTION

The blending of atomic and molecular lines in the G band is both real and instrumental. If very high dispersions were available, many of the band lines would undoubtedly be seen free of atomic lines, but some would be associated with the wings and cores of atomic lines. For the former, subtraction of the atomic absorption from the total absorption in the region would give the molecular absorption; for the latter, the theory of blended absorption lines would have to be applied. If one assumes a scattering atmosphere in which the

molecules and atoms are well mixed, and neglects collisions, Doppler effect, and variation of η with depth ($\eta = l/k$, where l is the coefficient of line absorption and k is the coefficient of continuous absorption), then Thackeray's[9] results could be applied. It can easily be shown that even in this simple case the mathematical complexity precludes a practical solution. However, those molecular lines falling near the cores of the much stronger atomic lines would be obliterated, for at such a frequency one sees but a small distance into

TABLE 1

MEASURE OF REDUCTION ACCURACY

Star	*V*	*R*	*G*	*S*	Plate
α Persei	7.1	9.8	6.1	23.0	PY 278P
α Persei	7.4	11.1	6.1	24.6	1R 10714
α Persei	7.9	9.5	5.7	23.1	PY 311P
Sun	11.0	10.1	9.4	30.5	PY 454P
Sun	10.9	10.2	9.3	30.4	PY 454P
Sun	10.4	9.8	8.5	28.7	PY 452P
Sun	11.9	11.9	9.4	33.2	PY 452P
o^2 Eridani	12.0	8.9	9.5	30.4	PY 245P
o^2 Eridani	13.8	9.6	9.8	33.2	PY 211P
η Coronae	9.7	9.2	7.2	26.1	1R 9147
η Coronae	10.4	9.3	7.3	27.0	PY 376P

the atmosphere, thus blocking out the *CH* molecules which lie below. In short, if inordinately high dispersion were available, one could merely subtract the atomic absorption from the total absorption and arrive at a good first approximation to the true *CH* absorption.

With the dispersions ordinarily available, however, the instrumental blending is probably far greater than the true blending, and any attempt to extrapolate the profiles of the atomic lines down to the true continuous background would vitiate the results. The equivalent atomic absorption may be estimated by the use of the adjacent regions *R* and *V*. These regions were chosen so that on an average microphotometer tracing each showed twice as many atomic

[9] *Ap. J.*, **84**, 433, 1936.

line-peaks as did the G region. The assumption that, on an average, $(V + R)/4$ would behave similarly to the atomic lines in the G region is open to some question, especially in the case of the supergiant stars in which we should expect inordinately strong ionized lines in the G region. To check this roughly we can examine the case of the supergiant α Persei. Weighting each absorption line in the regions V, R, and G by the listed[10] intensity and summing over each region, we obtain for the G region a count of 129 and for $(V + R)/4$ a count of 123. Thus, even though the G region is known to be rich in ionized lines, this assumption apparently does not vitiate the results.

Rather than use a statistical method, it might seem more logical to observe equivalent individual lines elsewhere in the spectrum for each atomic line found in the G region and to subtract this sum from the total absorption of the G region. This method was found impracticable, primarily because equivalent unblended lines of the same theoretical intensity as those in the G region cannot be found with the dispersion employed (30 A/mm at $H\gamma$.) It is questionable whether the method would be feasible even with considerably higher dispersion, for few strictly equivalent lines could be found, and allowance for these differences for some fifty lines would involve considerable uncertainty, even if all the comparison lines could be found in the unblended state. When both factors are taken into account, the method is even less certain than the one employed. The writers wish to emphasize, however, that the present method is an approximate one and that the results must be taken as only a relative measure of the *CH* absorption. Since, however, no better method of attacking this interesting problem was available, it was felt that its use was warranted.

Most previous observers have agreed that the *CH* absorption earlier than F5 is entirely negligible and that the intensity of the G band is due to atomic lines alone. We have taken the mean of the differences $G - (V + R)/4$ for two Fo and two F2 stars (amounting to 1.1 A) as the zero correction. Attempts were made to deduce a further correction to allow for the possible variation of this excess G atomic absorption with spectral class and luminosity, but it was

[10] T. Dunham, *Contr. Princeton Obs.*, No. 9, 1929.

concluded that with the present material such attempts would be too arbitrary and they were abandoned. We have thus: $A \equiv G - (V + R)/4$, and $B \equiv A - 1.1$, the latter taken as a measure of the molecular part of the G band.

OBSERVATIONAL RESULTS

In addition to the G, V, R, A, and B defined above, it seemed interesting to record the quantity S, the sum of V, G, and R, also

TABLE 2

EQUIVALENT WIDTHS IN G-BAND REGION FOR TWENTY-FIVE STARS

STAR	*Sp.*	M_I	M_S	V	R	G	S	A	B	V/R	CN
η Leporis	Fo	2.3	2.8	6.8	8.9	4.5	20.2	0.6	.....	0.8	o
20 Can. Ven.	Fo	−0.3	1.0	6.4	9.7	4.9	21.0	0.9	.....	0.7	o
81 Leonis	F2	.....	2.7	4.1	6.2	3.6	13.9	1.0	.....	0.7	o+
53 Virginis	F2	0.7	3.2	5.2	5.7	4.5	15.4	1.8	.....	0.9	o+
τ Boötis	F5	3.4	3.6	4.3	5.5	4.6	14.4	2.2	1.1	0.8	o+
α Persei	F5	−3.3	−1.1	7.5	10.1	6.0	23.6	1.6	0.5	0.7	o+
η Cassiopeiae	F8	4.9	4.5	13.5	13.4	10.9	37.8	4.2	3.1	1.0	o
ρ Coronae	F8	3.4	4.0	11.5	10.7	9.9	32.1	4.3	3.2	1.1	o
ϵ Hydrae	F8	−1.1*	2.4	8.6	11.4	6.6	26.6	1.6	0.5	0.8	1
ρ Cassiopeiae	F8p	1.4	−2.7	11.1	13.7	9.9	34.7	3.2	2.1	0.8	.....
Sun	Go	4.8	4.8	11.0	10.1	9.4	30.5	4.1	3.0	1.1	1
η Coronae	Go	4.3	3.9	10.0	9.2	7.3	26.5	2.5	1.4	1.1	2
β Leporis	Go	−2.2	0.2	14.4	13.0	11.5	38.9	4.7	3.6	1.1	2
η Pegasi	Go	neg.	0.0	14.2	13.3	10.6	38.1	3.7	2.6	1.1	2+
o^2 Eridani	G5	6.0	6.2	12.9	9.3	9.6	31.8	4.1	3.0	1.4	1
ϵ Geminorum	G5	−2.3	−1.8	20.5	18.2	13.2	51.9	3.5	2.4	1.1	3
ϵ Eridani	Ko	6.2	6.1	16.9	14.0	12.3	43.2	4.6	3.5	1.2	1+
τ Ceti	Ko	6.0	5.9	19.0	15.3	12.8	47.1	4.2	3.1	1.2	1
α Boötis	Ko	−0.2	0.6	23.0	19.6	14.5	57.1	3.8	2.7	1.2	3
ϵ Boötis	Ko	−1.4	−0.5	18.7	13.7	12.6	45.0	4.6	3.5	1.4	3+
ι Aurigae	K2	−0.8	−0.4	22.4	20.9	14.0	57.3	3.2	2.1	1.1	2+
α Orionis	Ma	−4.1	−4.0	19.7	14.7	10.7	45.1	2.1	1.0	1.3	3
R Coronae	Go	3.8	.....	11.3	13.5	8.1	32.2	1.9	0.9	0.8	3+
γ Persei	F5A3	−1.7	−0.1	13.2	15.7	9.8	38.7	2.6	1.5	0.8	1
5 Lacertae	KoAo	−2.4	−3.0	10.5	16.3	8.8	35.6	2.1	1.0	0.7	3+

* The dynamical parallax gives $M = +0.1$ for ϵ Hydrae, and this value was adopted.

the ratio V/R. Finally, for comparison purposes, the means of several independent estimates of the CN absorption at λ 4200 were noted. These quantities are listed in successive columns of Table 2 along with the star's name—stars are arranged primarily according to spectral class and secondarily according to luminosity—and its trigonometric and spectroscopic absolute magnitudes.

DISCUSSION OF THE RESULTS

Perhaps the most interesting point illustrated in Table 2 is the difference in behavior of *G*, the total absorption of the entire G region, and of *B*, the probable *CH*-band absorption. The *G* intensities follow the curve given by Rufus, and the *B* intensities follow, generally, the theoretical curves given for *CH* by Russell and substantiate the visual estimates by Struve and Swings. But whereas almost invariably the *G* intensity, which closely parallels the behavior of *S* (the sum of all measured absorptions), in giants is equal to, or greater than, its value in dwarfs, just the opposite result is noted for *B*. The latter is in accord with theory; dissociation is greater in a giant's atmosphere than in a dwarf's. In the G stars the greatest absolute-magnitude effect for *G* occurs, an increase of 30 per cent in total *G* absorption being noted in passing from dwarf to giant. Thus, for a G5 dwarf ($M = 6.1$) $G = 9.6$ A and for a G5 giant ($M = -2.0$) $G = 13.2$ A. In other classes this difference is smaller but is of the same nature. In the F8 stars for which there is a good range in absolute luminosity, the curve representing the *G* absorption and also the curve for *S*, if drawn, would have a minimum for intermediate luminosities. This may be due to the effect, noted previously,[11] that the curves relating total absorptions to absolute luminosities in classes F8 and Go are concave upward: both pronounced dwarfs and supergiants have more intense atomic lines than the stars intermediate in luminosity.

The variation of *B* is in agreement with Russell's predicted curves except that the maxima observed are flatter, especially for the dwarfs. The maximum values for *B* are nearly the same from F8 to Ko. A somewhat better agreement with the theoretical curves would be obtained if the latter were shifted about one spectral subdivision for the giants and about four for the dwarfs, toward the higher temperature side of the graph.

The mean value of *B* for the dwarfs of classes F8 to Ko is slightly greater than three angstroms of total absorption, or about 30 per cent of the total absorption in the G band. For giants this is found to be less than 20 per cent.

The variance of previous results concerning the behavior of the

[11] J. A. Hynek, *Contr. Perkins Obs.*, No. 1, 1935.

G band and the *CH* band are thus seen to be apparently due to the lack of discrimination between the principal components of the G band. The atomic lines grow stronger and the *CH* lines weaker as brighter stars are observed, but with small dispersions the net result will appear different from that with high dispersions. This is especially so with visual estimates. The differences in the *G* values in Table 2 for different stars of the same spectral class, and corresponding stars of different spectral classes, are thus probably real, especially considering the small probable error, and are due to the conflicting absolute-magnitude effects of the three components of the G band: the neutral and ionized lines, and the band lines. *G*, which thus represents the total of these effects, is therefore unreliable as an exact criterion of luminosity or of spectral class, although, in the mean, *G* increases to a maximum at K2 and then decreases slowly, in accordance with the results by Rufus.

It will be observed that *B* in a giant Go is about equal to that in a dwarf F8. If we assume that *B* is a measure of *CH* absorption, as appears to be the case from the foregoing, we can compute the ratio of association into molecules in the atmosphere of the giant and dwarf. Adapting the equation given by Russell[7] to our needs, we have

$$\log K_{CH} = 4.05 + \tfrac{1}{2} \log T - \frac{21{,}000}{T},$$

where K_{CH} is the dissociation constant for *CH*, and T is the absolute temperature. If we assume $T = 6150°$ for the F8 dwarf and $T = 5200°$ for the Go giant, then $\log K^d = 2.62$ and $\log K^g = 1.87$. But, by definition,

$$K_{CH} = \frac{p_C p_H}{p_{CH}},$$

where the p's refer to partial pressures. Taking the ratio of the two K's, we have

$$\frac{K^d}{K^g} = \frac{p^d_C p^d_H}{p^g_C p^g_H} \times \frac{p^g_{CH}}{p^d_{CH}}. \tag{1}$$

If S_x refers to the number of particles of substance x per unit area,

$$S_x = \frac{C p_x}{g y}, \tag{2}$$

C being a constant and g and y referring, respectively, to the surface gravity and the mean degree of association into molecules in a star's atmosphere. From the last two equations we can write, assuming that $S_{CH}^{d} = S_{CH}^{g}$, since we have taken a case in which the observed total absorptions are equal:

$$\frac{K_{CH}^{d}}{K_{CH}^{g}} = \frac{(S_H \cdot S_C \cdot g \cdot y)^d}{(S_H \cdot S_C \cdot g \cdot y)^g}.$$

Inserting the values of $\log S_H$ and $\log S_C$ from the published data of Russell, and computing the g's from his formulae, we have

$$y^d = 4.5 y^g .$$

The mean degree of association into molecules in a dwarf star of type F8 is, therefore, more than four times greater than in a giant star of type Go. Using the well-known formulae of Russell, we obtain

$$p_{CH}^{d} = 83.0 p_{CH}^{g} ,$$

where p is the partial pressure.

It appears that the ratio V/R increases 40 per cent in passing from Fo to K5, independently of the luminosity.

THE QUANTITY S

Since the measures of equivalent width of a line depend only upon the intensity of the continuous background in the immediate vicinity of the line, many troublesome factors—variable extinction factor, color equation, variation of color sensitivity of the plate, etc.—which make the deduction of true spectral energy-curves and similar photometric problems most difficult, do not enter. If heterochromatic spectrophotometry is employed and the plates are standardized at the same intensity level as the stellar image, and if a uniform processing technique is employed throughout, the sum of the total absorptions in, say, the region λλ 3800–5000 becomes a fundamental observable quantity. Results by Williams[12] indicate that the equivalent widths are independent of the dispersion employed, and thus the observations could be extended to very faint stars. Further-

[12] *Ap. J.*, **83**, 279, 1936.

more, the ratio of total Balmer absorption to the remaining absorption in the given region would provide a sensitive observational criterion of opacity in stellar atmospheres.

The present quantity S has been included to test the applicability of such an absorption index. The region covered is but 150 A, and not all the spectrophotometric precautions were taken, but the variations are significant. S shows a 60 per cent increase in passing from a dwarf to a giant G5. It appears to be influenced by the same effect noted before in F8 and Go stars, though the material is too scanty to allow any generalization.

G, B, AND S FOR COMPOSITE AND PECULIAR STARS

Two composite stars, γ Persei, F5A3, and 5 Lacertae, KoAo, were included in Table 2 so that the quantities, G, B, and S might be used as a check upon their spectral classification. We should expect that the spectrum of the A star superposed upon that of the later type would reduce the total absorption, especially when the hydrogen lines are not included in the measures. This is the case for 5 Lacertae, for which S is 35.6 as against the mean of 51.0 for Ko giants, but in the case of γ Persei S is 38.7 as against 23.6 for α Persei, another F5 giant. Visual estimates bear out this result, and also the color of this star indicates that its mean spectral class is F9 rather than intermediate between F5 and A3. Furthermore, B for this star is three times greater than for α Persei, whereas for 5 Lacertae B is less than one-half the value found for the corresponding Ko giant. Thus 5 Lacertae appears to be correctly classified but γ Persei is anomalous, and the primary star is probably considerably later than F5.

R Coronae Borealis was also measured at a recent maximum. Although the spectrum has "c" characteristics, its S is in agreement with that of dwarf G stars, as is the quantity G, but B is much smaller than normal, in spite of the great carbon content of the star, thus emphasizing the hydrogen deficiency in this star.

PERKINS OBSERVATORY
July 9, 1937

ON THE ORIGIN OF THE SOLAR SYSTEM

W. J. LUYTEN AND E. L. HILL

ABSTRACT

The theory of the origin of the solar system recently proposed by Lyttleton has been reconsidered. It is shown that Lyttleton's vector diagram is not applicable to the case of a planet-generating stellar encounter. Two factors overlooked by Lyttleton are shown to be of considerable importance. The first concerns the energy required to generate the planets. This is found to be so large as to require the intruding star to have an initial velocity of the order of 100 km/sec, which in turn results in the center of the planetary ribbon acquiring a velocity far beyond the escape velocity, relative to the sun. The second is that the action of the colliding stars on the filament cannot be neglected after the collision, and it is found that together these two stars retain roughly 94 per cent of the length of the planetary ribbon, leaving only 6 per cent available for possible capture by a third star. This makes it very difficult to understand how the sun could have acquired its planetary system by the mechanism suggested by Lyttleton.

A new solution for the origin of the solar system has recently been proposed by Lyttleton.[1] He considers that the sun (A) may have formed a binary system with another star (B), similar in mass and size, and that a third star (C), likewise similar in mass and size, may have entered the system and by a close collision may have divorced the sun from its companion. It is then proposed to show: (1) that B acquires and C retains sufficient momentum so that the three stars escape permanently from one another and (2) that some of the filament formed between B and C during the collision may be captured by the sun A and may remain behind to form our planetary system.

The binary-star phase of the theory was originally proposed by Professor H. N. Russell in order to avoid the principal dynamical objection to the collision theory, viz., that of the insufficiency of the angular momentum, which was originally pointed out by Nölke and by Russell. However, he did not publish any detailed theory along these lines, and the present version was developed by Lyttleton.

Of course, since this problem is essentially one of many bodies, and at best involves the solution for three bodies with unknown initial conditions, it is impossible to discuss the mechanism in any great detail. We feel, however, that it may be pertinent to add a few remarks to those of Lyttleton in an attempt to define the problem a little more closely.

[1] R. A. Lyttleton, *M.N.*, **96**, 559, 1936.

The discussion of the problem may be conveniently divided into two parts, the first dealing with the physics of the collision and the generation of the planetary matter and the second with the dynamics of the encounter. In order to simplify matters we shall, in the main, adopt assumptions concerning the numerical factors in the problem similar to those used by Lyttleton.

The sun and its identical companion are supposed to be revolving initially in a circular orbit about their common center of mass at a relative distance of 18 astronomical units and, hence, have a relative orbital velocity of 10 km/sec. Star C is also taken to be identical in mass and size with A and B.

I. CONSIDERATION OF THE HYDROGEN CONTENT

If we follow Jeffreys on the internal constitution of the planets we may assume, roughly, that Saturn has a central core of about four times the diameter of the earth and of similar composition. This leaves an outer layer about 32,000 km in thickness and a total mass some thirty times that of the earth, which might be composed, say, first of a layer of ice, then possibly of oceans of liquid NH_3 and CH_4 surrounded by an extensive atmosphere which may contain large quantities of free hydrogen but which certainly still contains gaseous ammonia on its outer boundary. It is rather difficult to estimate the actual percentage of hydrogen on Saturn now, but we might perhaps put it at roughly 15 per cent by mass. For Jupiter, the only planet which really counts, it would presumably be less, and for the average of all the planets we may adopt the value of 10 per cent by mass.

According to Russell, the H-content of the solar atmosphere is about 300:1 by number or about 12:1, or 92 per cent, by mass if we adopt Unsöld's mixture of other elements. B. Strömgren has indicated an H-content for the sun as a whole of about 37 per cent by mass. Hence, if the planets were formed by collision, out of stars similar to the sun, it would seem only reasonable to suppose that the original matrix of our planets contained at least 50 per cent hydrogen by mass, so that as a minimum this original planetary matrix must have had twice the present mass of the planets, or about $0.003\ \odot$.

Following the assumptions made by Jeffreys on the mechanism of a collision (and these seem to be the only ones proposed thus far which render the collision theory amenable to quantitative treatment), Luyten[2] has shown that the collision must be extremely close before so much matter as this can be sheared off. It seems reasonable, therefore, to assume that the periastron distance must have been of the order of a solar radius. It follows that the relative velocity of the two stars at periastron must have been of the order of 1000 km/sec or more. As Russell has suggested, the velocities acquired by the ions and electrons in the planetary matrix will be of the same order of magnitude, and the temperature of the filament will then depend upon the molecular weight. At any rate, it seems reasonable to suppose that a great deal of the filament originally sheared off will dissipate into space—hydrogen as well as heavier elements. Parts of the original filament will fall back into *B* and *C*, while other parts will remain within their respective velocities of escape. Only the very central part of the ribbon, where the forces of the other two stars more or less balance, would seem to be favorably situated for capture by the sun. Since it will be shown later that this central part is always moving with a velocity exceeding the parabolic velocity relative to the sun, it follows also that the actual fraction of the original filament (not counting the parts which fall back into *B* or *C*) which may come to form our present planetary system must be very small indeed; and, even if the foregoing argument on the hydrogen content is discounted, it would seem conservative to estimate that this original filament must have had a mass of at least $0.01\odot$. No account has been taken in this of the amount required for the resisting medium apparently still needed to account for the present circularity of the planetary orbits. The allowance made here for matter allotted to the two participants of the collision may need further elaboration in view of the fact that Lyttleton apparently ignores the existence not only of *A* before and during the collision but also of both *B* and *C* after the collision. We believe that this is not justified, since it is apparent that both *B* and *C* will remain closer to the center of the planetary ribbon than

[2] W. J. Luyten, *Zs. f. Ap.*, **7**, 46, 1933.

will A, for ten years or so. In section iii we give a short discussion of the effects of B and C on the filament.

II. INITIAL CONDITIONS

The first problem is to calculate the energy required to remove this much matter from the surfaces of B and C. Let **B** and **C** be the masses with which the participants of the collision escape, and β and γ the small amounts sheared off. We then have:

Before the Collision	After the Collision
B at an infinite distance from **C**	**B** at an infinite distance from **C**
β at an infinite distance from **C**	β at an infinite distance from **C**
γ at an infinite distance from **B**	γ at an infinite distance from **B**
β on the surface of **B**	β at an infinite distance from **B**
γ on the surface of **C**	γ at an infinite distance from **C**

In addition, β and γ were originally at an infinite distance from each other, while we cannot say just what the situation is later. Presumably, owing to dissipation into space, the constituents are farther apart after the collision than they were before, but the amount of energy involved is very small and, moreover, is immaterial for the present purpose, since β and γ have to be removed from B and C in the first place, so that whatever happens afterward cannot benefit the energy content of B and C.

The first three lines in both columns remain unchanged by the collision, but the fourth and fifth indicate a marked gain in potential energy after the collision. This, it would seem, could only have been brought about by a diminution in the kinetic energy of the system BC, and the change involved is seen to be equal to the energy required to remove this much matter—0.01 ⊙—from the surface of a star like the sun (i.e., to give it a velocity of 620 km/sec). Using the solar mass and km/sec as units, this kinetic energy is 1900, while with the foregoing assumptions the amount required to "ionize" B from A is only 50. Lyttleton has considered the latter but has apparently overlooked the former which, it now appears, is about forty times as large.

Using the center of mass of B and C as origin, we see that, if the two stars ultimately are to separate with no more than their relative parabolic velocity, their velocity at a distance while they approached

must have been about 43.5 km/sec each, making their original relative velocity at least 87 km/sec.

Since A is supposedly ignored during the collision, the approach velocity of C relative to A must have been at least 77 km/sec (the relative orbital velocity of B being 10 km/sec). As will appear later on, in the case most favorable for capture of the planetary filament by the sun the star C automatically removes itself from A, and no further allowance need be made for it. If the mass of the original planetary filament should have been more than the amount assumed here, this value of 77 km/sec must be correspondingly increased, and a value for the initial velocity of C relative to the system AB of 80 km/sec would seem entirely reasonable as a lower limit. While at the present time such a value appears higher than that observed for the average star, there seems to be nothing inherently improbable in it at the time of the presumable origin of the solar system.

III. DYNAMICS OF THE COLLISION

We now come to the dynamical part of the problem. After the collision is over, B and C must both escape from A, but in directions roughly opposite to each other and with velocities much less than their approach velocities. If we admit the reasonable assumption that the velocities at different points in the planetary filament are roughly linearly distributed between the extreme velocities of B and C, it might be thought that some part of this filament could have elliptic velocities relative to the sun. To study this a vector diagram similar to that used by Lyttleton might be constructed.

Unfortunately, the diagram drawn by Lyttleton illustrates a situation very different from that which his theory considers. His diagram indicates a deflection of about 20° in the relative velocity of B and C before and after the collision, which in turn indicates an eccentricity of $e=5.7$ in the relative hyperbolic orbit. If a is the semi-axis major and q the periastron distance in this orbit, we have $q = a(e - 1)$, and hence for the velocity at infinity:

$$V_\infty^2 = \frac{k^2 M(e-1)}{q}; \qquad V_\infty = \frac{90}{\sqrt{q}}$$

(since the total mass $= 2\odot$, $e = 5.7$. V is given in km/sec, q in astronomical units).

If V is to be at all reasonable, q must be large—of the order of one astronomical unit or more—so that no collision can occur, or we must assume M to be very small. For a collision between two planets similar to Neptune we might have $M = m_1 + m_2 = 10^{-4}\odot$, $q = 3 \times 10^{-4}$ astronomical units, and $V_\infty = 38$ km/sec. It is clear, however, that for a planet-generating encounter between two stars similar to the sun, q can hardly be as large as the solar radius, or $q = 4.6 \times 10^{-3}$ astronomical units, in which case V becomes 1300 km/sec. To assume this to have been the case not only would increase excessively the improbability of the event but also would give the planetary matter a velocity well outside the escape limit relative to the sun.

We can redraw Lyttleton's diagram, making use of the value of 80 km/sec for the initial velocity of C derived above. The chief difficulty lies in choosing the times when the collision effectively "begins" and "ends," but we may specify these somewhat by assuming them to be when the separation of B and C is of the order of a few astronomical units. Until the beginning of the collision, then, we may assume that the velocity of C increases relative to both A and B but that from then on and until the end of the collision, the motion of B and C can be treated as if A did not exist. At the beginning of the collision the velocity of C relative to the system AB may still be taken to be of the order of 80 km/sec, while at the end of the collision the velocity of C relative to B may be of the order of, say, 30 km/sec—but it may be much less.

It seems reasonable to assume that the thickest part of the planetary ribbon lies about midway between B and C, so that the most favorable situation for the capture of planetary matter by the sun occurs when the velocity of this halfway point (which is presumably equal to the velocity of the center of mass of B and C) has the smallest value relative to A. This will occur if C comes in with a velocity opposite to the instantaneous orbital velocity of B around A. Figure 1 illustrates this case: relative to A the velocities of B and C before the collision are as indicated by the vectors so labeled

and amount to 10 and 80 km/sec, respectively. Circles *I* and *II* are drawn around *A* as center with radii equal, respectively, to the velocity of escape of a particle relative to *A* at the distance of *B* (i.e., 10 km/sec) and to the velocity of escape of a solar mass relative to *A* at the same distance (i.e., 14.1 km/sec). The line *BC* represents the relative velocity of *B* and *C* before the collision. If *P* be the point midway between *B* and *C*, then *AP* represents the velocity of the centroid of *B* and *C* relative to *A*. The velocities of both *B* and *C* relative to their center of mass are greatly reduced by the generation of planets as shown above, but it is clear that the velocity of this center of mass relative to *A* is not affected, and the vector *AP* con-

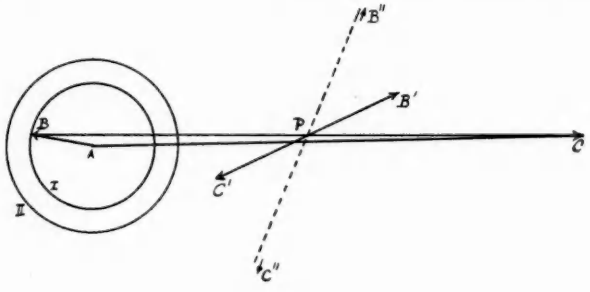

FIG. 1

tinues to represent this velocity after the collision. This same vector, then, also represents the velocity of the center of the planetary filament relative to *A*. It is easily seen that *AP* must be of the order of 35 km/sec, or three and one-half times the escape velocity relative to *A*.

Let *B'* and *C'* represent the velocity points of the stars *B* and *C* after the collision; the angles *CPC'* and *BPB'* must be large, but less than 180°, and the velocities of the various parts of the planetary filament will be represented by the continuum of points along the whole length of *B'C'*. If the sun is to retain any part of the filament, but both *B* and *C* are to escape, the necessary conditions are, as has been shown by Lyttleton: (1) both points *B'* and *C'* must lie outside circle *II* and (2) the line *B'C'* must intersect circle *I* between *B'* and *C'*.

The radius of circle *II* is 14.1 km/sec, and *AP* is of the order of

35 km/sec, and, as it was remarked above that B and C will escape from each other if their relative velocity at this time is of the order of 30 km/sec, the condition that both B' and C' lie outside II is seen to be easily satisfiable. Since both B' and C' lie on the same side of the circle II, the second requirement cannot be met in the present instance, and the entire planetary filament possesses velocities well outside the escape limit relative to the sun.

It is easily seen that this same condition has persisted throughout the duration of the collision; for example, at "last contact" the velocities of B and C will have been about as indicated by the dotted lines B'' and C'', having then been turned through roughly 120° and amounting to about 320 km/sec each.

From the point of view of the solar system it is, of course, not necessary that B and C escape from each other, so that it would also be unnecessary for the initial velocity of C to be as large as 80 km/sec. The point P might, therefore, lie much closer to A. But if the combined system $B + C$ escapes from A, the point P must lie farther than $10 \cdot \sqrt{3}$ from A, and in that case the length of $B'C'$ after the collision would be very small and it would not intersect circle I.

Next we consider whether a remedy could be found in a possible increase of the initial velocity of C and hence also of PC' to such an extent that C' lies to the left of circle II. In this case C comes in with a very high velocity, and B and C likewise part with a velocity much in excess of the parabolic value. But as long as the masses of B and C are equal, the distance from P to the left-hand side of circle II, lying within the angle subtended by circle I as seen from P, is always greater than PC, whereas the vector PC' must be less than PC. We again conclude that as long as the masses of B and C are equal, planetary masses generated in this way by a collision between them will not be captured by the sun.

From this conclusion we derive an indication that a solution might be found by assuming C to have been less massive than B. By way of illustration[3] we examine the case

$$M_A = M_B = \odot, M_C = \tfrac{5}{8} \odot ,$$

[3] We are indebted to Professor H. N. Russell for this suggestion.

for which the corresponding vector diagram is shown in Figure 2. It is evident that the initial velocity of C must now have been much greater, the radius of circle II in so far as C is concerned is now 12.8 instead of 14.1 km/sec, and the periastron distance during the collision of B and C should perhaps be slightly diminished. We may adopt $q = 4 \times 10^{-3}$ astronomical units and may likewise adopt a value of 1800 units for the energy now required to generate the planetary filament. A few numerical trials indicate that the most favorable case occurs for $V_c = 120$ km/sec, initially, relative to A. We then find: $PB = 50$ km/sec, $PC = 80$ km/sec, and $PA = 40$ km/sec. The kinetic energy of the system BC previous to the collision is 3200 units, and we assume a diminution of this to 1400 units. Hence $PB' = 33$ km/sec, $PC' = 54$ km/sec, and the relative velocity of

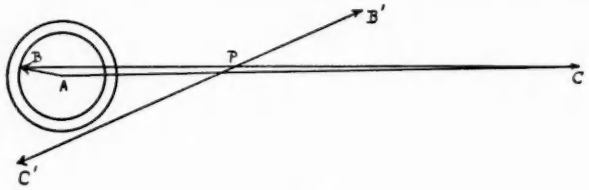

FIG. 2

B and C, which amounted to 130 km/sec before the collision, is reduced to 87 km/sec afterward. Treating their relative path as a hyperbola with a velocity at infinity of 108 km/sec, we find $a = 0.19$ astronomical unit, and with the foregoing value of $q = 0.004$ astronomical unit we have $e = 1.021$ and hence an angle between the asymptotes[4] of about 156°. This is the angle CPC' through which the velocities are turned. But from the position of P we see that an angle of at least 165° is required before $B'C'$ will intersect circle I. Any further increase in the initial velocity of C not only increases AP but also decreases the angle CPC'.

Again we see that, in this instance, while it is easy to have both B and C escape from A, all the planetary filament formed escapes with them.

It is perhaps conceivable that by choosing specific values for the

[4] Strictly speaking, the angle between the asymptotes is the supplement of this, viz., 24°, but the velocity vector is turned through 156°.

masses and diameters of the stars or for the distance AB, C' could be kept outside II but $B'C'$ would be made to intersect circle I. It is clear that in this case only a small fraction of the line $B'C'$—and hence of the planetary filament also—could fall within the sun's sphere of influence, but this would also largely or wholly lie within the elliptic limit relative to C.

A rigorous treatment of the motion of the particles in the planetary filament seems out of the question, but it can be easily seen that the fraction which escapes from both B and C is probably always quite small. Let $\mathbf{B}$ and $\mathbf{C}$ be the masses of the two stars B and C which are assumed to be separating with exactly the parabolic velocity, and let r be their distance of separation at the time when the planetary filament breaks. Let us further assume, with Lyttleton, that the velocities of the various points in the filament lie roughly linearly between the velocities of B and C, and that, after the filament breaks, each part of the ribbon pursues its course solely under the influence of the attracting masses of B and C, not being perturbed by adjacent parts of the filament.

At that instant, then, the velocity of B relative to C will be

$$V = k\left[\frac{2(\mathbf{B}+\mathbf{C})}{r}\right]^{1/2},$$

in which k is the Gauss constant. Consider the motion of a particle Q at a distance ar from C. Its velocity relative to C at that time will be

$$V_Q = aV = ak\left[\frac{2(\mathbf{B}+\mathbf{C})}{r}\right]^{1/2}.$$

It is subject to an acceleration directed toward C, of amount

$$\frac{k^2\mathbf{C}}{a^2r^2} - \frac{k^2\mathbf{B}}{(1-a)^2r^2} = \frac{k^2\mathbf{C}}{a^2r^2}\left[1 - \frac{\mathbf{B}}{\mathbf{C}}\frac{a^2}{(1-a)^2}\right].$$

Since star B is moving away with a high velocity, its attraction on Q diminishes more rapidly than does that of C, so that the expression given above for the acceleration toward C is a minimum value, and capture by C might well be expected if this value for the accelera-

tion is sufficient for it. Instantaneously the particle Q moves as if it were attracted by an effective mass,

$$\mathbf{C}\left[1 - \frac{\mathbf{B}}{\mathbf{C}}\frac{a^2}{(1-a)^2}\right],$$

situated at C. Relative to this mass the velocity of escape will be

$$V_{\text{esc}} = k\left(\frac{2\mathbf{C}}{ar}\right)^{1/2}\left[1 - \frac{\mathbf{B}}{\mathbf{C}}\frac{a^2}{(1-a)^2}\right]^{1/2}.$$

The necessary requirement for capture is $V_Q < V_{\text{esc}}$. It is seen, as might have been expected, that r cancels out of this inequality so that we do not need to make any special assumptions as to the time and the separation when the planetary ribbon breaks. If we let $a_0 r$ designate the distance of a point for which the combined attraction of B and C vanishes, and $\mathbf{C}/\mathbf{B} = h$, we have

$$a_0 = \frac{h^{1/2}}{1 + h^{1/2}}.$$

If we now set $a = a_0 - \epsilon$, and neglect second and higher powers of ϵ, we obtain

$$\epsilon > \frac{h(1+h)}{(1+h^{1/2})(2 + 11h^{1/2} + 10h + 11h^{3/2})}.$$

We might similarly calculate the fraction retained by the other star simply by replacing h in all the foregoing formulae by $1/h$. The essential element, however, is not what B and C retain, but how much matter can escape. In the foregoing notation this can be indicated by $\eta = \epsilon(h) + \epsilon(1/h)$. A rigorous numerical calculation shows that η remains virtually constant over a large range in h, increasing from $\eta = 0.0584$ for $h = 1$ (equal masses) to $\eta = 0.0611$ for $h = 0.1$ ($\mathbf{B} = 10\mathbf{C}$). Hence we conclude that ordinarily not more than 6 per cent, linearly, is available for possible capture by another star. This alone makes the theory highly improbable and shows that the assumption made in the present paper that, inclusive of hydrogen loss, the present planets constitute 14 per cent of the matter sheared off

is chosen as favorably as possible to Lyttleton's theory. The linear density of the ribbon would probably be greatest in the middle; but, since it has been shown that in all cases considered this same portion of the ribbon has a velocity well outside the escape velocity relative to the sun, we conclude that the sun's possible share of the filament must be very small indeed.

If the stars depart from each other with hyperbolic velocities, V_Q is somewhat greater than the value adopted here, but B also gets away more quickly. As a concrete case, let us take $\mathbf{B} = \mathbf{C}$, with a relative velocity at infinity of 100 km/sec, and assume that the ribbon breaks at $r = 0.05$ astronomical unit. The parabolic speed under these conditions would be 266 km/sec, the hyperbolic value 285 km/sec, resulting in only a small change in the final value of a.

In our opinion the analysis presented here shows that if the solar system did originate from such a collision process in a binary-star system, the actual course of events must have been quite different from that pictured by Lyttleton. Even if it could be proved possible for the sun to obtain planets in some such way, the theory would still be faced with the formidable physical difficulties of the older collision theory, such as the condensation into planets of the gaseous, low-density matrix having a temperature of the order of 10^6 degrees, and the difficult question of the resisting medium required to change the original highly eccentric orbits into nearly circular ones.

Summarizing our conclusions, we may state them as follows: The sun and its similar companion B are initially supposed to form a binary system. The intruder C, which must be less massive than B in the case most favorable for the theory, approaches with an original hyperbolic velocity of the order of 100 km/sec. If all circumstances are favorable, C may collide with B, and a planetary ribbon may be formed. It seems doubtful whether enough matter can be sheared off in this way to account for the present planetary system, but this portion of the theory is not now subject to definite proof or disproof. Granting it to be possible, we find that C loses most of its original kinetic energy in the process and that, surprisingly enough, it is much easier for C to "ionize" B from A than for B and C to get away from each other and from the filament, as was pointed out many years ago by Bickerton. B and C now depart, together retain-

ing some 94 per cent of the planetary ribbon. The small, but probably relatively massive, central portion is left with a velocity well outside the escape limit relative to the sun. Since for a period of about ten years this central part of the ribbon remains closer to both B and C than to A and is subjected to the equal but oppositely directed gravitational attractions of the two stars B and C, and since it presumably came from deep within the interior of the stars and was consequently at a high temperature, it might be expected to largely dissipate into space.

The sun may have been a witness, in the past, to such a catastrophe, but our present investigation indicates, rather definitely we believe, that it can hardly have acquired its present planetary system in this way.

UNIVERSITY OF MINNESOTA
July 12, 1937

NOTES

CONSIDERATIONS REGARDING INTERSTELLAR MOLECULES

ABSTRACT

An attempt has been made to compute the numbers of certain molecules in interstellar space. The results obtained are unfavorable to Saha's identification of one of Merrill's interstellar lines with Na_2. A search for the bands of CH, OH, NH, CN, and C_2 would appear to be promising.

Attention has recently been drawn to the subject of molecules in interstellar space by H. N. Russell,[1] P. Swings,[2] A. S. Eddington,[3] and M. N. Saha,[4] whose aims were essentially the interpretation of new interstellar lines of rather diffuse character, discovered by P. W. Merrill.[5] In the paper by Swings, a tentative identification of two of Merrill's lines with rotatory oscillation bands of CO_2 is suggested; the theoretical width of molecular interstellar bands is calculated and found to be in good agreement with the observations; and finally the importance of the dissociation of molecules in a radiation field is advocated. Later on, Saha published the statement that one of Merrill's bands (λ 6283) was certainly due to the Na_2 molecule (transition $^1\Sigma \leftrightarrow {}^1\Sigma$; $v'' = 0$, $v' = 8$) and that another line (λ 5780) might provisionally be attributed to NaK ($v'' = 0$, $v' = 5$). We do not believe that Saha's identification is correct; actually the experimental and theoretical investigations of the Na_2 spectrum and the determination of the corresponding Franck-Condon diagram by Loomis and Nile[6] and by Loomis and Nusbaum[7] indicate clearly that several other bands of Na_2 ($v'' = 0$ to $v' = 5, 6, 7, 9, 10$) are

[1] *M.N.*, **95**, 635, 1935.

[2] *Ibid.*, **97**, 212, 1937.

[3] *Observatory*, **60**, 99, 1937.

[4] *Nature*, **139**, 840, 1937.

[5] *Pub. A.S.P.*, **46**, 206, 1934; *Ap. J.*, **83**, 126, 1936.

[6] *Phys. Rev.*, **32**, 873, 1928.

[7] *Ibid.*, **40**, 380, 1932.

of the same intensity as $v'' = 0$, $v' = 8$, and, therefore, ought to be present also.

In any case, an estimate of the number of interstellar molecules seems important. If we assume that the density of radiation in the region of molecular absorption leading to dissociation is identical with black-body radiation at temperature T "diluted" by the factor δ, the number of molecules in dissociative equilibrium will be given by the usual formula, except that the numbers of atoms have to be multiplied by $\sqrt{\delta}$ (for diatomic molecules). Indeed, compared with black-body radiation, the number of dissociations in unit time is now reduced by the factor δ, while the number of recombinations is proportional to the product of the numbers of the engaged atoms.

We have, thus, as a first approximation:[8]

$$\frac{n_{AB}}{n_A \cdot n_B} = \frac{G_{AB}}{G_A G_B} \cdot \frac{hr_0^2}{1 - e^{-\frac{h\omega}{kT}}} \cdot \sqrt{\frac{8\pi}{mkT}} \cdot e^{D/kT} \cdot \delta ,$$

where n_A, n_B, and n_{AB} = the numbers of atoms (A and B) and molecules (AB) per cubic centimeter; r_0 = the nuclear distance in the molecule; ω = the fundamental frequency of vibration; D = the heat of dissociation; m = the reduced mass of the molecule [$m = (m_A m_B / m_{AB})$]; G_A, G_B, G_{AB} = statistical weights of the electronic levels concerned.

If we assume $T = 10{,}000^\circ K$; $\delta = 2 \cdot 10^{+14}$; $r_0 = 10^{-8}$cm; $\omega = 2000\ \text{cm}^{-1}$; $m = 10 m_H = 10^{-23}$; $\frac{G_{AB}}{G_A G_B} = 10$, we find for $D = 5$ volts:

$$\frac{n_{AB}}{n_A n_B} = 6 \cdot 10^{-9} ;$$

for $D = 10$ volts (case of CO):

$$\frac{n_{AB}}{n_A n_B} = 6 \cdot 10^{-7} ;$$

for $D = 1$ volt (case of Na_2):

$$\frac{n_{AB}}{n_A n_B} = 2 \cdot 10^{-10} .$$

[8] Cf. S. Rosseland, *Theoretical Astrophysics*, p. 247.

For a triatomic molecule (such as CO_2, assuming the reaction $CO + O$), we get

$$\frac{n_{AB_2}}{n_A n_B^2} = 4 \cdot 10^{-15} .$$

Thus triatomic molecules like CO_2 must be rare compared with diatomic compounds. In the case of Na_2, Eddington has given the maximum value to 10^{-6} atom per cubic centimeter for the density of neutral Na atoms in interstellar space. This would give us

$$n_{Na_2} = 2 \cdot 10^{-22} ,$$

which seems an extremely low value.

On the other hand, most of the H, O, N, and C atoms must be in their neutral state in interstellar space; we may safely assume that for these elements the atomic populations per cubic centimeter are not much smaller than unity, say between 1 and 10^{-3} atom per cubic centimeter. For diatomic compounds, such as H_2, OH, CH, NH, O_2, CO, CN, etc., the numbers of molecules would thus not be much smaller than the numbers of interstellar Ca^+ and Na atoms; but there would be less than 10^{-14} CO_2 molecules per cubic centimeter; this is rather unfavorable to the identification of CO_2. A search for the interstellar bands of CH, OH, NH, CN, and C_2 seems most interesting and promising. An interstellar line observed by Dunham[9] at λ 4300.3 may be due to CH. The only absorption lines of the (0, 0), $^2\Delta \leftarrow {}^2\Pi$ transition of this molecule, starting from the lowest rotational level, are λ 4300.24 and λ 4303.86. The second line could not be observed as a stationary line in an early B star, as it would be blended with λ 4303.82 *O* II. But the first would give an interpretation of the interstellar line observed by Dunham; the corresponding absorbing molecules would all be in their lowest level, in complete analogy with the case of Ti^+ atoms.

We may notice the influence of the adopted values for the temperature, the dilution factor, and the abundances. Actually if the temperature of radiation T_0 and the temperature of matter T_1 are identical, we may apply the formulae of thermodynamic equilibrium with the dilution factor δ and obtain the foregoing formula. If we suppose

[9] Pub. *A.S.P.* **49**, 26, 1937.

$T_1 \neq T_0$, we have to consider separately all the possibilities of transitions to and from the various states of the systems and to examine how these processes balance. But this could not modify substantially the numerical results. It is obvious also that the value of the density of interstellar radiation is rather uncertain. Finally, the problem of relative abundances of atoms in interstellar space is still at its very beginning; it may be that the usual assumption of relative abundances similar to those of the stellar atmospheres is not right.

P. SWINGS
L. ROSENFELD

DEPARTMENT OF ASTROPHYSICS
UNIVERSITY OF LIÉGE, BELGIUM
May 1937

NOTE ON THE INTERPRETATION OF UNIDENTIFIED INTERSTELLAR LINES

ABSTRACT

Spectroscopic objections to recent assignments of Merrill's unidentified stationary lines to molecular absorption bands are outlined.

Since the suggestion of the possible molecular origin[1] of Merrill's four interstellar lines,[2] attempts to correlate them with absorption bands of known molecules have been made.[3,4] The resulting identifications are, unfortunately, open to purely spectroscopic criticism, and indeed it seems highly improbable that these lines can be interpreted as molecular bands.

Molecular absorption in the visible spectrum might be formally attributed either to rotation-vibration bands or to electronic bands. In considering the absorption due to the small number of molecules which could conceivably exist in interstellar space, however, bands of the first type must surely be excluded, for the intensities of the high harmonics and combinations which lie in the visible are so extremely small that one could hope to observe such bands only in the relatively dense, cool planetary atmospheres. For this reason alone Swings's[3] identification of the interstellar lines λ 6283.91 and

[1] Russell, *M. N.*, **95**, 635, 1935.

[2] *Pub., A.S.P.*, **46**, 206, 1934; *Ap. J.*, **83**, 826, 1936.

[3] Swings, *M.N.*, **97**, 212, 1937.

[4] Saha, *Nature*, **139**, 840, 1937.

λ 6613.9 with $7\nu_3$ and $\nu_1 + 4\nu_2 + 5\nu_3$, respectively, of carbon dioxide seems very doubtful. The absence of the very much stronger Venus bands in interstellar absorption[5] confirms this conclusion.

On the other hand, it would appear reasonable to investigate the intense electronic absorption bands arising from molecular ground states. To identify satisfactorily an interstellar line with a given absorption band, however, it must be possible to show that (1) the shape of the line is compatible with the predicted envelope of the band at some reasonable temperature; (2) the wave-length of the line is equal to the wave-length of the intensity maximum in the band; and (3) the identification is compatible with the intensity distribution in the band system. These three requirements can best be illustrated by a brief outline of the extent to which each is satisfied in Saha's assignment of the interstellar line λ 6283.91 to the (11, 0)[6] band of the sodium molecule.[4]

1. *Shape.*—The *R* branch of the (11, 0) band has formed a head at its third line, so that even at 3.2° absolute the band would be strongly asymmetric, with a sharp, intense head on the short wave-length side. The interstellar line is observed to be approximately symmetric, although a definite statement as to its symmetry is impossible because of the proximity of an atmospheric oxygen band.

2. *Wave-length.*—The best absorption and magnetic rotation data[7] show that the center of the interstellar line is at a wave-length 3.60 A shorter than that of the (11, 0) band head. So large a discrepancy is surely real, and is obviously independent of assumptions concerning the effective temperature of the absorbing molecules.

3. *Intensity distribution.*—Absorption measurements in sodium vapor[8] lead one to expect the red system of the sodium molecule in interstellar absorption to consist solely of those bands originating in the lowest vibrational state—i.e., of the v' progression ($v'' = 0$)—which includes at least seven bands of greater intensity than (11, 0), none of which is observed as an interstellar line.

[5] Private communication from Dr. Merrill.

[6] The vibrational analysis of this system has been revised so that the band called (8, 0) by Saha is now recognized to be (11, 0).

[7] Fredrickson and Stannard, *Phys. Rev.*, **44**, 632, 1933.

[8] Fredrickson and Watson, *ibid.*, **30**, 431, 1927.

Saha's tentative identification of the λ 5780.55 interstellar line with the (5, 0) band of *NaK* is subject to essentially the same criticism. The wave-length discrepancy[9] in this case is 3.38 A.

Because of extremely low pressures in interstellar space, and the relatively high probability of the dissociation of molecules either by collisions with "high temperature" atoms and electrons or by photodissociation, it seems very reasonable to consider the probability of the existence of an appreciable concentration of polyatomic molecules as negligible and to rule out, as well, all diatomic molecules of low dissociation energy. Furthermore, since there is no experimental evidence for v' progressions ($v'' = 0$) of more than one member, only those electronic transitions which would produce such spectra—i.e., transitions involving only small changes of the moment of inertia—need be considered. A careful survey of the spectra of all known diatomic molecules which satisfy these conditions has revealed no possible identification of the strong interstellar lines, and it seems highly probable that their explanation will be found elsewhere.

It is a pleasure to thank Dr. Paul W. Merrill both for the privilege of inspecting his microphotometer tracings of the interstellar lines and for a number of helpful discussions during the preparation of this note.

EUGENE H. EYSTER

CALIFORNIA INSTITUTE OF TECHNOLOGY
PASADENA, CALIFORNIA
August 14, 1937

[9] Loomis and Arvin, *ibid.*, **46**, 286, 1934.